THE ROLE OF KININ SIGNALLING PATHWAYS IN GLIOBLASTOMA CELLS UPON CO-CULTURING WITH HUMAN MESENCHYMAL STEM CELLS

Mona das Neves Oliveira

Doctoral Dissertation for Double PhD
Jožef Stefan International Postgraduate School
Ljubljana, Slovenia

In collaboration with:
Institute of Chemistry of the University of São Paulo
São Paulo, Brazil

Supervisor: Prof. Dr. Tamara Lah Turnšek, National Institute of Biology, Ljubljana, Slovenia

Co-Supervisor: Prof. Dr. Alexander Henning Ulrich, Institute of Chemistry of the University of São Paulo, São Paulo, Brazil

Evaluation Board:
Prof. Dr. Igor Križaj, Chair, Jožef Stefan International Postgraduate School and Jožef Stefan Institute, Ljubljana, Slovenia

Prof. Dr. Radovan Komel, Member, Faculty of Medicine, University of Ljubljana, Slovenia

Prof. Dr. Vivaldo Moura Neto, Member, Institute of Biomedical Sciences, Federal University of Rio de Janeiro, Rio de Janeiro, Brazil

MEDNARODNA PODIPLOMSKA ŠOLA JOŽEFA STEFANA
JOŽEF STEFAN INTERNATIONAL POSTGRADUATE SCHOOL

Mona das Neves Oliveira

THE ROLE OF KININ SIGNALLING PATHWAYS IN GLIOBLASTOMA CELLS UPON CO-CULTURING WITH HUMAN MESENCHYMAL STEM CELLS

Doctoral Dissertation

VLOGA SIGNALIZIRANJA KININOV V CELICAH GLIOBLASTOMA V SO-KULTURAH Z MEZENHIMSKIMI MATIČNIMI CELICAMI

Doktorska disertacija

Supervisor: Prof. Dr. Tamara Lah Turnšek

Co-Supervisor: Prof. Dr. Alexander Henning Ulrich

Ljubljana, Slovenia, March 2019

Dedico este trabalho a minha família e em especial a minha amada mãe e meu querido esposo e aos meus filhos que me ajudaram a sonhar mais alto e perseverar no caminho ...

Acknowledgments

I would like to express my gratitude to all those who directly or indirectly helped in the creating of this work. I am very proud to be the researcher I have become and this is thanks to everyone's great contribution to this process. My many thanks to my relatives who endured my absence and Sundays in the laboratory and vibrated when I published. Aurora Oliveira, my beloved mother who always gave me support and love, my husband Sandi Ravbar, and my beautiful children Lana Oliveira and Dario Ravbar Oliveira. My advisors, who are like father and mother in the scientific journey, taught me to follow every step I took and they helped me to polish my data in the best way for publications. My many thanks to Prof. Dr. Henning Ulrich and Prof. Tamara Lah. I appreciate specially Prof. Henning Ulrich for the doctorate opportunity and confidence in my work, enabling my internationalization process and always supporting me during this journey in science. I want to explicitly thank Professor Dr. Tamara Lah Turnšek for the welcome and care in Slovenia and all efforts that made it possible for my family to get the visa to stay and help me during my stay in Slovenia. Many thanks to my deputy chiefs and post-doc friends Dr. Helena Motaln and Dr. Micheli Pillat who guided me on the bench and gave valuable training. I also thank the friends Archimedes Cheffar, Gunther Kriechhammer, Vashendryia Hira, Meta Novak, José Gonçalves, Maja Zagorščak, Janko Kosel, Arianje, Anna Cool and Tjaša Stare. You have made my day-to-day life lighter or pushed me to be better. I thank my non-academic friends Gisele Correia, Carolina Peixinho and Alice Schan who often showed me that there is a world outside the lab too. My special thanks to my friend Ricardo Lima and Prof. Dr. Roger Pain for the time dedicated to correcting English. I thank the Laboratory of Neurochemistry of UFBA for contribution and experimental partnership for the in vivo experiments. I also thank the whole team of the Laboratory of Neuroscience of USP, specifically Denise Yamamoto and Zilda Meendonça, by teaching me and working together in the process of learning new techniques. I thank the Institute of Chemistry and the Jožef Stefan Institute for the educational support and the National Institute of Biology for the use of laboratories and experimental support. And the ones I didn't mentioned, but I also have special affection for all my family members for having indirectly helped in this incessant search for knowledge that life is academic.

This doctoral dissertation was funded by the Slovenian Research Agency (ARRS) grant (Project J1–02474; awarded to TTL) and National Counsel of Technological and Scientific Development (CNPq Linha 2 – Bolsa Pesquisador Visitante Especial, Edital No 61/2011 [Proc. No. 402468/2012-0]; São Paulo Research Foundation [FAPESP] Proc. No. 2012/50880-4, granted to H.U.) in Brazil. I was the recipient of a CNPq Doctorate Fellowship in Brazil and of a sandwich Doctorate Fellowship for performing part of my PhD at the National Institute of Biology in Ljubljana, Slovenia, and I was a PhD student of the Jožef Stefan International Postgraduate School, Ljubljana, Slovenia. In addition, I would like to thank the National Institute of Biology in Slovenia, whose scholarship enabled me to study at the Jožef Stefan International Postgraduate School.

Abstract

Glioblastoma multiforme (GBM) represents the most lethal brain tumor with very limited treatment options. Mesenchymal stem cells (MSCs) are considered as candidates for advanced cell therapy, due to their tropism towards GBM, either directly affecting their malignancy or acting as a potential therapeutic vector. Here, we aimed to compare the effects of bone marrow (BM) and adipose tissue (AT) MSC on two different tumor cells lines of GBM population. The interplay of these cells was addressed with U87 and U373 GBM cell lines by in vitro two-dimensional (monolayer) and three-dimensional (spheroid) co-culture models. Indirect co-cultures, where the cells interacted by paracrine mechanism, as well as direct interactions in co-cultures promoted an increase in kinin-B1(B1R) and kinin-B2 (B2R) receptor expression levels in U87 cells, which was not observed in MSCs. The functionality of B1 and B2R was monitored by stimulation of intracellular calcium fluxes upon their respective agonists des-arg9-bradykinin (DBK) and bradykinin (BK), respectively. Moreover, BK induced a feedback control on kinin-receptor expression in direct and indirect co-cultures, as the treatment with BK increased expression levels of both receptors in U87 cells. This suggests that BK functions in the flow of information between GBM-MSC, being important for tumor progression. U87 cell migration and invasion in 3D co-cultures with BM-MSCs were greatly enhanced by kinin receptor agonists and blocked antagonists of these receptors. Enhanced migration and invasion correlated with significantly higher cell-cell interactions, such as more frequent heterotypic cell fusions and even cell cannibalism, as well as vesicle transfer between U87 and BM-MSC cells in direct co-cultures. These cell-cell interactions were also reduced after B1R antagonism. Further, CD105 and CD90 MSC phenotype biomarker acquisition occurred in U87 cells after these had been co-cultured with MSCs. BK promoted upregulation of epithelial-to-mesenchymal transition (EMT) gene expression together with F-actin expression in U87 cells which is associated with cell-cell interaction and invasion. In conclusion, GBM-MSC interactions promote tumor cell invasion, migration and EMT by inducing kinin receptor expression. Supposedly, kinin receptor activation favors these events by increasing tumor aggressiveness and, thus, may provide a novel therapeutic target.

Key terms: Bradykinin; kinin-B1 receptor; kinin-B2 receptor; glioblastoma; mesenchymal stem cells (MSCs); cell co-cultures; receptors; epithelial-to-mesenchymal transition (EMT); cell invasion.

Povzetek

Glioblastom multiforme (GBM) je najbolj smrtonosni možganski tumor z zelo omejenimi možnostmi zdravljenja. Mezenhimske matične celice (MSC) predstavljajo možen način naprednega celičnega zdravljenja zaradi svojega tropizma proti GBM, kjer bodisi neposredno vplivajo na njegovo malignost bodisi kot potencialni terapevtski vektorji. Tukaj smo želeli primerjati učinke MSC celic kostnega mozga (bone marrow=BM) ali maščobnega tkiva (adipose tissue=AT) na dve različni vrsti tumorskih celic. Medsebojni vpliv teh celic in GBM celičnih linij U87 in U373 smo proučevali z in vitro dvo-dimenzionalnimi (monoslojnimi) in tro-dimenzionalnimi (sferoidnimi) modeli so-kultur. Posredne so-kulture, kjer celice komunicirajo preko parakrinskih mehanizmov in njihove neposredne interakcije v so-kulturah spodbujajo povečanje izražanja kinin-B1 receptorjev (B1R) in kinin-B2 (B2R) receptorjev v celicah U87, ne pa tudi v MSCs. Funkcionalnost receptorjev B1R in B2R smo spremljali s stimulacijo znotraj-celičnega pretoka kalcijevih ionov z agonisti obeh BR, des-arg9-bradikinina (DBK) oz. bradikinina (BK). Izkazalo se je, da je BK ključen v krmiljenju povratnih informacij med nivoji kininskih receptorjev, tako v posredni kulturi kot tudi v neposredni so-kulturi. Kininski agonisti so pospešili migracijo / invazijo U87 celic v 3D-kulturah z BM-MSC, kininski antagonisti pa so jih inhibirali. Povečana migracija in invazija sta bili povezani z bistveno večjimi interakcijami celic, kot so npr. pogostejše fuzije heterotipnih celic in kanibalizem U87 in BM-MSC celic ter izločanje izvenceličnih veziklov (EV) v so-kulturah. Ob dodajanju B1 antagonista so bile celične interakcije manj pogoste. Poleg tega so celice U87 v interakciji z MSC začele izražati biomarkerje mezenhimskega fenotipa, kot so CD105 in CD90. Predpostavljamo, da v U 87 celicah BK regulira izražanje genov, ki posredujejo epitelno-mezenhimsko tranzicijo (EMT), skupaj z ekspresijo F-aktina, ki je povezan s celično invazijo. Na splošno lahko zaključimo, da smo odkrili, da interakcije med GBM in MSC celicami spodbujajo invazijo in migracijo tumorskih celic preko EMT, ki jo inducirajo kininski receptorji. Domnevamo, da aktivacija kininskih receptorjev tako spodbuja agresivnost tumorja, zato bi ti lahko predstavljali nove terapevtske tarče.

Ključni pojmi: Bradikinin; kinin-B1 receptor; kinin-B2 receptor; glioblastom; mezenhimske matične celice; receptorji; epitelijsko-mezenhimski prehod (EMT); celična invazija.

Contents

List of Figures

List of Tables

Abbreviations

2D	...	Two-Dimensional
3D	...	Three-Dimensional
AAP.	...	Arginine Aminopeptidase
ACE	...	Angiotensin Converting Enzyme
B1R or B1BKR	...	Kinin-B1 Receptor
B2R or B2BKR	...	Kinin-B2 Receptor
BK	...	Bradykinin
BM	...	Bone Marrow
BM-MSC	...	Bone Marrow-Derived Mesenchymal Stem Cells
DAG	...	Diacylglycerol
DBK	...	Des-Arg9-Bradykinin
DMEM	...	Dulbecco'S Modified Eagle'S Medium
EMT	...	Epithelial-to-Mesenchymal Transition
EVS	...	Extracellular Vesicles
FBS	...	Fetal Bovine Serum
FDA	...	Food and Drug Administration
GBM	...	Glioblastoma
GPCR	...	G Protein-Coupled Receptors
HK	...	High-Molecular-Weight Kininogen
IND	...	Investigational New Drug
IP3	...	Inositol 1,4,5 Triphosphate
KKS	...	Kallikrein-Kinin System
LK	...	Low-Molecular-Weight Kininogen
M1	...	Cytotoxic Macrophages
MMPs	...	Matrix Metalloproteinases
MSCs	...	Mesenchymal Stem Cells
PLC	...	Phospholipase C
TAF	...	Tumor-Associated Fibroblasts
TCGA	...	The Cancer Genome Atlas
U87dsRed	...	dsRed-transfected U87 Cells
u-PA	...	Urokinase Plasminogen Activator

Chapter 1

Introduction

1.1 The Kallikrein-Kinin System

Bradykinin (BK) was first described in isolated plasma globulins in 1949 by Rocha et al. It was observed that treatment with Bothrops jararaca viper venom led to reduction in cardiac contractions (E Silva, Beraldo and Rosenfeld, 1949). This peptide is a potent endothelium-dependent vasodilator that contributes to hypotension in the systemic circulation (Maurer et al. 2011). BK is a low molecular weight nonapeptide (1060.21 Da, C50H73N15O11), which is rapidly degraded by plasma and tissue metalloproteinases. BK sequences are relatively conserved among different vertebrate lineages (Table 1). It has a half-life of 17 seconds; therefore, its blood levels are relatively low under physiological conditions (0.2-7.1pM) (Negraes et al. 2015; Maurer et al. 2011). While BK has a greater affinity for the kinin-B2 receptor (B2R or B2BKR) DBK, its derivative has affinity for the kinin B1 receptor (B1R or B1BKR)(Leeb-Lundberg et al., 2001). Both receptors are G protein-coupled (GPCR) and trigger calcium signaling events, typical for GPCRs. The genes encoding the two receptors from several mammalian species were cloned (Cayla, Merino, and Cabrini 2002; Pesquero et al. 1994; Wong 2016). In humans, both genes are located at the same chromosome 14 residing in region 14q32 (Cayla, Merino, and Cabrini 2002).

Table 1.1: Bradykinin sequences in vertebrates

Table 1. Bradykinin Sequences in Vertebrates

Human	KRPPGFSPFR
Tasmanian devil	KRPPGFSPFR
Chicken	RRPPGFTPLR
Lizard	RRPPGFTPFR
Turtle	RRPPGFTPFR
Lungfish	-YGPGFSAPFR
Coelacanths	RLPAGMSPFR
Medaka	RRPPGWSPLR
Zebrafish	KRPPGWSPLR
Fugu	RRPPGWTPLR
Tilapia	RRPPGWSPLR
Stickleback	RRPAGWSPLR
Gar	RRPPGWSPFR
Sturgeon	-MPPGMSPFR
Skate	-GITSWLPF-
Lamprey	-RRPGFMHIA

The shaded residues indicate difference in amino acids compared to human. Adapted from: Marty K.S.Wong 2016

Kallikrein-Kinin metabolism begins with higher molecular weight (HK) and low molecular weight (LK) kininogens, which can be found in plasma and tissue, respectively. These proteins are proteolytically cleaved by Kallikreins, generating either bradykinin (plasma) or kallidin (tissue), depending on a location. BK can also be obtained through cleavage of lysine on the amino-terminal end of kallidin by arginine aminopeptidase (AAP). These peptides can be further processed to their des-Arg metabolites by kininase-1 and carboxypeptidases (CPM), respectively. The des-Arg kinin binds to the B1 receptor (B1R). Kinins are rapidly inactivated, mainly by angiotensin converting enzyme (ACE, i.e. kininase II). Kinin receptor stimulation through kinins is involved in diverse (patho)physiological processes, such as control of blood pressure, inflammation and cancer (Kashuba et al. 2013; Obiezu and Diamandis 2005; Article et al. 2013), as shown in Figure 1.1.

The B2R is constitutively and widely expressed throughout the central and peripheral nervous system, mediating most of the physiological effects of kinins (Negraes et al. 2015). The B1R on the other hand is not expressed in most tissues under normal conditions, but displays an essential role and is quickly activated under inflammatory conditions (Ehrenfeld et al., 2006), infectious or traumatic stimuli (Marceau 1995) or cancer (Raidoo et al., 1999). Kinins are important inflammatory mediators that are involved in many pathophysiological processes. It has been reported that the B1R plays a pro-tumor role via cross-talking with the B2R (Barki-Harrington et al., 2003). The activation of the B1R induces cell migration (D. Y. Lu et al. 2010), which is assisted by expression of matrix metalloproteinases (MMPs) MMP-2 and MMP-9 (Ehrenfeld et al. 2011). It has also been reported that B1R antagonists decrease proliferation of breast cancer cells (Molina et al. 2009).

Our group has previously demonstrated that treatment with BK promotes neural cell differentiation (Trujillo et al. 2015) and that the Erk/Akt pathway is involved in

proliferation and migration (Pillat et al 2016). However, the role of kinins in the brain microenvironment of malignant tumors still remains unexplored. Kinin receptors are known to be involved in cell proliferation, chemotaxis and invasion in breast cancer and glioma cells (Da Costa et al;. 2014 Kashuba et al;. 2013 Nicoletti et al 2014).

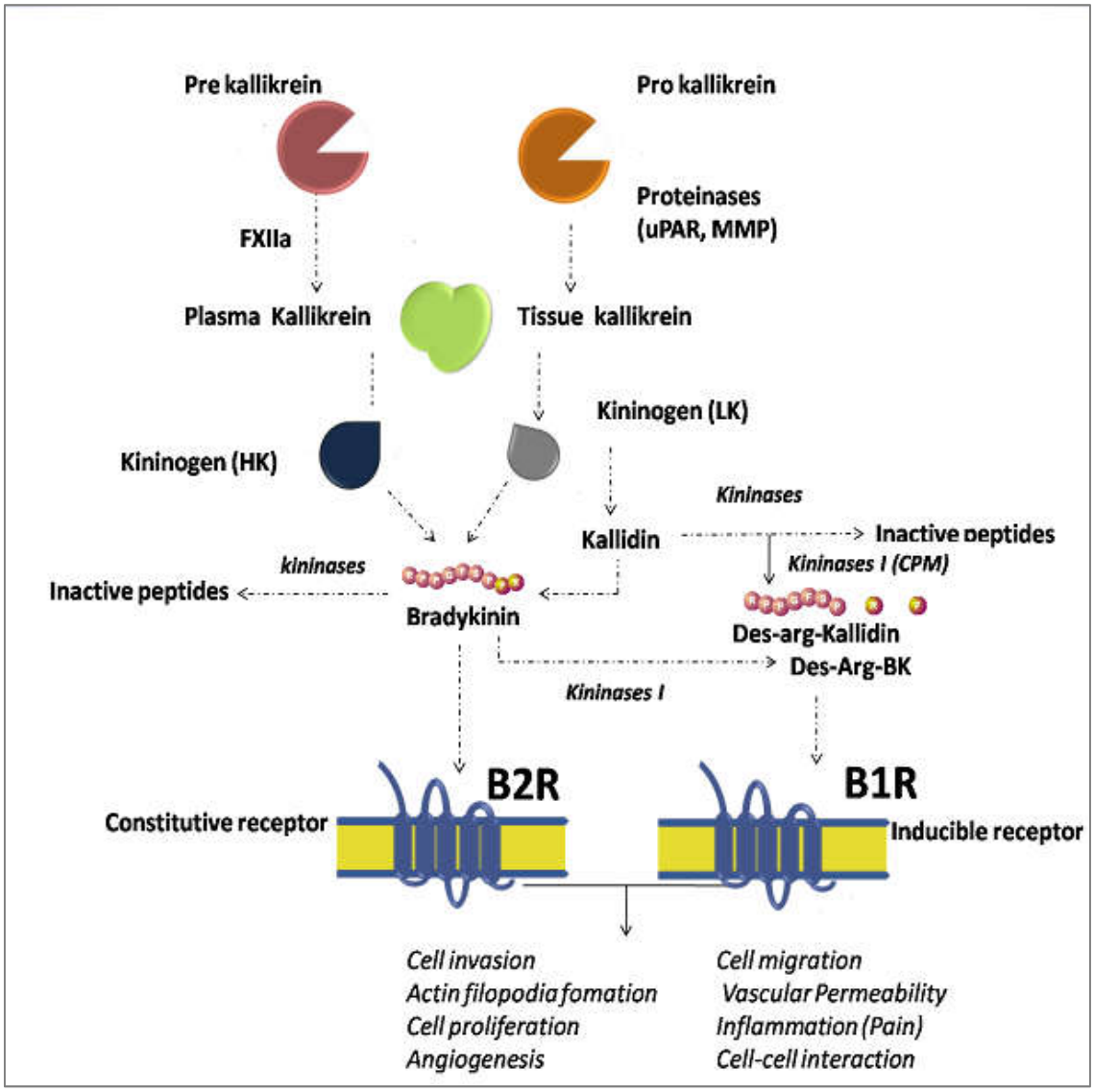

Figure 1.1: Schematic diagram of the Kallikrein-Kinin system (KKS) metabolic cascade.

Plasma and Kallikrein-related peptidases are secreted as zymogens and become activated by proteolytic cleavage. They act on high molecular weight (HK) and low molecular weight (LK) kininogens to generate bradykinin (BK) and kallidin, which act through the B2 receptor (B2R). BK is generated from kallidin by the action of an arginine aminopeptidase (AAP). These peptides can be further processed to their des-Arg metabolites by the kininases carboxypeptidases (kininases I). The Des-Arg kinin binds to the B1 receptor (B1R). Kinins are rapidly inactivated mainly by angiotensin converting enzyme (ACE,

kininase II). Bradykinin receptor stimulation through kinin is involved in diverse (patho)physiological processes, such as for example control of blood pressure, inflammation and cancer.

1.2 Glioblastoma Multiforme

Glioblastoma (GBM) are high-grade malignant gliomas (WHO grade III and IV), characterized by fast proliferation, migration and invasiveness, as well as high resistance against treatment (Louis et al. 2016). GBM are diffuse tumors that infiltrated its microenvironments and stromal cells, such as astrocytes, microglia, and inflammatory cells (Quali and Joyce, 2017), required for tumor growth, and endothelial cells during the angiogenesis process (Hardee and Zagzag 2012). This process is partly dependent on tumor cell derived cytokines, IL-1β and TNF-α that trigger expression and activity of the B1R, thereby having impact on the microcirculatory tumor system (Hardee and Zagzag 2012). In the central nervous tissue, the B1R also appears to modulate the permeability of brain tumors (Cote et al. 2012).

The high-grade glioma rarely metastasizes, neither through lymph vessels nor the hematological system. However, glioma cells invade normal tissue surrounding the tumor, and this is one of the main challenges for a more effective treatment (Rao 2003). Moreover, the intra-tumor genetic heterogeneity emerged from the dynamism of clonal selection processes within spatially distinct niches, allowing glioma cells to escape from conventional chemotherapeutic and radiological treatment (Bougnaud et al. 2016). Similarly, radiotherapy was shown to enrich for stemness genotypes and phenotypes in some tumor subpopulations, which cause tumor resistance and propagate disease progression (Mohr, Zänker, and Dittmar 2015). Likewise, the recruitment of brain tumor-derived MSCs has been associated with brain tumor heterogeneity (Behnan et al. 2013).

The presence of a heterogenic population is one of the hallmarks of GBM that can be promoted to one of the four different tumor subtypes- proneural, neural, mesenchymal and classical, according to The Cancer Genome Atlas (TCGA). These have been defined by genomic characteristics, survival length, patient age and treatment response (Verhaak et al., 2010). Interestingly, a comparison of the differentially regulated genes in the GBM cell lines with that of GBM tumor tissue transcriptome data (derived from TCGA) gave a genome concordance of ~73%, suggesting that the transcriptomes of the GBM tumor and tissue cell lines closely resemble (Patil, Pal, and Somasundaram 2015). In contrast, attempts to detect comparable transcriptional subtypes in immortalized cell lines were uninformative, as described from TCGA (Verhaak et al. 2010)

Mutations in characteristic genes following the TCGA classification were checked and cross linked with the genomic information of the exon sequences U87 and U373 from whole genome sequencing, as described by Patil et al., (2015) (see Table 1.2). We found a hybrid subtype classification. Both cell lines present proneural and mesenchymal gene mutations. The U87 cell line presents mutation in NF-1 and RB genes, similar as observed in tissue samples from mesenchymal subtypes and mutations in PDGFR, PDGFRA, PI3KCA and TP53 genes, like those observed in tissue samples from proneural subtypes according to the classification from Verhaak et al (2010). Moreover, the U373 cell line had a mutation in PTEN and RB genes similar to the one observed in tissue samples from mesenchymal subtypes and PDGFR, PDGFRA, PI3KR1, TP53 genes, such as observed in tissues samples from proneural subtypes (Table 1.2).

Table 1.2: Frequently mutated genes of GBM subtypes observed in cell lines.

Table 2. Presence of frequently mutated gene in GBM subtype observed in cell line

Gene	Subtype	U87	U373
IDH	Proneural	Wild Type	Wild Type
PDGFR	Proneural	Mutated	Mutated
EGFR		Wild Type	Wild Type
NF1	Mesenchymal	Mutated	Wild type
TP53	Proneural	Mutated	Mutated
ERBB2	Neural	Wild Type	Wild Type
RB	Mesenchymal	Mutated	Mutated
PIK3R1	Proneural	Wild Type	Mutated
PDGFRA	Proneural	Mutated	Mutated
PIK3CA	Proneural	Mutated	Wild Type
PTEN	Mesenchymal	Wild Type	Mutated

The recent work from Patel et al 2014 showed by single cell PCR analysis across RNAseq from primary GBM samples that these have a higher hybrid state, and highlights intra tumoral heterogeneity. The group found several GBM subtype mutations in tumor samples of a single patient (each sample obtained from a single cell). Tumor heterogeneity poses a major challenge in cancer diagnosis and treatment. Single cell analysis allowed to determine the highest heterogeneity inside the tumor and validates the cell line as a good model for evaluation of heterogeneity. Cells do not follow the genetic subtype classification, but show a hybrid genetic cell statement (Patel et al. 2014; Patil, Pal, and Somasundaram 2015).

Although it is widely accepted that most cancers exhibit some degree of intra-tumor heterogeneity, the dynamics that characterize the tumor subpopulations interactions are still not well understood. There is growing evidence suggesting that various subclones of cancer cells develop in competition with each other during cancer progression (Barber, Davies, and Gerlinger 2015; Zellmer et al. 2014). Lately, this approach was modified, and scientists now see this behavior not so much as competitive, but as cooperative, regarding the subclones that can influence disease progression (Tabassum and Polyak 2015). It is thus generally recognized that tumor cell heterogeneity is a very dynamic state of the neoplasm, with subpopulations that are appearing and subsiding during tumor progression and in particular as a response to altered tumor cell microenvironment.

1.3 Mesenchymal Stem Cells

Mesenchymal stem cells (MSCs) are non-hematopoietic stromal cells that are capable of differentiating into different cell lines, and contribute to the regeneration of mesenchymal tissues, such as bone, cartilage, muscle, ligament, tendon and adipose tissue (Chamberlain et al. 2007). They provide a promising tool for cell therapy in regenerative medicine (Ishii

et al., 2005). In addition to the release of immuno-modulators, MSCs directly suppress the activation of immune cells through cell-cell contact (Appaix 2014). Moreover, it has been noted that MSCs induce the anergy of T cells by downregulation of CD80 and CD86 expression on antigen presenting cells (Augello et al. 2005). MSC-promoted regulation of the immunological system affects the release of various modulatory factors that regulate inflammation, cell death, angiogenesis, fibrosis and tissue regeneration (Baglio, Pegtel and Baldini 2012). However, the controversial effect of interaction between MSCs and gliomas has been reported to promote tumor growth, invasion and chemoresistance (Melzer, Von Der Ohe, and Hass 2018; Bahnan2013 ; Del Fattore et al. 2014).

MSCs are employed for tissue regeneration in various clinical studies and are known to be attracted to sites of injury and inflammation (reviewed by Chen, 2013). Upon tumor infiltration, MSCs become part of the heterogeneous tumor microenvironment and participate in regulation of tumor progression. Whether MSCs promote or suppress tumor progression, is a controversial issue (Baglio, Pegtel, and Baldini 2012; Z. Li, Fan, and Xiong 2015). For instance, modified MSC used in GBM for expressing a single chain antibody to EGFRvIII promoted tumor growth inhibition (Balyasnikova et al. 2010). However, MSCs have also been reported to be involved in tumor progression (Yoon et al. 2016). Recently, it has been proposed that pro-inflammatory stimuli can be decisive in driving MSC polarization into cells with either tumor-supportive or tumor-repressive phenotypes, named MSC1 and MSC2 (Bracellos de Souza, 2014). Thus, elucidation of the dual roles of MSCs in glioma microenvironment is a prerequisite for any clinical applications (Yagi and Kitagawa 2013).

The molecular mechanism of paracrine interactions between bone marrow-derived MSCs and established GBM cell lines has been studied previously (Motaln et al., 2011). The cross-talk between both cell types in the indirect co-culture resulted in alterations of expression patterns of over 500 and 300 genes in MSCs and GBM, respectively. These were most likely responsible for the impairment of GBM growth and invasion, which was most likely hindered by enhanced expression of cell adhesion-related genes in GBM cell line. Thus, in direct co-cultures of these cells in vitro, Schichor et al., (2012) demonstrated that GBM cells display signs of functional as well as structural syncytium formation with MSCs, enabling direct molecular exchange.

1.4 Targeting Kinin Receptors for Cancer Therapy

In recent years, the understanding of the roles of bradykinin in cancer therapy has significantly improved. Kinin receptor antagonists have shown their efficacy in blocking tumor progression in preclinical and clinical studies. The Food and Drug Administration (FDA) has recently approved a request by Investigational New Drug (IND) for the clinical evaluation of B9870 as a tool for lung cancer treatment (Stewart et al., 2002). B9870 is a potent dual B2R and B1R antagonist with excellent antitumor activity in vivo. Dual B1R and B2R activation controls permeability of the blood brain barrier, and therefore this compound may be important for drug delivery, such as carboplatin, to the tumor site. Carboplatin has been proven to be effective in the rat glioma model F98 (Cote et al. 2012). However, in a random phase II study, where patients with glioma were treated with carboplatin with and/or without RMP-7, a B2R agonist of B2R, no improvements of carboplatin efficacy were registered (Whalley et al. 2012). Thus, the continuation of investigating the role of kinins in tumor progression (da Costa et al. 2014) and identification of the factors, which influence the effectiveness of kinin receptor antagonists and agonists, will be important for future therapeutic approaches.

1.5 GBM-MSC Cell-Cell Interaction

Recent advances suggest that comprehension of factors, such as tumor cell plasticity, the so-called "genetic noise", micro-environmental signaling and physical cues from the extracellular matrix are crucial for understanding cancer biology (Brock, Krause, and Ingber 2015). In addition to ECM and structural variations in the local tumor environment, diverse types of cells within the stroma contribute to tumor phenotypic differentiation (Patel et al. 2014). This becomes even more complex, considering simultaneous switches in stromal cell phenotypes. For instance, cytotoxic macrophages (M1) can switch to tumor growth induction by promoting M2 states depending on hypoxic environment, metabolic conditions and presence of chemokines (Bergamin et al. 2015). Similarly, and actually related to our study, bone marrow-derived mesenchymal stem cells (BM-MSC) switch from immunosuppressive to immune supporting cells, when infiltrating the tumors, as a consequence of Toll receptor priming upon interactions with T reg cells (Gwendal and Paula Y 2016). By the same token, immunomodulatory MSCs, being highly attracted by the tumor cells (Hass and Otte 2012; S. M. Kim et al. 2015; Melzer, Yang, and Hass 2016), play important roles in tumor microenvironment (Motaln and Turnšek 2015; Rhee, Lee, and Eom 2015).

Communication between cancer cells is an important issue for clonal cooperation as stated by Tabassum and Polyak 2015. Further, cooperation between tumor and stroma (i.e. the heterogeneous cellular cross-talk within the tumor microenvironments) results from paracrine and juxtacrine interactions. In paracrine interactions, the effects are caused by a set of diffusible factors, such as chemokines, that stimulate the growth of one or both populations, whereas in juxtacrine interactions shorter distances between the cells permit direct signaling (Figure 1.2). Complex interactions between various cell types in general create a potentially favorable environment for tumor growth stimulation (Quail and Joyce 2017; Skog et al. 2008).

In addition to inter-tumor interactions between tumor and stromal cells, extensive literature has demonstrated that tumor cell subpopulations are heterogenous, termed intra-tumor heterogeneity. For example, one sub-clone might secrete angiogenic factors to enhance blood vessel formation and nutrients and oxygen uptake, whereas the other is more invasive. In addition, collaborative crosstalk among multiple subpopulations may occur also through paracrine and juxtracrine effects, or it could also be an indirect outcome of micro environmental remodeling (Patel, 2014).

In this project, we have focused on investigating: (I) how GBM and MSCs can affect each other regarding proliferation, invasiveness and differentiation, and (II) understanding the role of kinin receptors in cellular cross-talk upon co-culture condition. Therefore, we divided this work into several chapters. In Chapter 2, we report the characteristics of B1R and B2R protein expression. We have also detected the activity of these receptors in direct and indirect co-culture and function of stimulation by bradykinin (BK) on expression of these receptors. In Chapter 3, we aimed to understand the mechanisms of B1 receptor activity in cell growth, invasiveness and cell fusion events. In Chapter 4, we discovered that after direct co-culture, a cross-talk following stimulation by bradykinin occurred involving kinin-B2 and B1 receptors, resulting in increased GBM cell drug resistance, survival rate and reversal of epithelial-to-mesenchymal transition.

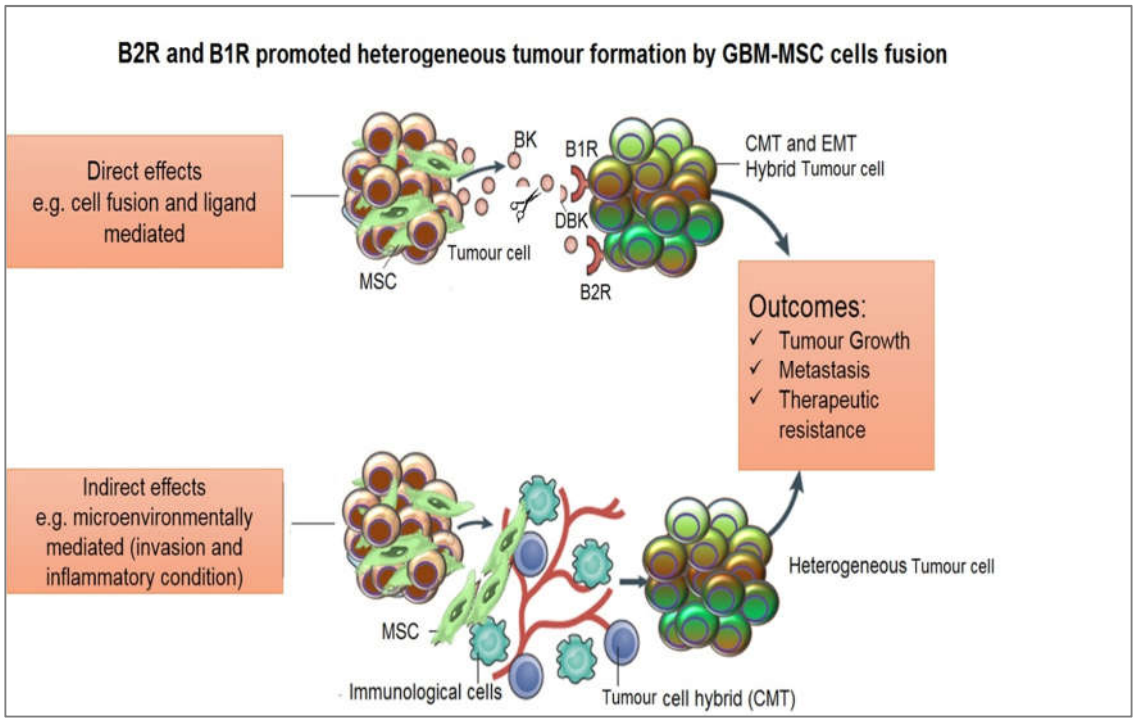

Figure 1.2: Schematic model of cell-cell interactions affected by kinin receptor action (paracrine, juxtracrine) involving variability of cells and altering the tumor cell microenvironment.

1.6 General Objective

The aim of this thesis was to define the roles for kinins in established GBM cell lines (U87, U373) and MSCs (bone marrow derived clones MSC2, MSC4 cells). Secondly, we aimed to elucidate the interplay between kinins and their receptors in complex GBM/MSC interactions, studied by several methodologies in co-cultures and compared to monocultures.

Specific objectives and methodological approaches:

1. Expression patterns (at mRNA levels) of selected kinin and protease signaling related genes were measured by quantitative RT-PCR.
2. Protein expression of the selected genes B1BKR, B2BKR, MMP2, MMP9, MMP14, CD90, CD29, CD105 and F-actin were revealed by specific antibody labelling and subsequent analysis by flow cytometry and immunofluorescence microscopy.
3. In the cell mixture of GBM/MSC of 1:1 cell ratio, vs monocultures, expression patterns of kinin receptors (B1R, B2R), cell invasion/migration related genes (MMP9, MMP2, calpain-1 and 2, cathepsin L and B, UPAR) and epithelium-to-mesenchymal transition related genes (TGF-b, Vimentin, Snail, CD44) were validated using qPCR-real time techniques.
4. Morphological and phenotypic characteristics, such as cell growth (proliferation), cell cycle distributions, senescence, migration/invasion and cell differentiation and fusion events were validated by cell counting, MTT, MTS, flow cytometry, ICC and 3D matrigel invasion/migration,

5. Validation of kinin receptor (B1R an B2R) activities was performed by inhibiting receptor signaling using selective agonists and antagonists of B1R and B2R and measured by calcium imaging.
6. Effects of kinin signaling on the phenotype changes were measured:
   6.1. Effects of agonists and antagonists of the kinin-B2 receptor, bradykinin and HOE-140, respectively, and of the kinin-B1 receptor, des-arg^9-bradykinin and R715, respectively, on viability / and differentiation of GBM and expression patterns of EMT genes was measured.
   6.2. Calcium imaging was performed with agonists and antagonists cited in 3.3.1. to verify kinin-specific receptor activities under varying experimental conditions.

Chapter 2

Glioblastoma-Mesenchymal Stem Cell Communication Modulates Expression Patterns of Kinin Receptors: Possible Involvement of Bradykinin on Information Flow

Micheli Pillat, Mona Oliveira, Helena Motaln, Barbara Breznik, Talita Glaser, Tamara Lah, Henning Ulrich

Reproduced from Cytometry part A. Accepted: 3 November 2015, published in December 2016

Cytometry
PART A
Journal of the International Society for Advancement of Cytometry

MIFlowCyt

Glioblastoma-Mesenchymal Stem Cell Communication Modulates Expression Patterns of Kinin Receptors: Possible Involvement of Bradykinin in Information Flow

Micheli M. Pillat,[1] Mona N. Oliveira,[1] Helena Motaln,[2] Barbara Breznik,[2,3] Talita Glaser,[1] Tamara T. Lah,[2,3]* Henning Ulrich[1]*

[1]Department of Biochemistry, Institute of Chemistry, University of São Paulo, Av. Prof. Lineu Prestes 748, São Paulo, S.P, 05508-000, Brazil

[2]Department of Genetic Toxicology and Cancer Biology, National Institute of Biology, Ljubljana, Slovenia

[3]Nanosciences and Nanotechnologies Programme, Jožef Stefan International Postgraduate School, Jamova 39, Ljubljana, 1000, Slovenia

Received 17 June 2015; Revised 8 October 2015; Accepted 3 November 2015

Grant sponsors: AARS Project J1-02474 (granted to T.T.L.) in Slovenia; National Counsel of Technological and Scientific Development (CNPq Linha 2 - Bolsa Pesquisador Visitante Especial, Edital No 61/2011 (Proc. No. 402468/2012-0); São Paulo Research Foundation (FAPESP) (Proc. No. 2012/50880-4, granted to H.U. in Brazil).

Additional Supporting Information may be found in the online version of this article.

*Correspondence to: Henning Ulrich, Department of Biochemistry, Institute of Chemistry, University of São Paulo, Av. Prof. Lineu Prestes 748, São Paulo, S.P. 05508-000, Brazil. E-mail: henning@iq.usp.br or Tamara T. Lah, Department of Genetic Toxicology and Cancer Biology, National Institute of Biology, Večna pot

ISAC
International Society for Advancement of Cytometry

Abstract

The most aggressive subtype of brain tumors is glioma WHO grade IV, the glioblastoma (GBM). The present work aims to elucidate the role of kinin receptors in interactions between GBM cells and mesenchymal stem cells (MSC). The GBM cell line U87-MG was stably transfected to express dsRed protein, single cell cloned, expanded, and cultured with MSC, both in the direct co-cultures (DC) and indirect co-cultures (IC) at equal cell number ratio for 72 h. Up- and down-regulation of matrix metalloproteases (MMP)−9 expression in U87-MG and MSC cells, respectively, in direct co-culture points to possible MSC participation in tumor invasion. MMP9 expression is in line with significantly increased expression of kinin B1 (B1R) and B2 receptor (B2R) in U87-MG cells and their decreased levels in MSC, as confirmed by quantitative assessment using flow cytometric analysis. Similarly, in indirect cultures (IC), lacking the contact between GBM and MSC cells, an increase of B1 and B2 receptor expression was again noted in U87-MG cells, and no significant changes in kinin receptors in MSC was observed. Functionality of kinin-B1 and B2 receptors was evidenced by stimulation of intracellular calcium fluxes by their respective agonists, des-Arg9-bradykinin (DBK) and bradykinin (BK). Moreover, BK showed a feedback control on kinin receptor expression in mono-cultures, direct and indirect co-cultures. The treatment with BK resulted in down-regulation of B1 and B2 receptors in MSC, with simultaneous up-regulation of these receptors in U87-MG cells, suggesting that functions of BK in information flow between these cells is important for tumor progression and invasion.

Key terms

Bradykinin; kinin-B1 receptor; kinin-B2 receptor; glioblastoma; bone-marrow mesenchymal stem cells; direct and indirect cell co-culture

Gliomas, although classified as a rare neoplastic disease, are still the most frequent brain tumors and their most malignant form (WHO stage IV astrocytoma). Glioblastoma (GBM) has an average postoperative survival of only 14.6 or 12.1 months when treated with radio- and chemo- therapy (temozolomide) or with radiotherapy alone, respectively (1). The major characteristic of these tumors is the high infiltration rate of single cells, the so called "guerrilla" cells into the brain parenchyma, even several cm away from the bulk tumor mass. These cells are hard to target by conventional therapies. In view of that, the development of novel therapeutic strategies for successful GBM treatment targeting tumor invasiveness has turned into an aim of priority.

11, 1000 Ljubljana, Slovenia.
E-mail: tamara.lah@nib.si
M.M.P., M.N.O., T.T.L., and H.U. contributed equally to this work.

Published online 15 December 2015 in Wiley Online Library (wileyonlinelibrary.com)
DOI: 10.1002/cyto.a.22800

Mesenchymal stem cells (MSC), subject for investigation of their therapeutic potential in various clinical studies are known to exhibit high tropism (2) toward sites of injury, inflammation, and neoplasms, including GBM cells (3,4) that is mediated by paracrine actions of secreted growth factors, chemokines, cytokines, other peptides, and macromolecules (5). Upon tumor infiltration, MSC become part of the heterogeneous tumor microenvironment and are believed to participate in tumor progression by augmenting stemness of tumor cells, enhancing migration and angiogenesis, and drug resistance, while suppressing immune response resistance (6). However, reports on MSC effects are contradictory as recently reviewed (7) and possibly depend on the tumor type and stage (8). Indeed, the cross-talk between both cells types in the indirect in vitro co-culture model resulted in alterations of expression of over 500 and 300 genes, respectively, in MSC and GBM (9). These are most likely responsible for the impairment of GBM growth and invasion, due to the enhanced expression of cell adhesion-related genes in the GBM cell line. On the other hand, GBM cells inversely affected growth and invasion of MSC, presumably via induced sets of cytokines, as described by Motaln et al. (9) In contrast, in direct co-cultures of these cells in vitro Schichor et al. (10) demonstrated that GBM cells display signs of functional as well as structural syncytium formation with MSC, enabling direct molecular exchange. Altogether, these resulted in enhanced migration of both, GBM cells and MSC, when in direct co-cultures. However, the molecular mechanisms of these interactions have not yet been revealed.

At the same time, recent studies demonstrate the influence of kinin B1 (B1R) and B2 receptors (B2R) on proliferation, chemotaxis, and tumor invasion (11), such as in melanoma (12), bladder cancer (13,14), and glioblastoma (15,16). Sontheimer and coworkers already reported that glioma cells show oscillatory changes in free intracellular calcium concentration $[Ca^{2+}]_i$, as cells migrate and that bradykinin (BK), acting via B2R stimulation caused intracellular $[Ca^{2+}]_i$ transients. Moreover, B2R expression positively correlates with pathological tumor grade in human glioma. Additionally, Guevara-Lora et al. (17) recently reported that the human GBM cell line U373 produced and bound kininogens, synthesized kallikreins, as well as carboxypeptidases M and E, resulting in the production of B1R and B2-activating kinins, affecting cell invasion. Therefore, considering the effects of GBM-MSC interaction and of kinin receptor activation on proliferation, chemotaxis, and tumor invasion of glioma cells, here we investigate whether direct and indirect co-cultures of bone marrow derived MSC with malignant GBM cells U87-MG would affect B1R and B2R expression, as well as consider possible inductions of protease mediated increase in GBM progression and invasion.

Material and Methods

Cell Lines – Mono-cultures

The human glioblastoma cell line U87-MG (ATCC® HTB-14™), was cultured in Dulbecco medium (DMEM, Sigma), 10% fetal bovine serum (FBS), 100 U penicillin, 1,000 U streptomycin, 2 mM L-glutamine, Na-Pyruvate, and non-essential amino acids. Cells were cultured at 37°C, 5% CO_2, and the culture medium was changed every three days. Cells were passaged after reaching 75% confluence and plated for culture maintenance at density of 15,000 cells/cm^2.

The U87-MG dsRed cell line was obtained by permanent pCMV DsRed-Express2 plasmid transfection of U87-MG. At 50% confluence, U87-MG cells were transfected with the circular form of the plasmid using Superfect Transfection Reagent (Qiagen, Valencia, CA) by 3 h preincubation at 37°C, 5% CO_2. Afterwards the transfection mix was removed and upon washing with 1X phosphate-buffered saline (PBS), fresh culture medium was added to the cells. Cells were left to grow for another 24 h, before the addition of 0.8 mg/ml Geneticin into the medium (G418, Gibco, Life Technologies, Grand Island, NY). After 2 weeks of selection, the cells were detached from T25 flasks using 1 mL of trypsin-EDTA solution for 5 min at 37°C. Uniformity of fluorescence staining was verified by flow cytometry. After verification of the best stably transfected U87-MG cell clone (> 99% fluorescent cells), only this was further used in our experimental work.

Human bone marrow mesenchymal stem cells (BM MSC) derived from bone marrow of a healthy volunteer (MSC4) were purchased from Lonza BioScience Walkersville (Walkersville, MD). After resuscitation, cells were plated and grown in the same medium as GBM. Cells were passaged after reaching 75% confluence at a density 7,000 cells/cm^2. MSC of passages 8–11 and U87-MG of passages 40–45 were used in the experiments all performed in culture medium containing 10% of FBS.

Indirect and Direct Cell Co-Cultures

The indirect co-cultures were set up in duplicates using six-well Transwell inserts (Corning Costar, Sigma) with 0.4 μm pore size and the corresponding six-well plate, as described previously (9). When indirectly co-cultured, MSC were always plated in the bottom and U87 were always plated in the insert at the density of 1.5×10^5 cells in 3 ml final volume of media per well and cultured for 72 h. MSC were left to attach for 4 h before adding the inserts with U87 cells. In the case of direct co-cultures, cells were plated into six-well plates at a total amount of 1.5×10^5 cells per well in the final volume of 3 ml and cultured for 72 h. Co-cultured cells were always set up in a 1:1 U87-MG dsRed:MSC cell number ratio.

Determination of Kinin Receptor Gene Expression by qRT-PCR

Total RNA was isolated from three biological replicates of mono-cultured and co-cultured MSC and U87-MG cells using Trizol reagent (Invitrogen Limited, Paisley, Scotland, UK) following the manufacturer's instructions. RNA was column purified with RNAeasy Mini Kit (Qiagen) and their integrity confirmed using the Agilent 2100 Bioanalyzer (Agilent Technologies, Santa Clara, CA). The cDNA was generated from 1 μg of total RNA using the High-Capacity cDNA Reverse Transcription Kit (Applied Biosystems, Hilden, Germany). Relative quantification of gene expression levels of B1R and B2R was done using a real-time PCR system (ABI 7900 HT Sequence Detection System, Applied Biosystems, ThermoFisher, Waltham, MA). Real-time PCR reactions were performed using 1:10 dilutions (1 μl/well) of each cDNA added to TaqMan Universal PCR Master Mix (Applied Biosystems) and TaqMan Gene Expression Assays (all from Applied Biosystems): For B1R-Hs00664201_s1 and for B2R-Hs00176121_m1 probes vs amplification of glyceraldehyde 3-phosphate dehydrogenase (GADPH; Pre-Developed TaqMan Assay Reagent No. 4310884E) probe as internal control. The 1, 1:10, 1:100, 1:1,000, and 1:10,000 dilutions of the template sample were used to allow for relative mRNA quantity determination in the samples. The SDS v2.2 software (Applied Biosystems) was used to analyze the data obtained from TaqMan Gene Expression Assays. Independent experiments were performed in duplicates and repeated three times. Statistical significance between mono-culture and indirect, direct co-cultures was determined by two-tailed Student's t test and a value of $P < 0.05$ was considered significant.

Immunofluorescence Studies

For immunofluorescence analyses of these mono-cultures of MSC and U87dsRed cells as well as co-cultures (1:1 ratio) were set up. Upon 72 h in co-cultures cells were fixed with 4% paraformaldehyde (PFA) in PBS for 15 min, washed three times and exposed for 30 min to a blocking solution containing 0.05% Triton-X 100 and 2% FBS. Cells were incubated overnight at 4°C with primary rabbit anti-human antibodies against B1R receptors (1:100, Abcam). Samples were washed three times with PBS, followed by incubation for 1 h with Alexa Fluor (AF) 488 goat anti-rabbit (1:800, Sigma). In control experiments, the primary antibody was omitted and immunostaining was never observed. Counterstaining of cell nuclei was done with 0.1% of 49,6-diamidino-2-phenylindole (DAPI). Following another washing step, slides were mounted with Vectashield (Vector Laboratories, Burlingame, CA) and analyzed on an Axiovert 200 epifluorescence microscope (Zeiss, Aalen, Germany), equipped with a Nikon DMX1200F camera and Metamorph image analysis program (Nikon, Melville, NY). ds-Red fluorescence emission was determined with a 605/70 nm bandpass filter. Alexa Fluor 488 and dsRed images were merged for detection of B1R expression in co-cultured U87-MG and MSC cells.

Flow Cytometry Analysis

When cells were plated into six-well plates as described above for direct culturing, at the 1:1 ratio (direct culture mix) in the sum amount 3×10^5, cells were detached from wells using 0.25% trypsin (1 ml; Gibco-Life Technologies, São Paulo, Brazil) for 5 min at 37°C and mechanically dissociated to a single cell suspension after FBS addition (0.5 ml). Cells were passed through a 40 μm cell strainer, centrifuged, then fixed for 20 min in 4% paraformaldehyde (PFA) at room temperature (RT), washed with PBS supplemented with 2% FBS, and incubated for 30 min at RT with mouse anti-B2R (1:100; BD Biosciences) and rabbit anti-B1R (1:100; Abcam) primary antibodies in PBS plus 0.1% Triton X-100 and 2% FBS. After washing with 900 μl of PBS plus 2% FBS, the secondary anti-mouse antibodies conjugated with Alexa Fluor (AF) 647 and anti-rabbit conjugated antibodies with AF 488 (both at 1:500 dilutions; Life Technologies) were added and incubated for 30 min at RT (18,19). After a final washing step, the cells were re-suspended in 400 μl of PBS and analyzed on a flow cytometer (BD Accuri C6, BD Biosciences). Thirty-thousand events were acquired per sample and data were displayed on logarithmic scales. Forward and side light scatter signals were used to exclude dead cells and debris. Kinin receptor-positive cells were determined as the percentage of cells stained positive out of total cells in each cell type. Data were analyzed using the FlowJo V10 software (Ashland, OR). MSC and U87-MG cells in absence of primary antibodies were used to assess the signal background (0.1%) and determine gate boundaries.

For detecting matrix metalloproteases-2 (MMP2) and matrix metalloproteases-9 (MMP9) protein expression with flow cytometry, MSC and U87-MG co-cultures were collected on Day 3 of co-culture by trypsinization and precipitated. Pelleted cells were washed in 1% PBS and fixed in 0.5% glutaraldehyde/PBS for 20 min. Permeabilization was performed for 30 min in 0.1% Triton X-100/PBS. Primary antibody diluted in 1% PBS (1:20 for mouse anti-human MMP2, and for rabbit anti-human MMP9 in 1:100 dilution, both Abcam) added and incubated for 30 min at 4°C. After washing with 900 μl of PBS, the anti-rabbit or anti-mouse secondary antibodies conjugated with AF 488 (1:300 dilution; Life Technologies) were added and incubated for 30 min at 4°C. After a final washing step, the cells were re-suspended in 400 μl of PBS and analyzed on a flow cytometer (BD FACSCalibur, BD Biosciences). Ten-thousand events were acquired per sample and data were displayed on logarithmic scales. Forward and side light scatter signals were used to exclude dead cells and debris. MMP2 and MMP9 positive cells were determined as the percentage of cells stained positive out of total cells in each cell type. Controls were conducted in absence of primary antibodies to assess signal background and determine gate boundaries. Data were analyzed using the BD CellQuest Pro software (Becton & Dickinson, Franklin Lakes, NJ). More details are given in the Supporting Information MIFlowCyt checklist.

Calcium Imaging

87-MG and human MSCs cells were seeded into 24 wells cell culture dish. Tumor cells were allowed to attach for 4 h to dish surfaces before adding MSC for indirect co-culture for

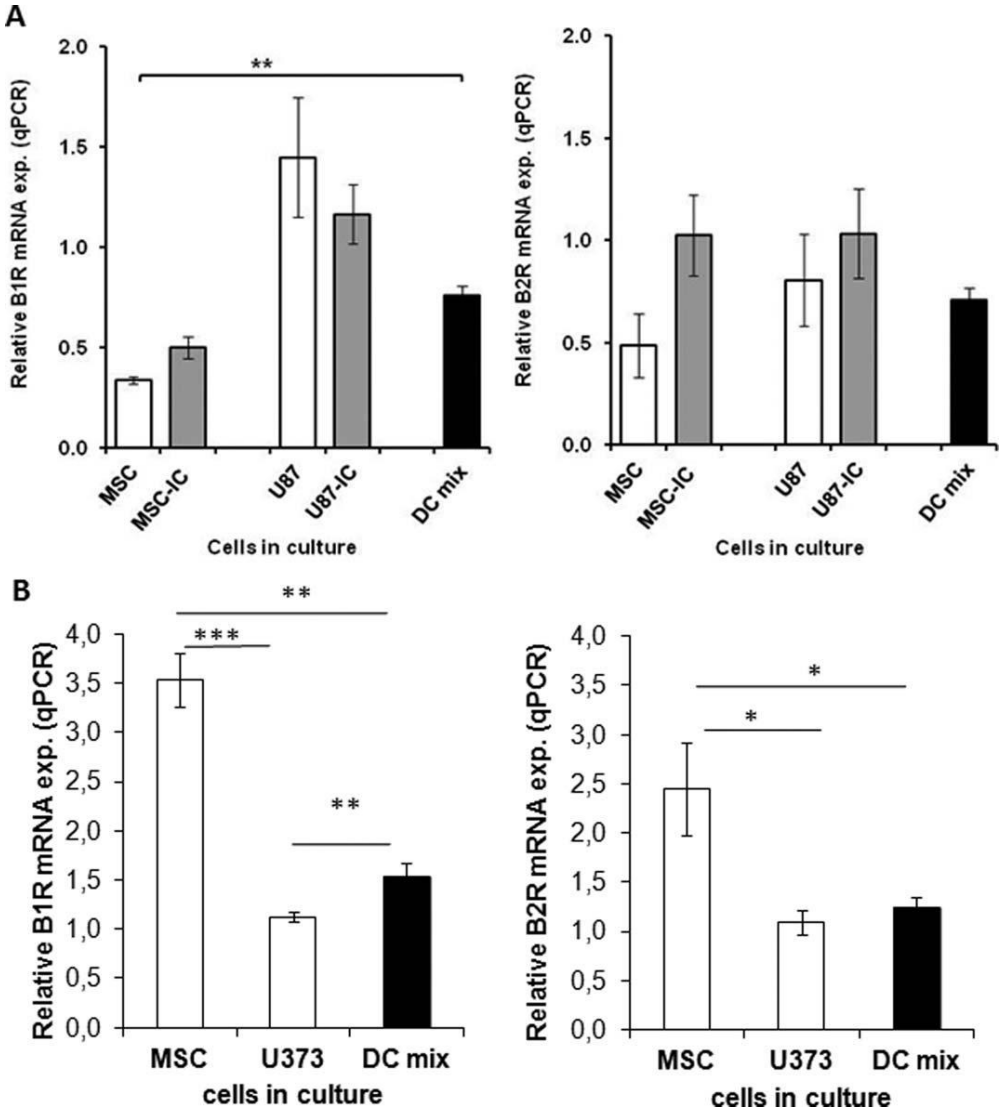

Figure 1. B1R and B2R gene expression in U87-GBM and MSC mono and co-cultures. Real time RT-PCR analysis of B1R mRNA (left panel) and B2R mRNA (right panel) levels in MSC and U87-MG cells, when in indirect co-cultures (IC) with the other cell type. In the direct co-cultures (DC), e.g. culture mix, expression levels of B1R (left panel) and B2R (right panel) are also shown, as the last column on the left in both panels. Prior to analysis, co-cultured cells were grown together for 72 h, as described in Material and Methods. The experiments were performed in triplicates, the error bars represent standard errors of the mean, $^{**}P < 0.01$ were considered as statistically significant differences between the expression rates.

24 h at a density of 16.8 cells/cm^2. For direct co-cultures, the mix of MSC and U87-MG cells (1:1 ratio) were seeded and cultured for 24 h. Prior to calcium imaging, the cells were washed with PBS and loaded with 5 μM of Fluo3-AM for 45 min at 37°C in serum-free medium containing 0.5% Me2SO and 0.06% of the nonionic surfactant pluronic acid F-127 (Sigma), as published previously (19–21). Cells were rinsed with serum-free medium and equilibrated in the chamber for 15 min before capturing calcium images using the Nikon fluorescence imaging microscope (ECLIPSE-TiS) (Nikon) equipped with a 14 bit high-resolution CCD camera CoolSNAP HQ2 (Photometrics, Tucson, AZ) and analyzed with the NISElement software (Nikon). Fluorescence excitation was done with a xenon lamp at 488 nm and the light emission was collected at 515–530 nm using a bandpass filter. Calcium concentration ($[Ca^{2+}]_i$) levels were recorded for 3 min at 1 frame/sec. Following imaging of resting cells, cells were stimulated by 1 μM bradykinin (BK) or des-Arg^9-bradykinin (DBK). The traces shown are average variations over time of at least 20 single cells. Calcium imaging of co-cultures of dsRed-U87 cells was performed with the Leica TCS STED 3X confocal microscope (Leica, Wetzlar, Germany), using the 488 nm argon and 543 nm helium neon laser lines for Fluo-3AM and dsRed excitation, respectively.

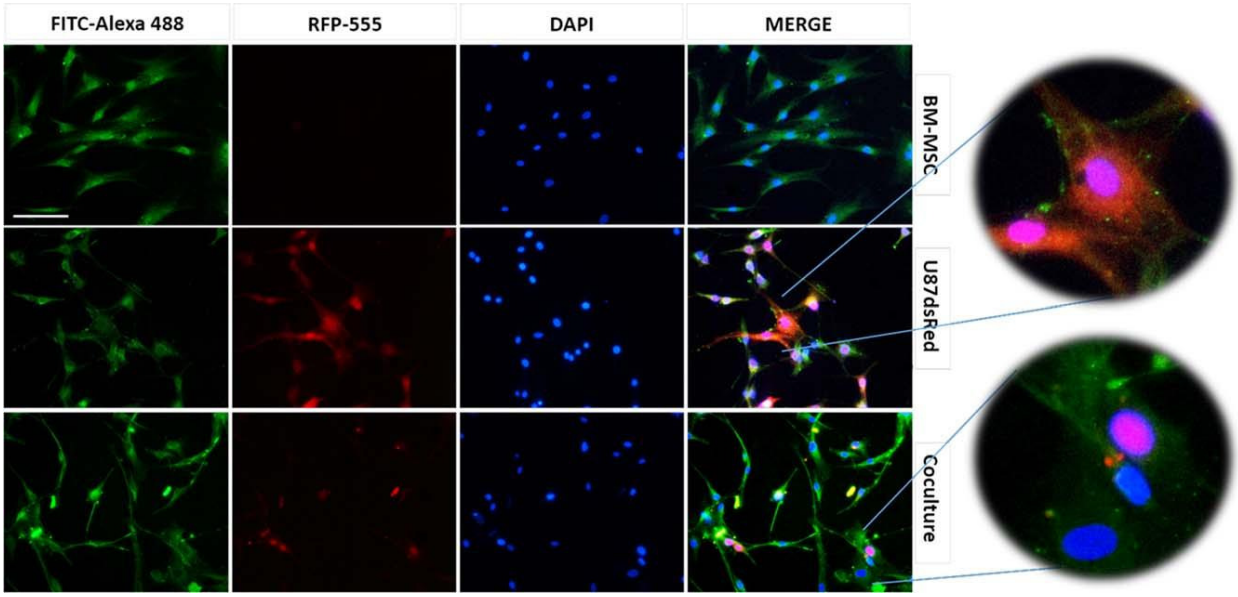

Figure 2. Immunofluorescence labelling of B1 receptor protein expression in mono cultures and direct co-cultures of MSC and U87-MGdsRed cells. Immunofluorescence labelling of MSC and U87-MGdsRed cells in mono- and direct co-cultures was performed after 72 h of mono- or co-culture on poly-L-lysine coated Lab Tek Chamber slides, cells were labelled with primary mouse anti-human B1R antibodies in 1:100 dilution and secondary Alexa Fluor 488 antibodies in 1:200 dilution (green). Counterstaining for cell nuclei was performed with DAPI (blue). U87-MGdsRed cells are visualized in red (RFP-555). Images were taken with the inverted microscope ECLIPSE-TiS (Nikon, Melville, NY) using a 20 X objective (Scale 50 μm).

Statistical Analysis

Statistical comparisons between different conditions were done by either a Student's *t* test or one-way analysis of variance (ANOVA) with Bonferroni *post hoc* test by using GraphPad Prism 5.1 software (Graph-Pad Software, La Jolla, CA). The results were expressed as mean values ± standard deviation (SD) from three or more independent experiments. For flow cytometry, a minimum of 10,000 cells was analyzed per sample. Traces of calcium responses are representative for 20 individual imaged cells. The criteria for statistical significance were set at $^{*}P < 0.05$ and $^{**}P < 0.01$.

Results

Kinin Receptor Gene and Protein Expression Levels in Mono- and Co-Cultures of GBM and MSC

Kinin receptors are expressed by tumor cells, where they are believed to be involved in regulation of proliferation, invasiveness and immunomodulation. MSC and U87-GBM cell interactions have lately drawn attention, since tumor cell features, including proliferation and invasiveness, are changed under these conditions. Transfection with pCMV-dsRed-Express2 plasmids was done for fluorescence-tracking of U87-MG dsRed labeled cells in direct co-cultures. Image and flow cytometry analyses revealed that 99% of transfected U87-MG cells expressed dsRed (data not shown). Gene expression levels of B1R and B2R were determined in mono-cultures as well as in indirect and direct co-cultures of U87-MG and MSC. As shown in Figure 1A, expression level of B1R was increased in MSC, whereas it was decreased in U87-MG dsRed cells. B2R expression rates were increased in both cell types upon indirect co-cultures of GBM-MSC (Fig. 1B). The resulting mRNA levels of both cell types in direct contact were intermediate, not allowing to distinguish between contribution rates of U87-MG cells and MSC.

The presence of B1R was confirmed by immunofluorescence studies, pointing at increased expression in conditions of co-cultures. The overlay of dsRed expression of U87 fluorescence images and DAPI stained co-cultures with anti-B1R Alexa 488-immunofluorescence revealed that B1R are expressed by both cell lines in conditions of direct co-cultures (Fig. 2).

In the following, flow cytometry analysis was employed to quantify relative expression levels and cell populations expressing kinin receptor subtypes (Fig. 3). The data corroborate mRNA expression rates of B1 and B2 receptors in MSC and U87-MGdsRed cells, with B1R being expressed by a higher percentage of cells than B2R. Indirect co-cultures resulted in an increase of the percentages of B1R and B2R positive cells. Direct co-cultures resulted in an increase of the percentages U87-MG DsRed cells expressing B1 and B2 receptors, whereas the number of MSC expressing these receptors decreased at the same time, as revealed by representative flow cytometry dot-blots (Fig. 3A) and statistical analysis of three independent performed experiments (Fig. 3B). Moreover, mean expression levels of B1R and B2R were estimated by mean fluorescence intensity (MFI; Fig. 3C). The MFI results were similar to percentages of positive cells.

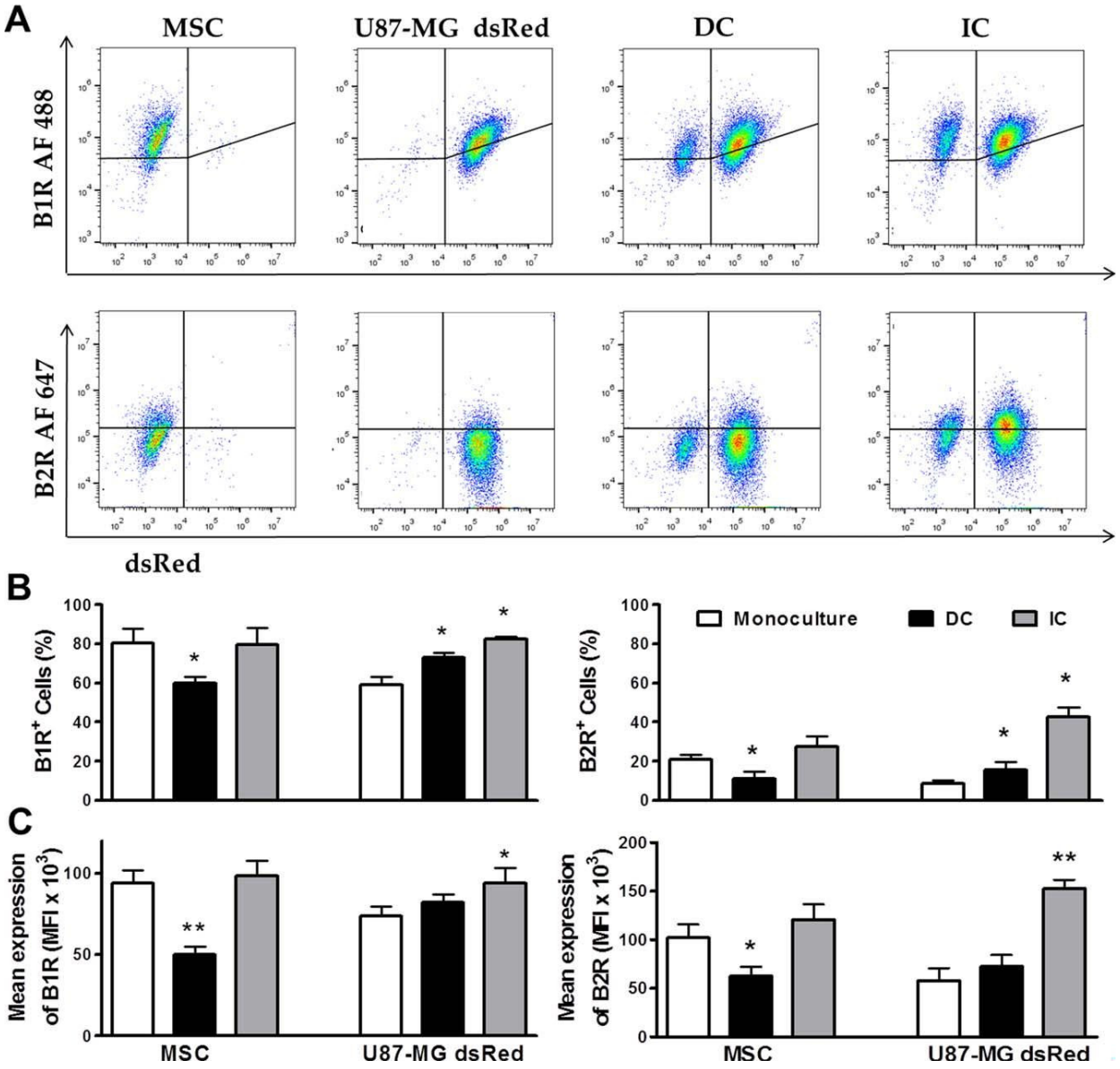

Figure 3. Flow cytometry analysis of B1R and B2R expression in mono-cultures, indirect and direct cell co-cultures of MSC and U87-MG dsRED cells. (**A**) B1R and B2R expression in U87-MG dsRed and MSC grown as mono- indirect (IC) and direct (DC) co-cultures for 72 h was determined by flow cytometry, as described in the Methods section. Cells samples were labelled with anti-B1R (AF 488 fluorophore) and anti-B2R (Alexa Fluor (AF) 647 fluorophore) antibodies and analyzed by flow cytometry. Representative dot-plots are shown. (**B**) Quantifications of $B1R^+$ and $B2R^+$ MSC and U87-MGdsRed cells. (**C**) Mean expression levels ± SEM of B1R and B2R were estimated by mean fluorescence intensity (MFI) for each sample. Sixty-thousand events were acquired for each example and analyzed with the Flowjo V10 software. Data are representative of three independent experiments and shown as mean ± SD (*$P < 0.05$; **$P < 0.01$). [Color figure can be viewed in the online issue, which is available at wileyonlinelibrary.com.]

MMP2 and MMP9 Protein Expression in Mono- and Co-Cultures of GBM and MSC

As matrix metalloproteases (MMPs) are crucial for extracellular matrix degradation and thus GBM invasion, we examined the protein expression levels of two MMPs, MMP2 and MMP9, also named gelatinases A and B, respectively in mono-cultures and in direct co-cultures of U87-MG and MSC using flow cytometry, as described in Material and Methods. We observed that in U87-MG cells, the level of MMP2 expression was not altered (Fig. 4A), while the MMP9 expression was significantly increased in U87 cells upon direct co-culturing with MSC at 1:1 ratio (Fig. 4B). In contrast, expression levels of both, MMP2 and MMP9, decreased in MSC after direct co-culturing with U87-MG for 72 h, compared to mono-cultures.

Functional Validation of B1 and B2 Receptors

The functionality of kinin receptors was determined by calcium imaging of cells stimulated with the DBK and BK as

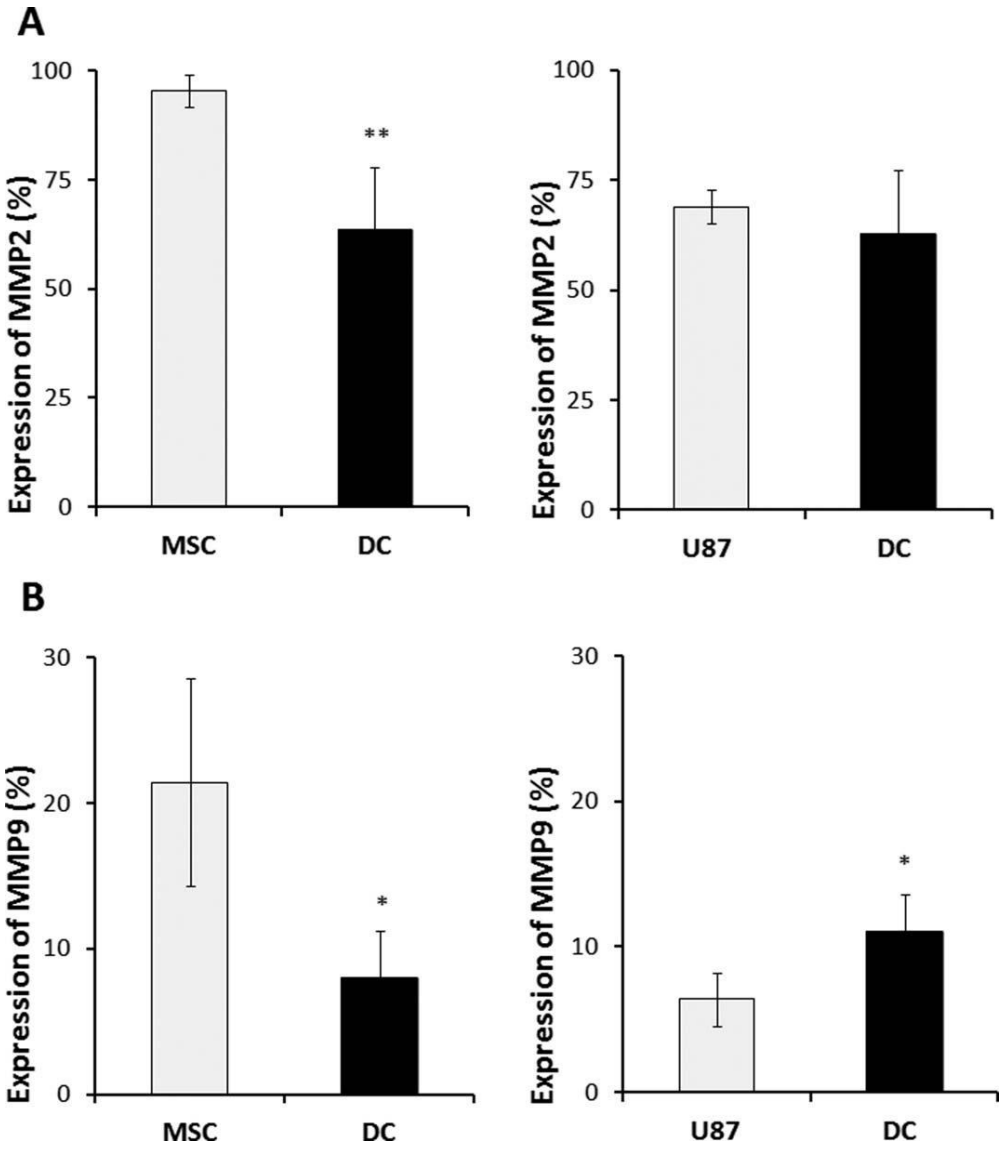

Figure 4. MMP2 and MMP9 expression in mono-culture and direct cell co-cultures. MMP2 and MMP9 expression in U87-MG dsRed and MSC grown for 72 h mono- and direct co-cultures (DC) in 1:1 ratio was determined by flow cytometry, as described in the Methods section. Cells samples were labelled with (**A**) anti-MMP2 Alexa Fluor (AF) 488 fluorophore antibody (mouse antihuman, Abcam) and (**B**) anti-MMP9 Alexa Fluor (AF) 488 fluorophore antibody (rabbit antihuman, Abcam). Ten-thousand events were acquired and analyzed with the FlowJo V10 software (Ashland, OR). Data are representative of three independent experiments and are shown as mean of $MMP2^+$ and $MMP9^+$ cells ± SD ($*P < 0.05$, $**P < 0.01$).

selective agonists of B1R and B2R, respectively (Fig. 5). B1R and B2R activities were noted in both, U87-MG dsRed and MSC, as well under indirect and direct co-culture conditions, demonstrating that kinins can participate in various signaling pathways in both cell types. Interestingly, the indirect or direct interaction between MSC and U87-MG dsRed cells changes magnitude of B1 and B2 receptors-mediated responses in both cell types, suggesting their involvement in GBM and MSC communication.

Previously published data obtained with an embryonal carcinoma cell line showed that B2R functionality is regulated under conditions of long term, mimicking chronic modulation of receptor activity (22). In view of that, we studied the effects of chronic, long term, chronic bradykinin treatments for 72 h on B1 and B2 receptors expression levels in mono-cultures and co-cultures of U87-MG dsRed cells and MSC. BK treatment diminished in a negative feedback–like reaction the percentage of B1 and B2 receptors-positive MSC in mono-culture and in indirect and direct co-cultures (Fig. 6A and B), while U87-MGdsRed cells increased by positive feedback the number of B1R-and B2R-expressing cells under conditions of indirect and direct co-cultures (Fig. 6C and 6D). It is important to note that these effects of BK treatment are similar to

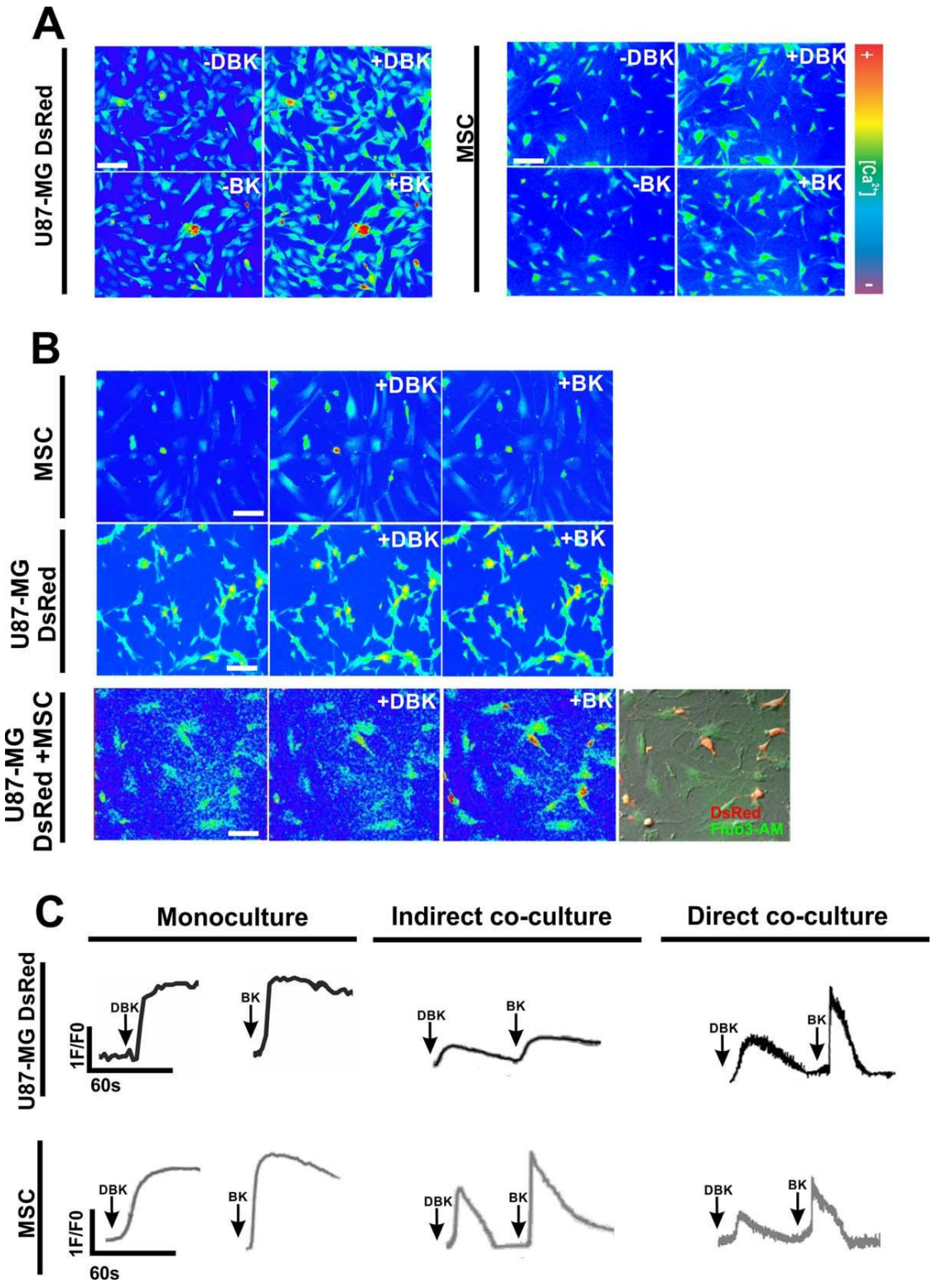

Figure 5. Elevations in free intracellular concentrations ($[Ca^{2+}]_i$) in MSC and U87-MG dsRed glioma cells in mono and co-culture, mediated through B1 and B2 receptors activation. Prior to calcium imaging, cells were loaded with the Ca^{2+}-sensitive fluorophore indicator Fluo-3AM. Non-stimulated cells were imaged for obtaining basal fluorescence values, followed by addition of 1 μM final concentration of des-Arg^9-bradykinin (DBK) or bradykinin (BK). Cells were rinsed with culture medium between DBK and BK administration. $[Ca^{2+}]_i$ levels at 1 frame/sec were recorded for 3 min and representative images of non-stimulated cells and cells following 10 s of ligand application are shown with (**A**) cells in mono-culture, (**B**) direct co-culture, showing stimulation levels of bone-marrow MSC and U87-MG dsRed glioma cells (upper and middle panels) and co-cultures of U87-MG dsRed cells with MSC (lower panel). Calcium imaging was performed with the Inverted Research Microscope ECLIPSE-TiS (Nikon, Melville, NY) equipped with a 14 bit high-resolution CCD camera CoolSNAP HQ2, except for the images obtained for direct co-cultures, which were obtained with a confocal microscope (Leica TCS SP8). Merges of dsRed and Fluo-3AM fluorescence levels were used for determination of the fraction of glioma cells responding to kinin receptor activation. (**C**) Kinetics of kinin receptor-induced $[Ca^{2+}]_i$ transients. The shown data are average responses of 20 cells. Scale bar = 50 μm.

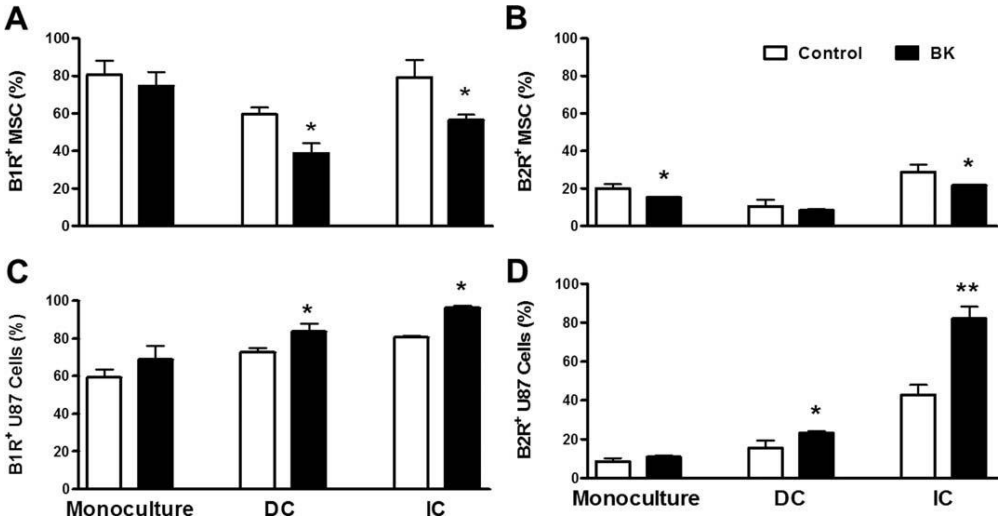

Figure 6. Effects of chronic bradykinin exposure on B1 and B2 receptor expression in mono-cultures, direct and indirect co-cultures of MSC and U87-MG dsRed cells. MSC and U87-MG dsRed cells were grown in absence (control) or presence of bradykinin (BK; 1 μM) in mono-cultures, direct (DC) or indirect (IC) cell co-cultures for 72 h. Cell samples were immune labelled with anti-B1R and anti-B2R antibodies and analyzed by flow cytometry. Mean percentages of (**A**) B1R and (**B**) B2R of MSC cultured in the absence (control) or presence of BK is presented. Mean percentages of (**C**) B1R and (**D**) B2R of U87dsRed cells in mono-cultures, indirect cultures (IC), and direct cultures (DC) for 72 h. Sixty-thousand events were acquired and the results were analyzed with the FlowJo V10 software. Data are representative of three independent experiments and are shown as mean values ± SD (*$P < 0.05$).

those observed with GBM:MSC co-cultures, suggesting its involvement in information flow (chemical messenger) between these cells.

In summary, our results indicate an increase of kinin receptor expression in GBM U87-MG cells when in co-culture with MSC, which is accompanied by a decrease of the percentage of MSC, expressing these receptors. Kinin receptor expression levels are yet enhanced under conditions of chronic exposure to bradykinin.

Discussion

Although kinin receptors in brain tumors have been studied mostly with respect to their physiological functions to possibly raise blood-tumor-barrier permeability (23) and affect angiogenesis (24,25), here we focused on their impact on glioblastoma (GBM) cell invasion. In vivo studies on kinin B1 (B1R) and B2 receptors (B2R) revealed that B2R was increasingly expressed with augmenting malignancy of glioma (16) and GBM cells (26). Reportedly, B1R was not relevant for GBM cell invasion (15); however, B1R expression upregulation in GBM cells was confirmed by Lu et al. (27). In GBM tissue, B1R expression may be induced by high levels of inflammatory cytokines produced by tumor infiltrating immune cells (28). Here, we are showing that both B2R and B1R are expressed in GBM U87-MG cells in vitro at mRNA and protein levels (Figs. 1–3). This is in accordance with recent results published by Lu et al. (27), demonstrating that two human GBM cell lines U-138-MG and U-251-MG express functional B1R and B2R. They showed that proliferative effects were induced by incubation with DBK and BK. These effects were most likely mediated by activation of phosphatidylinositol 3 kinase (PI3) Akt and extracellular signal-regulated kinases (ERK) pathways (29). Kinin receptor-modulated proliferation was also observed for microglial cells (30) as well as for bladder carcinoma (14) and other cancers (25).

Co-culturing of GBM cells with MSC, mimicking in vivo MSC tropism, and direct cellular cross-talk altered GBM invasion (10). The key finding of our present results is that indirect and direct effects of MSC on GBM U87-MG cells were associated with increased expression levels of both, B1 and B2 receptors, possibly triggering increased invasiveness. By the same token, increased levels of kinin receptor expression would not support previously observed inhibition of invasion of GBM cells in indirect interactions with MSC (9). With respect to the underlying mechanism, Montana and Sontheimer (16) showed that bradykinin via B2R-induced $[Ca^{2+}]_i$ transients enhanced and directed invasion of glioma cells toward blood vessels. Moreover, Seifert and Sontheimer (15) recently revealed that bradykinin through $[Ca^{2+}]_i$ transients in GBM cells in vitro induced the formation of small bleb-like protrusions at the plasma membrane, which stimulated an amoeboid phenotype of cell migration.

As a consequence of direct co-culturing and in parallel to enhanced B2 and B1 receptor expression, expression of metalloprotease MMP9, but not MMP2, was increased in U87-MG cells. This was not surprising, as the same was described by Hsieh et al. (31), showing that BK induced MMP9 expression and enhanced cell migration via a PKC-delta-dependent ERK/Elk-1 pathway in astrocytes. This pathway (32,33) and/or alternative possibilities, such as induction of reactive oxygen

species (ROS)-dependent pathways, were also shown in brain astrocytes (34). Furthermore, trans-activation of epidermal growth factor receptors (25,35,36), known to be often amplified in its expression rates or mutated in GBM cells, may play a role in the protease cascade activation, where MMP9 is pivotal in modifying extracellular matrix proteins (32,37). Taken together, we hypothesize that kinin receptor expression induction upon direct co-culture with MSC induced calcium influx, possibly promoting MMP9 production in tumor cells. This suggests a possible role of bradykinin as extracellular messenger in communication between MSC and U87-MG cells, triggering changes in the kinin receptors' expression and also tumor cell migration in vivo.

A possible role for bradykinin as extracellular messenger in glioblastoma is supported by previously collected evidence. Guevara-Lora et al. (17) showed that kininogen and kallikreins are indeed expressed by GBM cells, such as shown for the U373 cell line. High molecular weight kininogen (HMWK) is the precursor of bradykinin. The strong binding of kininogen to the cell surface and the enzymatic degradation of this protein by cells and their secreted proteases (kallikreins and plasmin) suggest the activation of kinin-generating systems. The tissue kallikrein protein is expressed in several tumors, where it was shown to be involved in metastasis and invasion (38–40). Likewise, MSC were shown previously to express and secrete interleukin (IL)−1β and tumor necrosis factor (TNF)-α cytokines, which have strong relationships with angiogenesis and the kallikrein–kinin system (17).

The kallikrein–kinin system has not been investigated at molecular levels so far, and to our knowledge, this is the first demonstration that bone marrow-derived MSC constitutively express functional B1 and B2 receptors. Srivastava et al. (41) showed that BK inhibits the migration of these cells, but did not affect their viability. Here we show that upon direct or indirect co-culture expression levels of both receptors were down regulated or not altered in MSC.

However, these data are not in line with increased MSC cell invasion observed in both types of co-culturing, but may be explained by GBM cells inducing an alternative signaling pathway to enhance MSC invasion via some of the numerous molecular messengers comprising GBM:MSC cellular cross-talk (9) and counterbalancing potential kinin receptor promotion of invasion. The importance of the kallikrein–kinin system in MSC, given regarding its therapeutic effects in regenerative medicine (42), will need to be further studied by using pharmacological inhibition studies and/or receptor expression down-regulation or knock-out constructs.

In conclusion, here we have shown that GBM cells express functional B1R and B2R genes and proteins that can be further activated under the influence of indirect and direct cellular cross-talk with MSC. It is suggested that kinin receptor-mediated downstream signaling, that in direct co-cultures may affect expression of MMP9, known as the key enzyme in pericellular proteolytic cascades favors GBM cell invasion. Possible mechanisms, including the participation of extracellular vesicles for the intercellular transport of molecular and oncogenic signatures (43), need further investigations.

Acknowledgements

M.O. and M.M.P. acknowledge fellowship support from CNPq. T.T.L. is visiting professor within the Science without Borders Program of the CNPq. M.O. is recipient of a sandwich doctorate fellowship for performing part of her Ph.D. theses at the National Institute of Biology at the University of Ljubljana. T.G.'s doctoral thesis research is supported by FAPESP.

Literature Cited

1. Stupp R, Mason WP, van den Bent MJ, et al. Radiotherapy plus concomitant and adjuvant temozolomide for glioblastoma. N Engl J Med 2005;352:987–996.
2. Nery AA, Nascimento IC, Glaser T, Bassaneze V, Krieger JE, Ulrich H. Human mesenchymal stem cells: From immunophenotyping by flow cytometry to clinical applications. Cytometry Part A 2013;83A:48–61.
3. Grisendi G, Bussolari R, Veronesi E, Piccinno S, Burns JS, De Santis G, Loschi P, Pignatti M, Di Benedetto F, Ballarin R, et al. Understanding tumor-stroma interplays for targeted therapies by armed mesenchymal stromal progenitors: The mesenkillers. Am J Cancer Res 2011;1:787–805.
4. Kim SM, Lim JY, Park SI, Yang HG, Kang MC, Choi YW, Kim SM, Jeun SS, Sung YC. Gene therapy using TRAIL-secreting human umbilical cord blood-derived mesenchymal stem cells against intracranial glioma. Cancer Res 2008;68:9614–9623.
5. Yagi H, Kitagawa Y. The role of mesenchymal stem cells in cancer development. Front Genet 2013;4:261
6. Guan J, Chen J. Mesenchymal stem cells in the tumor microenvironment. Biomed Rep 2013;1:517–521.
7. Motaln H, Turnsek TL. Cytokines play a key role in communication between mesenchymal stem cells and brain cancer cells. Protein Pept Lett 2015;22:322–331.
8. Motaln H, Schichor C, Lah TT. Human mesenchymal stem cells and their use in cell-based therapies. Cancer 2010;116:2519–2530.
9. Motaln H, Gruden K, Hren M, Schichor C, Primon M, Rotter A, Lah TT. Human mesenchymal stem cells exploit the immune response mediating chemokines to impact the phenotype of glioblastoma. Cell Transplant 2012;21:1529–1545.
10. Schichor C, Albrecht V, Korte B, Buchner A, Riesenberg R, Mysliwietz J, Paron I, Motaln H, Turnšek TL, Jürchott K, Selbig J, Tonn JC. Mesenchymal stem cells and glioma cells form a structural as well as a functional syncytium in vitro. Exp Neurol 2012;234:208–219.
11. Molina L, Matus CE, Astroza A, Pavicic F, Tapia E, Toledo C, Perez JA, Nualart F, Gonzalez CB, Burgos RA, Figueroa CD, Ehrenfeld P, Poblete MT. Stimulation of the bradykinin B(1) receptor induces the proliferation of estrogen-sensitive breast cancer cells and activates the ERK1/2 signaling pathway. Breast Cancer Res Treat 2009;118:499–510.
12. Dillenburg-Pilla P, Maria AG, Reis RI, Floriano EM, Pereira CD, De Lucca FL, Ramos SG, Pesquero JB, Jasiulionis MG, Costa-Neto CM. Activation of the kinin B1 receptor attenuates melanoma tumor growth and metastasis. PLoS One 2013;8:e64453.
13. Baba K, Yamaguchi O. Effects of bradykinin on cytoplasmic calcium and motility in murine bladder tumor cells. J Urol 2001;165:259–262.
14. Sgnaolin V, Pereira TCB, Bogo MR, Zanin R, Battastini AM, Morrone FB, Campos MM. Functional and molecular characterization of kinin B1 and B2 receptors in human bladder cancer: Implication of the PI3Kγ pathway. Invest New Drugs 2013;31:812–822.
15. Seifert S, Sontheimer H. Bradykinin enhances invasion of malignant glioma into the brain parenchyma by inducing cells to undergo amoeboid migration. J Physiol 2014;592:5109–5127.
16. Montana V, Sontheimer H. Bradykinin promotes the chemotactic invasion of primary brain tumors. J Neurosci 2011;31:4858–4867.
17. Guevara-Lora I, Blonska B, Faussner A, Kozik A. Kinin-generating cellular model obtained from human glioblastoma cell line U-373. Acta Biochim Pol 2013;60:299–305.
18. Pillat MM, Cheffer A, de Andrade CM, Morsch VM, Schetinger MR, Ulrich H. Autoregulation of bradykinin receptors: agonists in the presence of interleukin-1beta shift the repertoire of receptor subtypes from B2 to B1 in human lung fibroblasts. Cytometry Part A 2015;87A:929–935.
19. Nascimento IC, Glaser T, Nery AA, Pillat MM, Pesquero JB, Ulrich H. Kinin-B1 and B2 receptor activity in proliferation and neural phenotype determination of mouse embryonic stem cells. Cytometry Part A 2015;87A:989–1000.
20. Montiel-Eulefi E, Nery Aa, Rodrigues LC, Sánchez R, Romero F, Ulrich H. Neural differentiation of rat aorta pericyte cells. Cytometry Part A 2012;81A:65–71.
21. Glaser T, de Oliveira SL1, Cheffer A, Beco R, Martins P, Fornazari M, Lameu C, Junior HM, Coutinho-Silva R, Ulrich H. Modulation of mouse embryonic stem cell proliferation and neural differentiation by the P2X7 receptor. PLoS One 2014;9:e9628.
22. Martins AH, Resende RR, Majumder P, Faria M, Casarini DE, Tárnok A, Colli W, Pesquero JB, Ulrich H. Neuronal differentiation of P19 embryonal carcinoma cells modulates kinin B2 receptor gene expression and function. J Biol Chem 2005;280:19576–19586.
23. Wang YB, Peng C, Liu YH. Low dose of bradykinin selectively increases intracellular calcium in glioma cells. J Neurol Sci 2007;258:44–51.
24. Figueroa CD, Ehrenfeld P, Bhoola KD. Kinin receptors as targets for cancer therapy. Expert Opin Ther Targets 2012;16:299–312.

25. da Costa PLN, Sirois P, Tannock IF, Chammas R. The role of kinin receptors in cancer and therapeutic opportunities. Cancer Lett 2014;345:27–38.
26. Côté J, Bovenzi V, Savard M, Dubuc C, Fortier A, Neugebauer W, Tremblay L, Müller-Esterl W, Tsanaclis AM, Lepage M, et al. Induction of selective blood-tumor barrier permeability and macromolecular transport by a biostable kinin B1 receptor agonist in a glioma rat model. PLoS One 2012;7:e37485.
27. Lu DY, Leung YM, Huang SM, Wong KL. Bradykinin-induced cell migration and COX-2 production mediated by the bradykinin B1 receptor in glioma cells. J Cell Biochem 2010;110:141–150.
28. Phagoo S, Poole Leeb-Lunder LMF. Autoregulation of bradykinin receptors: agonists in the presence of interleukin-1beta shift the repertoire of receptor subtypes from B2 to B1 in human lung fibroblasts. Mol Pharmacol 1999;56:325–333.
29. Nicoletti NF, Erig TC, Zanin RF, Pereira TC, Bogo MR, Campos MM, Morrone FB. Mechanisms involved in kinin-induced glioma cells proliferation: The role of ERK1/2 and PI3K/Akt pathways. J Neurooncol 2014;120:235–244.
30. Ifuku M, Färber K, Okuno Y, Yamakawa Y, Miyamoto T, Nolte C, Merrino VF, Kita S, Iwamoto T, Komuro I, Wang B, Cheung G, Ishikawa E, Ooboshi H, Bader M, Wada K, Kettenmann H, Noda M. Bradykinin-induced microglial migration mediated by B1-bradykinin receptors depends on Ca2+ influx via reverse-mode activity of the Na+/Ca2+ exchanger. J Neurosci 2007;27:13065–13073.
31. Hsieh HL, Wu CY, Yang CM. Bradykinin induces matrix metalloproteinase-9 expression and cell migration through a PKC-delta-dependent ERK/Elk-1 pathway in astrocytes. Glia 2008;56:619–623.
32. López-Otín C, Matrisian LM. Emerging roles of proteases in tumor suppression. Nat Rev Cancer. 2007;7:800–808.
33. Maeda H, Wu J, Okamoto T, Maruo K, Akaike T. Kallikrein–kinin in infection and cancer. Immunopharmacology 1999;43:115–128.
34. Lin CC, Hsieh HL, Shih RH, Chi PL, Cheng SE, Chen JC, Yang CM. NADPH oxidase 2-derived reactive oxygen species signal contributes to bradykinin-induced matrix metalloproteinase-9 expression and cell migration in brain astrocytes. Cell Commun Signal 2012;10:35.
35. Toledo C, Matus CE, Barraza X, Arroyo P, Ehrenfeld P, Figueroa CD, Bhoola KD, Del Pozo M, Poblete MT. Expression of HER2 and bradykinin B_1 receptors in precursor lesions of gallbladder carcinoma. World J Gastroenterol 2012;18:1208–1215.
36. Levicar N, Nuttall RK, Lah TT. Proteases in brain tumor progression. Acta Neurochir (Wien) 2003;145:825–838.
37. Lah TT, Durán Alonso MB, Van Noorden CJ. Antiprotease therapy in cancer: Hot or not? Expert Opin Biol Ther 2006;6:257–279.
38. Obiezua CV, Diamandis EP. Human tissue kallikrein gene family: Applications in cancer. Cancer Letters 2005;224:1–22.
39. Borgoño CA, Michael IP, Diamandis EP. Human tissue kallikreins: Physiologic roles and applications in cancer. Mol Cancer Res 2004;2:257–280.
40. Chee J, Naran A, Misso NL, Thompson PJ, Bhoola KD. Expression of tissue and plasma kallikreins and kinin B1 and B2 receptors in lung cancer. Biol Chem 2008; 389:1225–1233.
41. Srivastava S, Sharma K, Kumar N, Roy P. Bradykinin regulates osteoblast differentiation by Akt/ERK/NFκB signaling axis. J Cell Physiol 2014;229: 2088–2105.
42. Chao J, Bledsoe G, Chao L. Kallikrein–kinin in stem cell therapy. World J Stem Cells 2014;6:448–457.
43. Nakano I, Garnier D, Minata M, Rak J. Extracellular vesicles in the biology of brain tumor stem cells–Implications for inter-cellular communication, therapy and biomarker development. Semin Cell Dev Biol 2015;40:17–26.

Chapter 3

Kinin-B1 Receptor Stimulation Promotes Invasion and is Involved in Cell-Cell Interaction of Co-Cultured Glioblastoma and Mesenchymal Stem Cells

Mona Oliveira, Helena Motaln, Micheli Pillat, Henning Ulrich, Tamara Lah

Reproduced from Scientific Reports. Accepted: December 21, 2017, published on January 18, 2018

SCIENTIFIC REPORTS

OPEN

Kinin-B1 Receptor Stimulation Promotes Invasion and is Involved in Cell-Cell Interaction of Co-Cultured Glioblastoma and Mesenchymal Stem Cells

Received: 4 July 2017
Accepted: 29 December 2017
Published online: 22 January 2018

Mona N. Oliveira[1,2,3], Micheli M. Pillat[1], Helena Motaln[2], Henning Ulrich[1,3] & Tamara T. Lah[2,3,4]

Glioblastoma multiforme (GBM) represents the most lethal brain tumour, and these tumours have very limited treatment options. Mesenchymal stem cells (MSC) are considered as candidates for advanced cell therapies, due to their tropism towards GBM, possibly affecting their malignancy, thus also representing a potential therapeutic vector. Therefore, we aimed to compare the effects of bone-marrow-derived *versus* adipose-tissue-derived MSC (BM-/AT-MSC) on heterogeneous populations of tumour cells. This cells' interplay was addressed by the *in-vitro* two-dimensional (monolayer) and three-dimensional (spheroid) co-culture models, using U87 and U373 GBM cell lines, expressing genotypically different mesenchymal transcriptome profiles. U87 cell low mesenchymal profile expressed high levels of kinin receptor 1 (B1R) and their invasion was greatly enhanced by the B1R agonist des-Arg^9-bradykinin upon BM-MSC co-culturing in 3D co-cultures. This correlated to significantly higher cell-cell interactions in U87/BM-MSC mixed spheroids. This was not observed with the U373 cells and not in AT-MSC co-cultures. Altogether, these data support the on-going exploration of B1R as target for adjuvant approach in GBM therapy. Secondly, the results emphasize the need for further careful exploration of the selectivity regarding the origin of MSC as potential candidates for cell therapies, particular in cancer, where they may adversely affect heterogeneous tumour cell populations.

Over the past few years, it has become evident that the tumour microenvironment is important for regulation of tumour progression[1]. Glioblastoma (GBM) is the most frequent and lethal neoplasia among brain tumours, and a vast body of literature refers to these malignant tumour cells[2]. In contrast, the dynamics and interactions of GBM cells with stromal cells within the tumour microenvironment need still to be explored. Among infiltrating glial cells/macrophages and other immune cells, astrocytes and endothelial cells, it has been shown that mesenchymal stem cells (MSC) also actively move to and reside in GBM tumours[3,4]. Tumour-infiltrating MSC have been associated with enhancement of malignancy and with induction of GBM cell proliferation and migration[5,6]. The anti-tumour effects of MSC are well known, and these include inhibition of proliferation and promotion of apoptosis and senescence of cancer cells (reviewed in[7,8]).

We have previously demonstrated that *in-vitro* cross-talk between bone-marrow-derived MSC (BM-MSC) and U87 GBM cells in an 'indirect' co-culture model (i.e., cells sharing medium, without direct cell-cell contact) resulted in their altered expression of over 500 and 300 genes, respectively[9]. On the other hand, in direct co-cultures of MSC and U373 GBM cells (i.e., in direct cell-cell contact), an enhancement of migration of both cell types was reported by Schichor *et al.*[3]. These authors also demonstrated that U373 cells can form structural and functional syncytium with MSC, which enables direct molecular exchange, and might also be accelerated by cell heterotypic fusion[10] to form

[1]Department of Biochemistry, Institute of Chemistry, University of São Paulo, Av. Prof. Lineus Prestes 748, São Paulo, SP, 05508-000, Brazil. [2]Department of Genetic Toxicology and Cancer Biology, National Institute of Biology, Večna pot 111, 1000, Ljubljana, Slovenia. [3]Jožef Stefan International Postgraduate School, Jamova 39, 1000, Ljubljana, Slovenia. [4]Department of Biochemistry, Faculty of Chemistry and Chemical Engineering, University of Ljubljana, Večna pot 113, 1000, Ljubljana, Slovenia. Correspondence and requests for materials should be addressed to H.U. (email: henning@iq.usp.br) or T.T.L. (email: Tamara.Lah@nib.si)

mixed hybrids. Recently, we addressed the effects of co-culturing MSC with two different GBM cell subtypes, as U87 and U373 cells, and we showed that the effects of MSC on glioma cells are subtype dependent[11].

Bradykinin (BK) has been shown to regulate proliferation and to promote migration of neural stem cells and neurogenic differentiation[12,13]. However, the role of kinins in the malignant brain microenvironment remains poorly explored. Kinins are generated by kininogen processing during inflammation, and they have diverse functions, which include regulation of neuroinflammation[14], endothelial cell activation and vasodilatation[15]. This kinin signalling system is associated with activation of proteases, which produce pharmacologically active BK and kallidin, as well as des-Arg^9-bradykinin (DBK) and des-Arg^9-kallidin, having pro-inflammatory effects upon binding to the two kinin receptors, B1R and B2R, respectively[16]. The B2R is constitutively expressed and has high affinity for the binding of BK and kallidin peptides; in contrast, B1R is an inducible receptor with affinity for DBK and des-Arg^9-kallidin. In cancer, these kinin receptors are involved in cell proliferation, chemotaxis and invasion[17], such as in breast carcinoma[18] and glioma cells[19]. Lu and co-workers[19] revealed that B1R expression up-regulation in GBM cells increases the cell proliferation mediated by DBK and BK. These might be induced by inflammatory cytokines secreted by tumour-infiltrating immune cells, with signalling via the phosphatidylinositol-4,5-bisphosphate 3-kinase (PI3K)/Akt (protein kinase B) and extracellular signal-regulated kinase (ERK) pathways. As MSC also have immunomodulatory properties[9,20], immunomodulation by MSC might also induce B1R expression.

Pillat *et al.*[21] previously showed that both B1R and B2R are expressed at the mRNA and protein levels in U87 cells and in BM-MSC *in vitro*. Additionally, they demonstrated that in indirect and direct co-cultures of U87 cells with BM-MSC, B1R gene and protein expression increased in U87 cells, which was correlated with their enhanced invasiveness via induction of metalloproteases. Here, we aimed to examine B1R involvement in direct cross-talk between two distinct GBM phenotypes (U87 and U373 cells) and MSC of two different origins (BM-MSC and adipose-tissue-derived, AT-MSC). We demonstrate differential responses of U87 and U373 GBM cells to MSC in terms of cell proliferation, cell cycle and GBM/MSC cell-cell interaction (vesicle transfer, fusion events and entosis), B1R agonist des-Arg^9-BK stimulation of U87/BM-MSC mixed spheroids and increased migration/invasion of U87 cells. To the best of our knowledge, this is the first report on B1R as a potential regulator of these processes. Possible clinical applications of our findings are supported by studies that have already suggested B1R as biomarker[22] for targeting in cancer therapy[17,23]. In addition, the present study has important implications for potential MSC therapies for GBM, providing mechanisms for their their interactions with tumour cells[24].

Results

Cell proliferation, cell size and the cell cycle effects in mixed spheroids of glioblastoma and bone-marrow-derived mesenchymal stem cells. The work-flow for the (co-)culturing of the cells as three-dimensional (3D) mono-cultures (termed 'mono-spheroids' of a single cell type) and mixed 3D co-cultures (termed 'mixed spheroids', formed from different cell types mixed in a 1:1 ratio) is shown in Fig. 1A. Briefly, these spheroids were formed as mono or mixed cells seeded with 4% methylcellulose in 96-well U-bottomed plates (2.5×10^3cells/well; see Methods for details). These were left in culture for 1 day at 37 °C under 5% CO_2, to form one spheroid per well.

The proliferation rates of the U87dsRed and U373eGFP GBM cells and BM-MSC as mono-spheroids and mixed spheroids were assessed for their viability using the 3-(4,5-dimethylthiazol-2-yl)-5(3-carboxymethonyphenol)-2-(4-sulfophenyl)-2H-tetrazolium (MTS) as say in terms of the metabolic activity of the cells (Fig. 1B), and for their population doubling times in terms of automated cell counting (Fig. 1C). These U87dsRed and U373eGFP GBM cells showed increased proliferation rates as mixed spheroids with BM-MSC, as compared to their mono-spheroid cultures. As BM-MSC proliferation was slower compared to these GBM cells, as shown by the lower metabolic activity of the BM-MSC *versus* GBM mono-spheroids, we can conclude that in our experimental condition the metabolically more active and proliferating GBM cells accounted for the increased metabolic activity of these GBM/BM-MSC mixed spheroids (Fig. 1B). Furthermore, the U87dsRed cells were more proliferative as both mono-spheroids and mixed spheroids than the U373eGFP cells (Fig. 1B). BM-MSC-induced proliferation of U87dsRed cells significantly halved their population-doubling time, showing a greater effect than that seen for U373eGFP cells (Fig. 1C). The predominance of U87dsRed cells in these mixed spheroids was confirmed using flow cytometry over this period of 5 days (Fig. 1D), and similar, although smaller, increases in U373eGFP cells over BM-MSC in the mixed spheroids were also seen. Direct cell counts confirmed that the U87dsRed cell numbers increased in the U87/BM-MSC mixed spheroids with time (up to 5 days), whereas the number of BM-MSC cell in these mixed spheroids decreased (Fig. 1E).

Figure 2 shows comparisons of the spheroid sizes after 3 and 5 days of co-culturing of the GBM cells with BM-MSC, using imaging and flow cytometry analysis of mono-spheroid and mixed spheroid cultures (Fig. 2A,B). U87dsRed mono-spheroids and U87/BM-MSC mixed spheroids increased their cross-sectional areas up to 5 days, whereas those for BM-MSC mono-spheroids and U373 and U373/BM-MSC mixed spheroids decreased (Fig. 2B). This decrease in the BM-MSC spheroid size paralleled the BM-MSC cell size decrease that was determined through the forward scattering of the BM-MSC as both mono-spheroids and mixed spheroids (Fig. 2C,D). The BM-MSC were becoming significantly smaller in size when cultured with the U87dsRed GBM cells in both 2D (monolayer) and in these 3D (spheroid) cultures in a time dependent manner (Fig. 2C–E,G). On the other hand, the BM-MSC in the U373/BM-MSC mixed spheroids did not decrease in size. Also, no changes were detected for the U87dsRed and U373eGFP GBM cell sizes when cultured as mono-spheroids and mixed spheroids. The GBM and BM-MSC cell cycle alterations were also followed after 2D (monolayer) co-culturing. These analyses confirmed that after 3 days, for U87dsRed cells in co-culture with BM-MSC there was a small but significant decrease in the G0/G1 phase population (Fig. 2F, right panel), where as the U373eGFP cells in co-culture with BM-MSC showed increased cell population in the G2/M phase already from the first day (Fig. 2F).

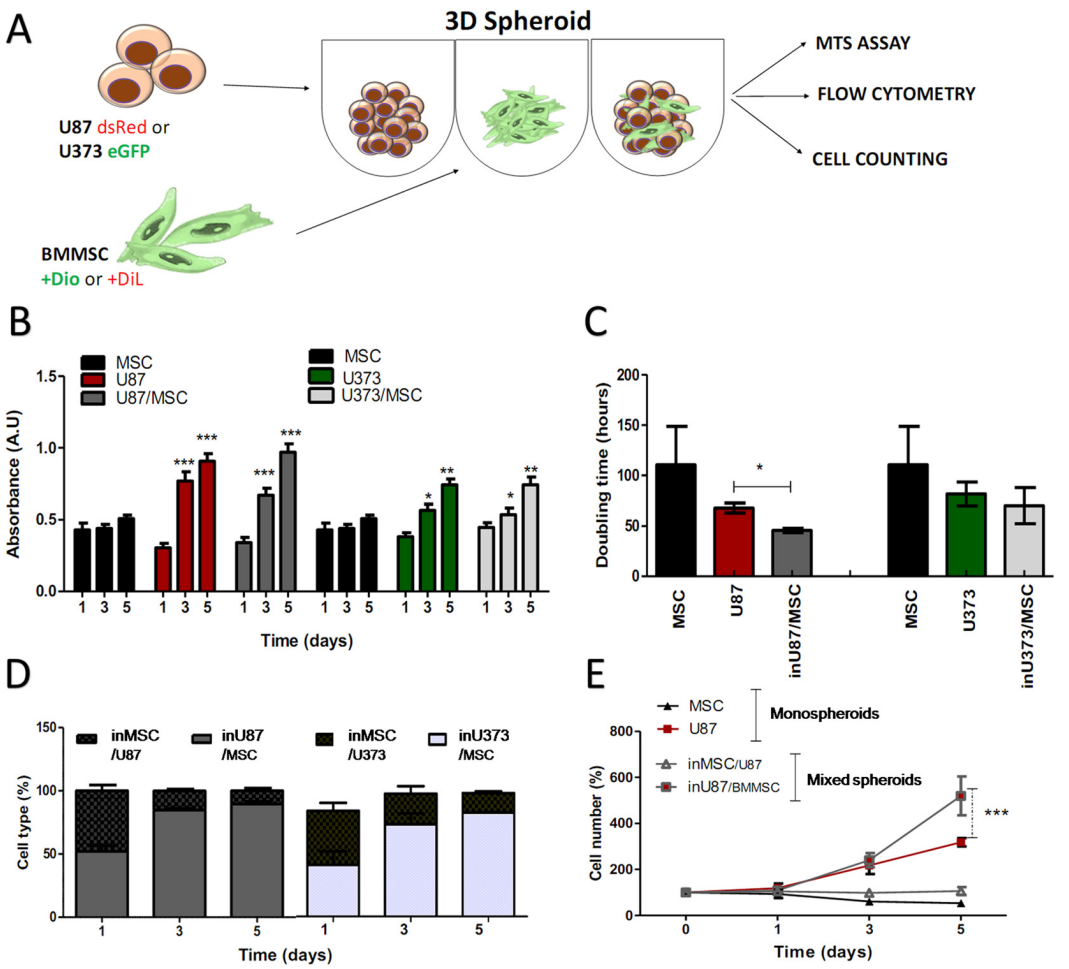

Figure 1. Bone-marrow (BM) MSC induce proliferation of GBM cells in mono-cultures and mixed spheroids. (**A**) Experimental scheme for mono-spheroids and mixed (co-cultured) spheroids for the studies of phenotype changes. (**B**) Total cell viability presented as metabolic activity (A.U. at λ 490/630 nm) in mono cultures of U87dsRed and U373eGFP GBM cells, and BM-MSC (=MSC), and in mixed spheroids (U87/MSC, U373/MSC), as determined by the MTS assay after 1, 3, and 5 days (see Methods). (**C**) Mean doubling times (h) as calculated from the cell counts (see Methods), for U87 and U373 cells, and MSC, in mono-spheroids and mixed spheroids. (**D**) Percentages of GBM cells and MSC in mixed spheroids, marked as in U87/MSC and inU373/MSC were determined by flow cytometry after 1, 3, and 5 days in co-culture. (**E**) Proliferation of U87 cells and MSC in mono-spheroids and mixed spheroids, as calculated from the cell counting after 1, 3, and 5 days, and normalized to the number of cells present in the spheroids on day 0. Data are means ± standard deviation (n = 3); $*P < 0.05$, $**P < 0.001$, $***P < 0.0001$.

Taken together, this supports the data showing that BM-MSC increase the proliferation of U87dsRed cells in mixed co-cultures more than seen for U373eGFP cells in mixed co-cultures. However, there were no changes in the GBM cell sizes, in contrast to BM-MSC, that were becoming particularly smaller in co-cultures with U87dsRed cells, but not with U373eGFP cells.

Glioblastoma and mesenchymal stem cell-cell interaction rate is cell-type dependent. Tumour cells have been reported to fuse with each other (i.e., to form homotypic hybrids) and to fuse with stromal cells (i.e. to form heterotypic hybrids)[10,25,26]. Vesicle-mediated transfer also are fundamental biological processes that are emerging as novel mechanisms for re-programming cells in the tumour microenvironment[27]. The question here was whether the cell-cell interaction (vesicle transfer and cell fusion) might be cell-phenotype dependent. Thus, the potential of these phenotypically different GBM cell lines, U87 and U373, to form heterotypic hybrids and vesicle transfer with BM-MSC was studied.

U87 and U373 cells expressing red fluorescence protein (dsRed) and green fluorescent protein (GFP), respectively, and BM-MSC pre-labelled with the vital fluorescent dyes DiO and DiI were grown as 2D monolayers as single cell types (2D mono-cultures) and mixed cell types (2D co-cultures) for 3 days, and then cell-cell interactions were imaged by fluorescence microscopy and flow cytometry, as described in the Methods. Figure 3(A,B) shows merged images of U87-dsRed cell-cell interaction with BM-MSC-DiO cells, recorded as the double fluorescent signals. Some of these hybrid cells retained double nuclei (i.e., green and red) derived from both cell

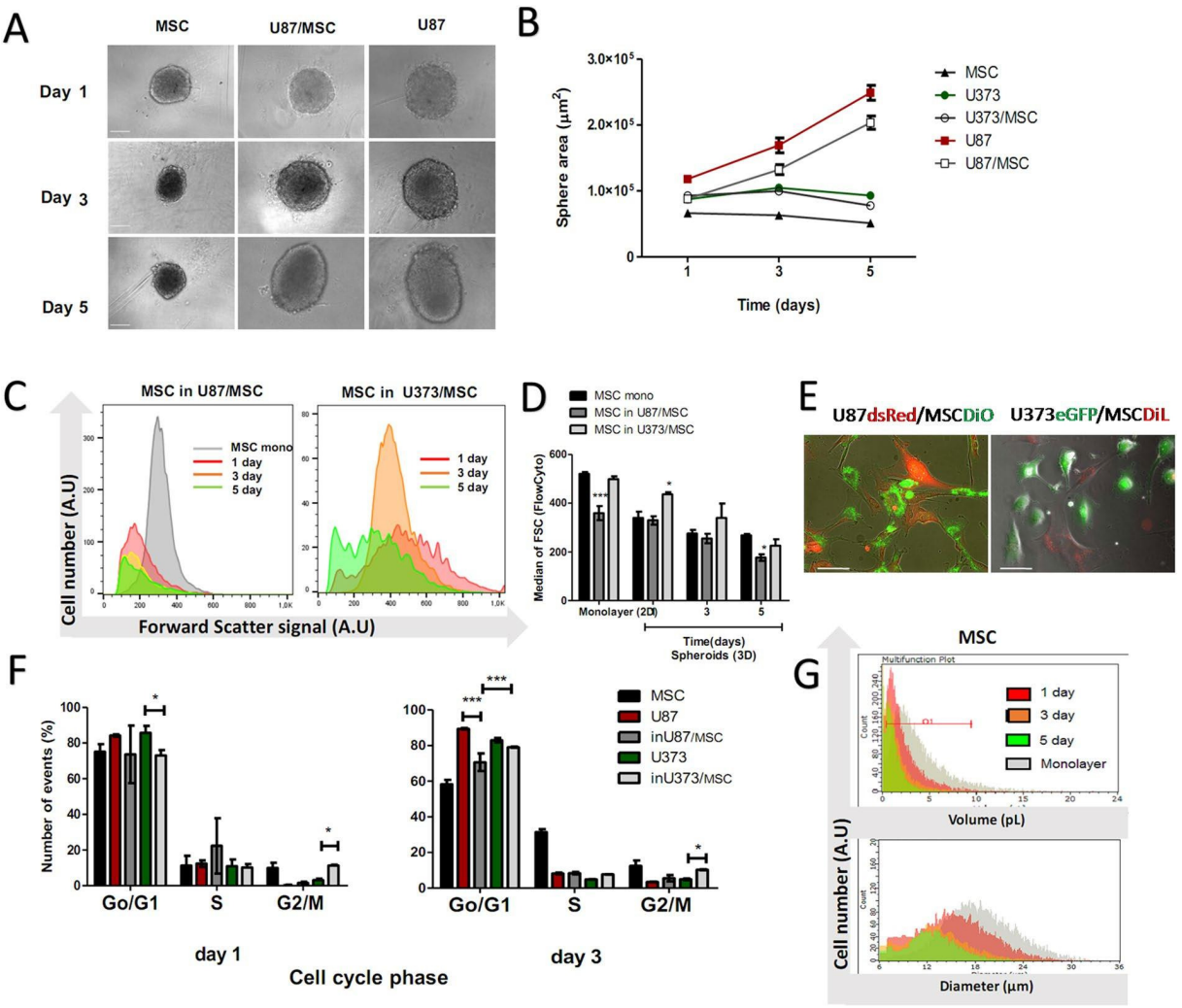

Figure 2. Bone-marrow MSC change in size and morphology when co-cultured with GBM cells of different origins. (**A**) Representative images of spheroids' sizes of BM-MSC (=MSC), U87/MSC, and U87 spheroids. (**B**) Quantification of the spheroids area size after 1, 3, and 5 days in culture, performed on micrographs using the NIS elements software, as described in Methods. (**C**) Changes in MSC area size in co-cultures with U87 and U373 cells after 1, 3, and 5 days in culture (increased forward scatter meaning increased cell size, as described in Methods. (**D**) Changes in cell size of MSC were quantified in 3D mono-spheroids and in mixed spheroids with U87 and U373 cells, after 1, 3, and 5 days in culture. The control MSC cell sizes were measured in 2D monolayer cultures and 2D co-cultures is shown (the first bar graph, left). (**E**) Representative phase-contrast microscopy images of cell morphology in 2D monolayer cultures of U87dsRed (in red) and U373eGFP (in green) GBM cells with MSC DiO (in green) and MSC DiL (in red) respectively; scale bar, 25 µm. (**F**) Quantification for cell cycle analyses of U87 and U373 cells and MSC as 2D monolayer cultures and co-cultures, for 1 and 3 days. (**G**) Representative data for diameter and volume measurements of MSC grown as 2D monolayer and as spheroid after 1, 3, and 5 days, determined by Scepter cell counting device. Data are means ± standard deviation (n = 3). $^{*}P < 0.05$, $^{***}P < 0.0001$.

types, and had either mosaic membrane (red and green). The frequency of cell-cell interaction of these cells in the 2D co-cultures apparently depended on the GBM cell phenotype: for U87-dsRed/BM-MSC-DiO 2D co-cultures after 1 day, cell-cell interaction were more abundant (25.8 ± 6.6%), when compared to U373-GFP/BM-MSC-DiL2D co-cultures (4.2 ± 2.0%). Moreover, the percentage of those events increased after 3 days in U87dsRed/BM-MSC-DiO2D co-cultures (41.4 ± 15.1%), whereas cell-cell interaction remained low in U373-GFP/BM-MSCDiL2D co-cultures (4.9 ± 0.8%) (Fig. 3C,D). This thus suggests that compared to U373 cells, U87 cells (which have been shown to have a less pronounced mesenchymal phenotype) have greater tendency to cell-cell interaction with vesicle transfer or fuse with the BM-MSC to form heterotypic hybrids and eventual entosis events (Supplementary Fig. 1). Tumour cells showing multiple nuclei and double labelling for dsRed and DiO after 3 days in these 2D co-culture are shown in Fig. 3E. Cell-cycle analyses performed after 1 and 3 days revealed that the U87-dsRed/BM-MSC-DiO double staining population in S phase decreased, whereas the proportion of these cell in G2/M phase increased after 3 days (Fig. 3F). The G2/M phase increase is most likely be

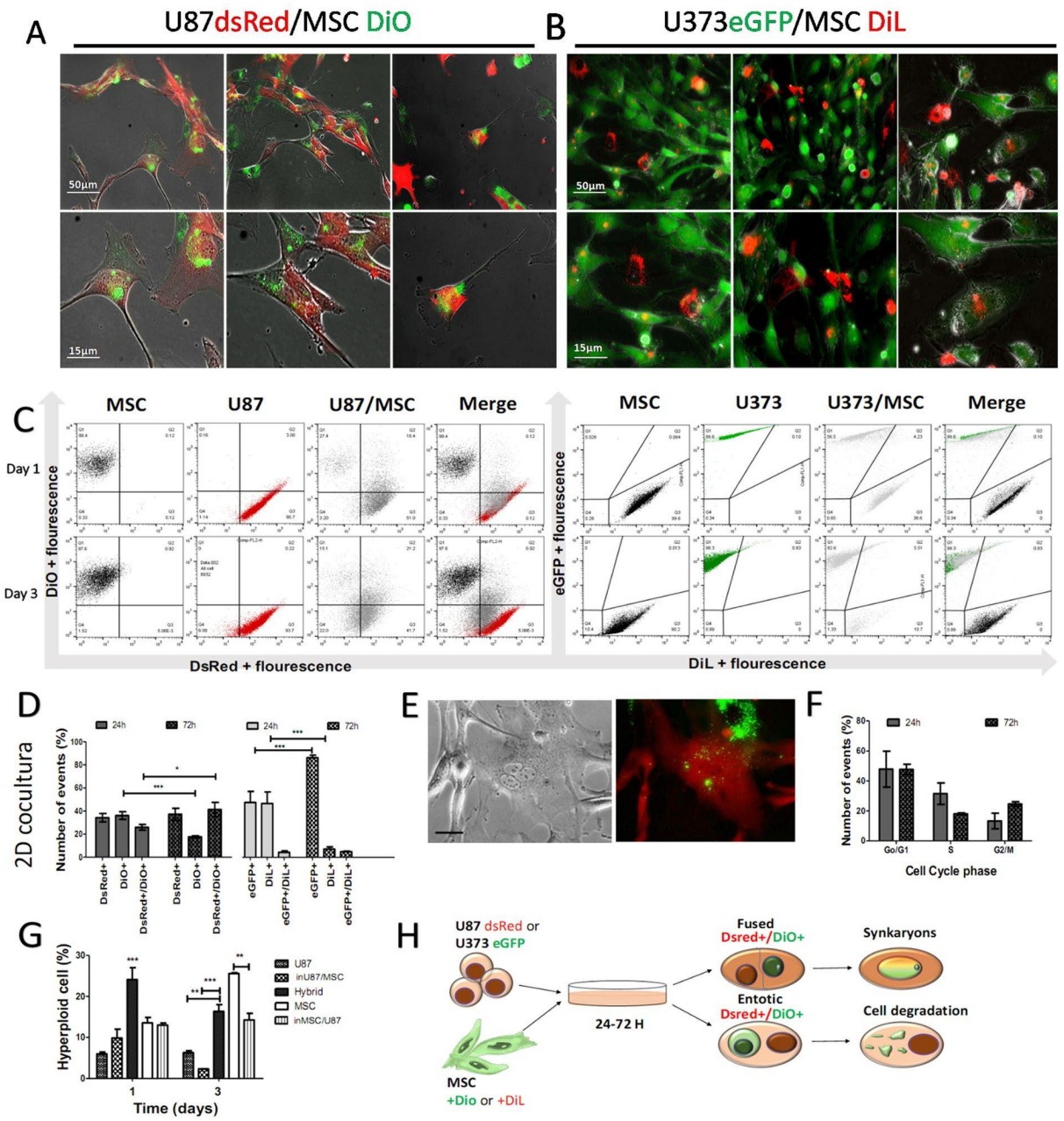

Figure 3. Cell-Cell interaction events in 2D monolayer co-cultures of GBM U87 and U373 cells with BM-MSC. (**A**) Representative images of heterotypic cell fusion (orange) between U87-dsRed cells (red) and BM-MSC (=MSC; green), indicated by arrow heads after 3 days in co-culture. (**B**) As for (**A**), between U373-GFP cells (green) and MSC; red) and rare events of cell fusion (orange). (**C**) Representative flow cytometry dot-plots after 1 and 3 days of co-culturing, showing the increase in the cell-cell interaction populations in the last (right) panel (Merge): Ds Red+= U87 in U87/MSC, DiO+= MSC in U87/MSC Dared+/DiO+= hybrid cells, entosis or vesicle transfer; eGFP+= U373 in U373/MSC, Dil+= MSC in U373/MSC eGFP+/Dil+= hybrid cells, entosis or vesicle transfer. (**D**) Quantification of cell-cell interaction events (cell hybrids) in U87/MSC and U373/MSC mixed spheroids, as derived from flow cytometry data in (**C**). (**E**) Representative images of heterotypic fusion or entotic events between U87dsRed cells (red) and MSCs (green) as 2D monolayer co-cultures, after 3 days. Scale bar, 20 µm. (**F**) Cell cycle analysis of the fused U87/BM-MSC cells in 2D monolayer co-cultures after 1 (24 h) and 3 (72 h) days. (**G**) Polyploidy of cell populations (quantified as described in Methods) in U87/MSC 2D monolayer co-cultures, after 1 and 3 days. (**H**) Scheme of the fusion or entotic events between the different types of cells, under the present experimental set-up. For quantifications, data are means ± standard deviations (n = 3). $*P < 0.05$, $**P < 0.001$, $***P < 0.0001$.

assigned to mitosis ploidy changes, as high levels of polyploidy persisted in the double labeled populations at both 1 and 3 days (Fig. 3G). Contrary to high polyploidy found in these double-labeled populations, polyploidy in 2D co-cultured U87 cells and BM-MSC decreased after 3 days, compared to U87 cells and BM-MSC grown alone

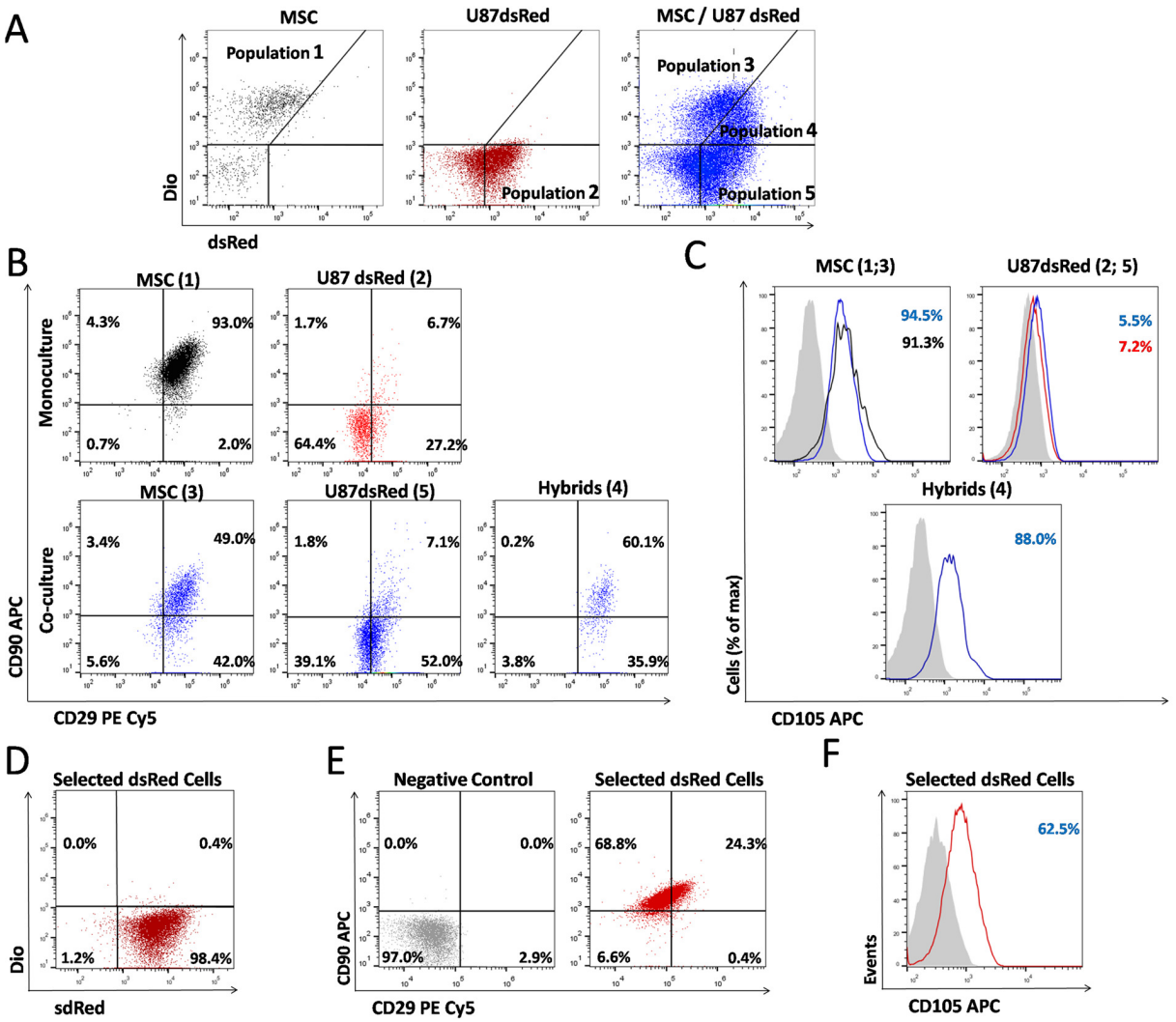

Figure 4. Glioblastoma U87dsRed cells acquire the mesenchymal phenotype upon co-culturing with MSC. (**A**) Flow cytometry dot-plots after 3 days of mono- and co-culture, DiO^+ MSC (population 1 in monoculture and population 3 in co-culture), $dsRed^+$ U87 cells (population 2 in monoculture and population 5 in co-culture), and DiO^+ $dsRed^+$ hybrid cells (population 4 in co-culture). (**B**) Dot-plots for mesenchymal stem cell markers CD90 and CD29 in MSC and U87 cells in mono- and co-culture, demonstrating that the hybrid population 4 is positive for CD90 and CD29, such as observed in MSC (populations 1 and 3). (**C**) Flow cytometry histograms, comparing expression of CD105 in MSC (upper left, monoculture in black line and co-culture in blue line); CD105 expression in U87 cells (upper right (monoculture in red line and co-culture in blue line), CD105 positivity in hybrid cells (lower histogram; co-culture in blue line. The data show expression of the MSC related marker also in hybrid cells. Gray histograms represent negative controls, as described in Methods. (**D**) Selection of U87 dsRed cell by geneticin treatment for 6 days, in co-cultures with MSC was efficiently selecting for 98.4% of $dsRed^+DiO^-$ cells. (**E**) Flow cytometry dot-plots of these selected dsRed cells evidenced high expression rates of CD90, CD29 and (**F**) CD105. Data were analyzed with Flowjo V10 software.

in 2D mono-cultures. These results suggest that through cell-cell interaction heterotypic fusion occurs, possibly involving transition from heterokaryon to syncharyon. Entosis, the process of the invasion of one cell into another might also have occurred here (Fig. 3E,H), although we have not distinguished both processes by molecular markers, as suggested by Sottile *et al.*[28] Altogether, these data suggest that U87 and U373 have distinct cell-cell interaction potentials, which are possibly linked to their differentially expressed mesenchymal phenotypes.

Glioblastoma U87 dsRed cells acquire mesenchymal phenotype when co-cultured with BM-MSC. We investigated the expression of mesenchymal-specific membrane markers, CD29, CD90 and CD105 in monoculture and co-culture of BM-MSC and U87dsRed cells by flow cytometry (Fig. 4). As expected, the majority (90%) of BM-MSC were highly positive for these markers, of which CD90 expression in BM-MSC decreased upon co-cultures from 93% to 49% (Fig. 4B), but a reduction of CD29 (97.3 to 91.0%) and CD105 (94.5 to 91.3%) was not significant (Fig. 4B,D). As expected, U87 cells expressed very low levels of these markers, not being

significantly altered upon co-culturing for CD90 (from 8.4% to 8.9%) and CD105 (from 5.5% to 7.2%), but was significantly increased for CD29 from 33.9% to 59.1%.

The double stained dsRed^{+}/DiO^{+} cells in co-cultures of U87dsRed/BM-MSCDiO, were separated after 3 days as population 4 in Fig. 4A, and the frequencies of CD29, CD90 and CD105 were again quantified by flow cytometry analysis, revealing that the double stained cells expressed higher levels of mesenchymal cell-specific markers, such as 88% of CD105, 96% of CD29, and 60% of CD90 (Fig. 4B,E). These data demonstrated that U87dsred/BM-MSCDiO double stained population expressed higher mesenchymal phenotype. This may enhance U87 migration, possibly triggered by cytokines secreted from mesenchymal stem cells[20,29,30]. Furthermore, after 6 days in co-culture, U87dsRed cells were selected by geneticin (G418), 1 mg/ml treatment to observe the CD29, CD90 and CD105 levels within the 2D coculture. As shown in Fig. 4D, G418 selected for survival of 98.4% U87dsRed cells, but no MSCDiO was present. Interestingly, some of these selected U87dsRed cells, presumably containing both U87 transdifferentiated and hybrid cell population, expressed rather high levels of the mesenchymal-specific markers, 24.7% of CD29, 93.1% of CD90, and 62.5% of CD105 (Fig. 4E,F).

B1R expression and alterations in U87 and U373 glioblastoma cells in response to mesenchymal stem cells are associated with heterotypic cell fusion and vary in MSC of different tissue origin. Induced expression of B1R in inflammation and cancers is well established[22]. Moreover, in our previous report[21] we showed that that indirect and direct effects of BM-MSC on U87dsRed GBM cells were associated with increased expression of both B1R and B2R, which possibly triggers increased cell invasiveness. However, to date, no links between B1R and cell fusion or vesicle transfer have been reported. In view of this, the effects on cell-cell interaction were investigated here in terms of B1R expression and its agonist DBK and antagonist AcLys[D beta Nal^{7}, Ile^{8}]desArg^{9}-bradykinin (R715), in both U87dsRed and U373eGFP GBM cells in 2D co-cultures with BM-MSC and AT-MSC. Previously, we have also showed higher B1R expression in U87 than U373 cells, and their labelled derivatives[21], as shown in Fig. 5A (left). Contrary to these GBM cells, both BM-MSC and AT-MSC showed lower B1R expression, although higher B1R expression was seen for BM-MSC *versus* AT-MSC (Fig. 5B, right). The B1R agonist (DBK) and antagonist (R-715) were used at the effective dose of 100 nM for B1R activation and chronic inhibition, respectively[31]. As also shown previously, these are not cytotoxic for any cell types and under any condition tested (Fig. 5C). Moreover, DBK enhanced the viability/metabolic activity (measured using spheroids and the MTS assay), and thus promoted the proliferation of MSC mono-spheroids and both U87/BM-MSC and U373/BM-MSC as mixed spheroids. Figure 5D shows that U87/BM-MSC and U373/BM-MSC 2D co-cultures responded to B1R agonist stimulation with increased free cytosolic calcium ion concentrations, as compared to the 2D mono-cultures, and that this was effectively blocked by the B1R antagonist. Figure 5E addresses the association between B1R activation and cell-cell interaction events in 2D mixed co-cultures using the R715 antagonist of B1R, decreasing the number of cell-cell interaction that reduced heterotypic U87dsRed/AT-MSCeGFP hybrids formation from $3.0 \pm 0.4\%$ to $0.35 \pm 0.21\%$, while for U87dsRed/BM-MSCDiO in 2D co-cultures the reduction was from $41.4 \pm 15.1\%$ to $27.6 \pm 5.9\%$ after 72 h (Fig. 5E and Supplementary Fig. 2). This also occurred for U87dsRed/AT-MSCeGFP 2D co-cultures, although these events were relatively rare compared to BM-MSCDiO. Interestingly, higher expression of B1R in U87 cells than in U373 cells also correlated with lower frequency of cell-cell interaction events in U373 cells in 2D co-cultures with BM-MSC (Fig. 3C). Taken together, negative modulation of B1R activity resulted in reduced heterotypic fusion and vesicle transfer between GBM cells and MSC in these 2D co-cultures. Moreover, we demonstrated that the frequency of cell-cell interaction events and expression of B1R differ in GBM cells of different subtype, being lower in U87 cells with a more proneural transcriptomic type than in U373cells, expressing typical mesenchymal transcriptome. Cell-cell interaction also depends on the tissue origin of MSC.

Invasion of U87 glioblastoma cells in co-cultures with BM-MSC is affected by B1R activity. The question was whether differential B1R expression in U87dsRed cells, BM-MSC and AT-MSC (Fig. 5B) would also mirror their differential agonist (DBK) and antagonist (R715) invasion responses. When mono-spheroids and mixed spheroids of U87dsRed cells and both BM-MSC and AT-MSC were incubated for 7 days they showed enhanced invasiveness of U87dsRed cells out of the spheroids, and this was further stimulated by DBK in coculture with BM-MSC (Fig. 6A,B). Treatment with the antagonist R715 efficiently abrogated this effect in U87dsRed mono-spheroids and U87/BM-MSC mixed spheroids, whereas no such effect was observed in U87/AT-MSC mixed spheroids. Accordingly, in U87/BM-MSC 2D co-cultures, gene expression analysis revealed elevated levels of the pro-invasive proteolytic enzymes matrix metalloprotease (MMP)14 and cathepsin B, but not of other proteases, such as cathepsin L, calpains 1/2 and the urokinase receptor when comparable with coculture U87/AT-MSC (Fig. 6C). Furthermore, cell migration of U87dsRed cells and BM-MSC from mono-spheroids and mixed spheroids was quantified after 3 days of treatment with DBK and R715 (Fig. 6D,E) DBK significantly increased the migration of U87dsRed cells and MSC, whereas the B1R antagonist R715 was a potent inhibitor of cell migration (Fig. 6E). Taken together, these data suggest that B1R activation may play a role in the regulation of cell-cell interactions between GBM cells, which express B1R receptor, and MSC. B1R/DBK-mediated activation was correlating with enhanced migration/invasion rates of GBM cells and MSC out of co-cultures. This is particularly relevant in co-cultures with BM-MSC, which affected U87 transition (transdifferentiation) to a more mesenchymal phenotype markers (Fig. 4D,E).

Discussion

Glioblastoma are malignant brain tumours that have the worst prognosis and high recurrence rates because of the tumour aggressiveness and resistance to chemotherapy and radiotherapy. In the tumour microenvironment, the interactions between tumour and stromal cells have been shown to modulate GBM aggressiveness and resistance

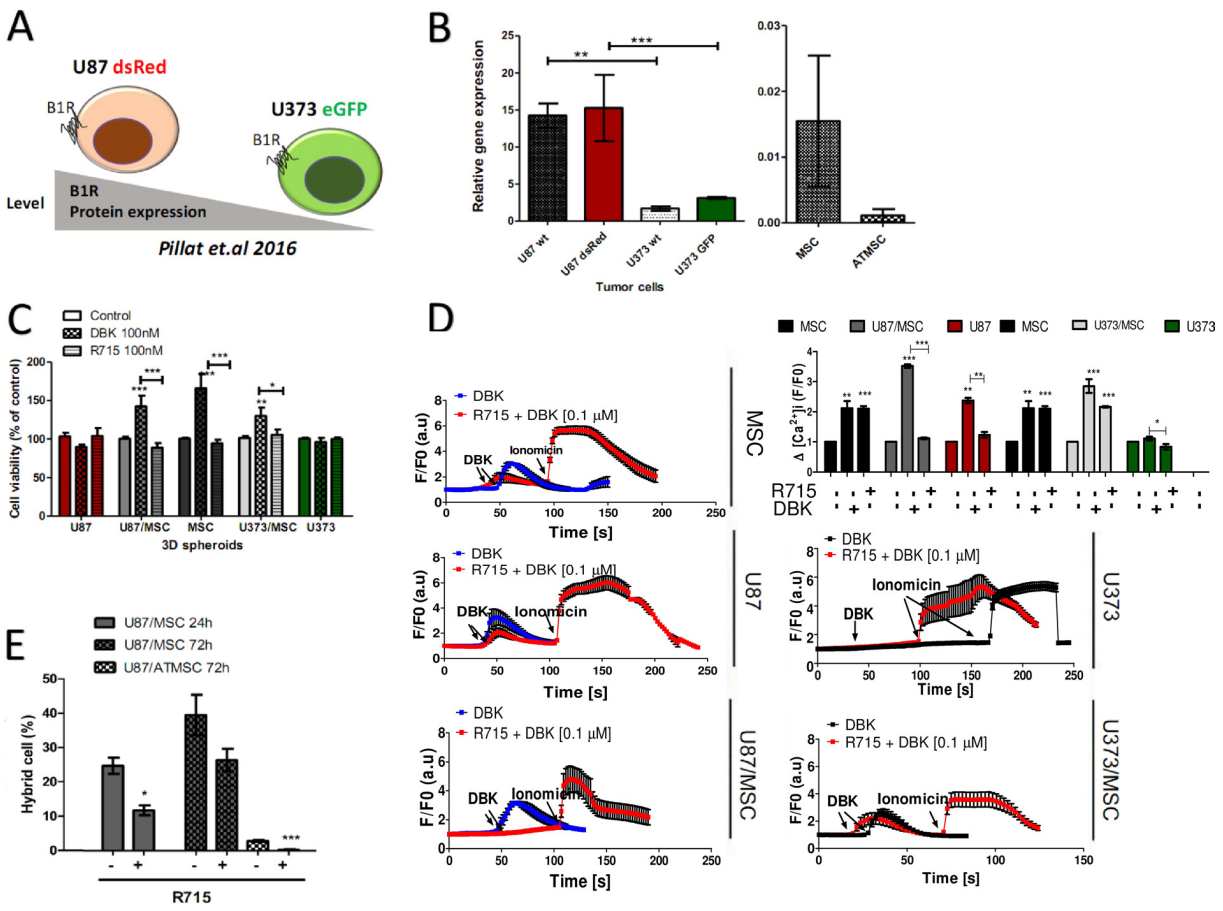

Figure 5. Fusion of GBM cells with BM-MSC and AT-MSC cells is associated with kinin-B1 receptor (B1R) expression and activity. (**A**) Scheme for B1R protein expression in GBM cell lines based on our previous report by Pillat *et al.*[21]. (**B**) Quantification of relative B1R mRNA expression levels in GBM cells (as indicated) and BM-MSCs (=MSC) and AT-MSCs as 2D monolayer mono-cultures, using qRT-PCR. (**C**) Quantification of cell viability of U87 and U373 cells and BM-MSC (MSC) in mono-spheroids and mixed spheroids for treatment with 100 nM des-Arg^9-bradykinin (DBK; B1R agonist) and 100 nM R715 (B1R antagonist) for 5 days, as determined using the MTS assay with normalization to control conditions. (**D**) Intracellular calcium elevations $[Ca^{2+}]_i$ in MSC and glioma cells (U87-MG and U373 MG) in 2D mono and co-culture, mediated upon B1 receptors activation and inhibition with (R715). Prior to calcium imaging, cells were loaded with the Ca^{2+}-sensitive fluorophore indicator Fluo-4AM. Non-stimulated cells were imaged for obtaining basal fluorescence values, followed by addition of 100 nM final concentration of des-Arg9-bradykinin (DBK) or R715. Kinetics of kinin receptor-induced $[Ca^{2+}]_i$ transients is shown in average (six trials) of the change in fluorescence ($\Delta F/F$) of DBK and R715 during time detection in the graph (right panel). The shown data are average responses of 10 cells. (**E**) Quantification of cells' hybrid formation of U87dsRed cells with BM-MSC (MSC) and AT-MSC in 2D monolayer co-cultures for treatment with 100 nM R715 (B1R antagonist), after 1 and 3 days, measured by flow cytometry. Data are means ± standard deviation. $*P < 0.05$, $**P < 0.001$, $***P < 0.0001$.

to therapy[1]. The presence of non-neoplastic cells within the tumour stroma and studies that have traced the origins of such cells in animal models suggest that these cells participate also in tumour formation[6]. These cells provide the so-called inter-tumour heterogeneity, or tumour non-autonomous heterogeneity, and may significantly affect the tumour cell environment[32], thus becoming an important target in cancer therapies. On the other hand, it is known that glioma stem cells can give rise to autonomous cellular tumour heterogeneity within different GBMs that have the same clinical appearance. Verhaak *et al.*[33], and later several other studies[6,34], postulated four different GBM transcriptome subtypes that appeared to co-exist within any single tumour. This has been recently demonstrated by Rickylefs *et al.*[35], showing that this heterogeneity suggests more aggressive tumours with worse prognosis. Heterogeneous populations of tumour cells are exposed to heterogeneous populations of stromal cells, which might thus affect the tumour cells in very different ways. For studying this diversity, we used MSC as our model, which can infiltrate into the brain, presumably, but not necessarily, from the bone marrow. The tropism to neoplasia of these cells has been well documented[36], which was also the basis for preclinical studies of MSC as vectors for cell-based cancer therapies[7,8]. Thus, their effects on heterogeneous populations of tumour cells should be considered before the application of any MSC therapies.

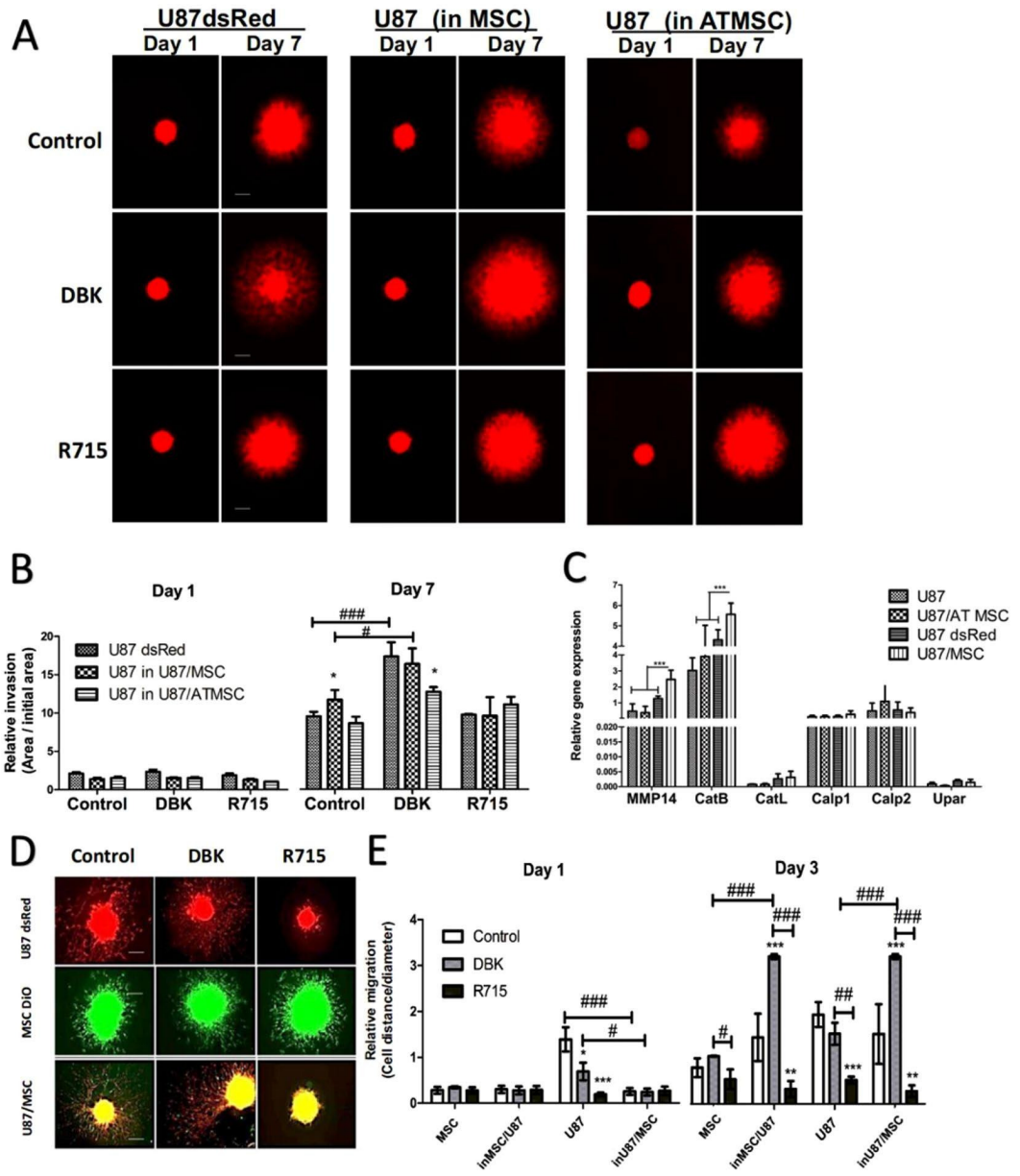

Figure 6. Bone-marrow (BM) MSC and adipose tissue (AT) MSC differentially affect U87 cell invasion responses to bradykinin receptor 1 (B1R) activation. (**A**) Representative images of U87dsRed cell growth and invasion with BM-MSC (=MSC) and AT-MSC as mono-spheroids and mixed spheroids for treatment with 100 nM DBK (B1R agonist) and 100 nM R715 (B1R antagonist), after 1 and 7 days. The spheroids were embedded in Matrigel (see Methods). Scale bar, 250 µm. (**B**) Quantification of the relative invasion as derived from data illustrated in (**A**), as the ratio of the invasion area *vs* initial spheroid area, after 1 and 7 days. (**C**) Quantification of relative gene expression (mRNA levels) of selected invasion-related proteases in U87 cells and BM-MSC (=MSC) and AT-MSC in 2D monolayer cultures and co-cultures, after 1 and 7 days. (**D**) Representative images of U87dsRed cells (red) and BM-MSC (MSC; green) migration/invasion from mono-spheroids and mixed spheroids, for treatment with 100 nM DBK (B1R agonist) and 100 nMR715 (B1R antagonist), after 3 days. The spheroids were embedded in Matrigel in 24-well plates. Scale bar, 250 µm. (**E**) Quantification of relative migration as derived from data illustrated in (**D**), calculated as the ratio of cell distance vs spheroid diameter for each time interval (see Methods). Data are means ± standard deviation (n = 3). $*P < 0.05$, $**P < 0.001$, $***P < 0.0001$.

Recently, we demonstrated GBM cell-type-specific responses to BM-MSC in 3D direct co-cultures, where BM-MSC inhibited invasion of U87 cells, while enhancing invasion of U373 cells after 4 days[11]. We assumed that this was due to significant differences in the intrinsic gene expression profiles of these two GBM cell lines, which show less (U87) and more (U373) mesenchymal-like features. Here, we also found differential proliferation responses of these U87 and U373 cell lines in mixed spheroids with BM-MSC, as evaluated also by the cell *versus*

spheroid size ratios. Although both U87 and U373 cells showed increased proliferation rates upon this direct contact with BM-MSC, the predominance of U87 cells, and to a lesser extent of U373 cells, over BM-MSC in these mixed spheroids was noted over 5 days, in parallel with reduced proliferation and size of the BM-MSC.

These data can be explained by the observed high rate of cell-cell interaction events between these GBM cells and BM-MSC, with levels of 25% and 3% for the U87 and U373 cells, respectively. Cell fusion has a crucial role in pathophysiological processes such as cancer, where it represents an efficient means of rapid phenotypic evolution, through the production of cells with new properties at rates that exceed random mutagenesis[36–38]. Consistent with our findings, higher fusion rates have also been observed in exponentially proliferating cells, compared to slowly proliferating cells[39,40]. These previous studies also indicated that cell hybrids formed by spontaneous fusion between GBM cells and normal hamster cells *in vivo* and showed modified GBM traits. Mercapide *et al.*[10] also showed that homotypic U87 and heterotypic U87/fibroblast hybrids had higher proliferative activity, which resulted in a larger fraction of polyploidy in tumour cells, which were shown to arise from cell fusion. This is similar to what we observed in the U87/BM-MSC 2D co-cultures, which were associated with increased heterotypic fusion rate and increased size of the U87/BM-MSC, which also contained higher numbers of polyploidy cells compared to the U373/BM-MSC. BM-MSC might have an impact on giant cell formation, as we also noted increased numbers of giant U87 cells. We speculate that these might arise by homotypic fusion among the U87 cells when exposed to the BM-MSC, as we have also already reported on giant U87 cells when these were exposed to BM-MSC conditioned-medium alone[9]. The heterotypic hybrids might be transformed into viable re-programmed cells, and are emerging as a plausible source of increased tumour heterogeneity *in vivo*[41], a process that is also stimulated by chemotherapy[42]. Such cells might contribute to cancer progression and metastasis, due to the genetic instability caused by their polyploidy[43,44]. Altogether, our data imply that even in the same tumour, cells of different tumour subtypes are differentially affected and more or less fuse with infiltrating BM-MSC, what accounts for their differential proliferation and polyploidy, mimicking the observations for GBM *in vivo*[32].

Tumour cells release different types of vesicles including extracellular microvesicles (MVs) and microparticles, membrane blebs, apoptotic bodies, etc[45]. Similarly, nanovesicles, transferring proteins, lipids and various types of RNAs to neighbouring cells have been described for MSC in regenerative medicine[7,46]. MSC also release a number of growth factors, such as TGF-β, which may trigger alterations in transcription factors required to initiate process, similar to EMT[47,48] in the neighbouring GBM cells resulting in enhanced migration, for example here out of the BM-MSC co-cultures, where we found increased levels of adherence junctions in U373/GBM cells[3]. Here we observed initial increase in the CD29[49], which is an integrin β1 that is involved in EMT, in U87 GBM cells, but CD29 expression decreased after prolonged co-culturing from of 59% to 24% of, possibly being related to slightly enhanced invasion (Fig. 6). Heterotypic cell fusion was imaged here in the coculture, presumably as a result of the "invasion" of the MSC cells into the U87 cells (Supplementary Fig. 1). However, in related work by Breznik *et al.*[11] we observed enhanced invasion of MSC, but not of U87 out of in U87/BM-MSC spheroids.

Here we also occasionally observed 'cell in cell' cytological features, as often observed in cancers, which is termed entosis[50]. Recently, Bartosch *et al.*[51] demonstrated a similar phenomenon, termed cell cannibalism, where BM-MSC were shown to enter breast cancer cells in 3D co-cultures. This enhanced the survival of the cancer cells, but at the same time suppressed their tumorigenicity, and promoted their dormancy. As suggested by these authors, the MSC were mobilised from the bone marrow and migrated into the tumour environment, promoting the formation of tumour cell spheroids that were finally internalised by the tumour cells. Moreover, our data demonstrate a significantly higher cell-cell interaction of these U87 cells with the BM-MSC (about 40% of cells) *versus* the fusion rate with AT-MSC (only 3% of cells), which provides the first evidence that the tendency of cancer cell interaction with MSC depends on the MSC tissue origin. Such data are supported by the observation of Akimoto *et al.*[52], and Del Fattore *et al.*[27], who showed differential effects of BM-MSC, AT-MSC and umbilical cord blood MSC on glioma cells *in vitro*, but most likely, this reflects the *in-vivo* situation, as BM-MSC tropism to the brain tumours have been demonstrated in mice and humans[53].

It is important to emphasize that the elevated number of double-stained cells in our experiments could also result from an exchange of microvesicles as well as transdifferentiation through. Recently, Vignais *et al.*[54] pointed at the potential of MSC in modelling nanotubules for syncytium formation by rearrangement of the cytoskeleton and cell-to-cell transfer of mitochondria under physiological and pathological conditions, changing cell metabolism and functions related to cellular energy. The importance of cell fusions in tissue remodelling has been documented as a physiological process during regeneration[55,56], to which MSC actively contribute.

Cell fusion is also triggered by chronic inflammation[55], and 10-fold to 100-fold increases in cell fusion frequency have been reported in liver, brain and intestinal tissue under chronic inflammatory conditions[57]. Furthermore, cell integration through cannibalism of MSC by tumour cells would augment the liberation of pro-inflammatory factors[58]. Along with a plethora of other cytokines, this would induce expression of B1R[14,17,21,59,60]. As these processes are orchestrated by GBM-derived factors, which include cytokines, we explored the possibility of a link between B1R in GBM cell fusion and invasion under chronic inflammatory conditions. Inflammatory signals *per se* and increased cell fusion were shown to enhance tumour progression, as many cancer hybrid cells showed more metastatic behaviour[60]. Shichor *et al.*[3] proposed that upon cell contact, molecular signals from MSC internalised by U373 GBM cells can result in transcriptional activation downstream of the mitogen-activated protein kinase/ERK cascade, which is known to regulate both cell motility and proliferation. We have demonstrated that the U87 cell invasion is suppressed by BM-MSC can be triggered by the addition of a B1R agonist (DBK), which is consistent with the very high B1R expression in these U87 cells. However, the induced invasiveness of U87cells in mixed spheroids with MSC appeared to be delayed, as this was observed between 1–4 but after long time of analysis with 7 days the invasiveness is observed in these co-cultures. This delay roughly coincides with the cell-cell interaction rate increase that was observed over this period of time. Consistent with the negligible B1R expression in U373 cells, no changes in cell invasion were noted upon either

agonist or antagonist treatment of U373/BM-MSC spheroids (data not shown). We demonstrated that the fusion is diminished by B1R blocking/or low expression and are involved with invasiveness potential *via* its agonist DBK, to enhance this signalling via the PI3K/Akt and ERK1/2 pathways[61]. The functionality of B1R was shown here by stimulation of the intracellular calcium ion flux. Our previous data showed that treatment of U87 GBM cells with bradykinin resulted in down-regulation of B1R and B2R expression in BM-MSC, with simultaneous expression up-regulation of B1R and B2R in U87 cells. This suggests that bradykinin mediates the information flow between these cells, to some extent regulating tumour progression and invasion[21]. As we did not detect significant changes in the invasiveness-related proteases in U87 cells, we believe that the MSC- and DBK-induced migration is related to the changes in intracellular calcium transients, through a mechanism described by Seifert and Sontheimer[62]. The intracellular calcium ion transients in GBM cells *in vitro* induced the formation of small bleb-like protrusions at the plasma membrane, which stimulated an amoeboid phenotype of cell migration that was unrelated to proteolytic activity and ECM degradation[63].

In conclusion, this study has shown that the frequency of cell-cell interaction by heterotypic fusogenic events, vesicle transfer and entosis in the two established GBM model cell lines, U87 and U373 cells, preferentially with BM-MSC (vs. AT-MSC) is related to cell genotypes /phenotypes, which include differential B1R expression levels. The mechanisms by which these cells respond to cues from the micro-environmental, such as infiltrating MSC, with induce epithelial to mesenchymal transition and activate invasion-related proteases in less-invasive GBM cells, such as these U373 cells, which are not higher cell-cell interaction. In contrast, the more invasive and fusogenic U87 cells need B1R activation, which would most likely depend on a more or less inflammatory environment within a tumour *in vivo*. Altogether, our study supports the on-going exploration of B1R agonists and antagonists as target candidates in the development of adjuvant approaches to GBM therapy. Secondly, our study indicates the need to further and carefully explore MSC as potential candidates for cell therapies, particularly with respect to tumour cell autonomous heterogeneity.

Materials and Methods

Cell lines and culture maintenance. The U87 and U373 human GBM cells lines were obtained from American Type Culture Collection (USA) and regularly authenticated, according to Torsvik *et al.*[64]. GFP-transfected U373 cells (U373eGFP) and dsRed-transfected U87 cells (U87dsRed) were established as previously stated[3,21]. Cells were grown in complete growth medium that consisted of Dulbecco's modified Eagle's medium (DMEM) supplemented with 10% foetal bovine serum (FBS), non-essential amino acids, 4mML-glutamine, 100 U/mL penicillin and 100 µg/mL streptomycin (Gibco). The U373eGFP and U87dsRed cells were routinely propagated in the medium with additional 1mg/mL G-418 (Sigma-Aldrich). The cells were cultured at 37 °C, in 5% CO_2, and the medium was changed every 3 days. These cells were passaged after reaching 75% confluence, and plated for culture maintenance at a density of 15000 cells/cm^2.

Human bone-marrow MSC derived from bone marrow of a healthy volunteer (MSC-2) were purchased from Lonza Bioscience Walkersville (Walkersville, MD, USA). The AT-MSC transfected with GFP were generously provided by Prof. Massimo Dominici (University Hospital of Modena, Italy). After resuscitation, the cells were plated and grown in the same medium as the GBM cells, however, without G-418. The MSC were passaged after reaching 75% confluence at a density of 7000 cells/cm^2. BM-MSC of passages 8–12, and U87/U87-dsRed and U373/U373-GFP GBM cells of passages 40–58 were used, in culture medium containing 10% FBS.

Two-dimensional and three-dimensional cell co-cultures. For 2D direct cell co-cultures (i.e., cell types in direct contact with each other), GBM cells and MSC were plated into 6-well plates at a 1:1 ratio, and cultured for 1–7days. Direct co-cultures of U87/BM-MSC, U87dsRed/BM-MSC, U373/BM-MSC, U373eGFP/BM-MSC and U87-dsRed/AT-MSC-GFP were prepared using different plates and time intervals, and also always at a 1:1 ratio. For preparation of the spheroid cultures (mono-spheroids, mixed spheroids), the corresponding cells (as 1:1 cell mixtures) were seeded in 200 µL complete DMEM growth medium containing 4% methylcellulose, into 96-well U-bottomed plates (2.5×10^3cells/well; Corning, Life Sciences, MA, USA). They were centrifuged for 90 min at 850 × *g* and left in culture for 1 day at 37 °C under 5% CO_2, to form one spheroid in each well. In the mixed spheroid or "hybrid cell, GBM and MSC cells can fuse, what we defined as "heterotypic fusion", or "hybrid cells" to distinguish these form "homotypic fusion", which occurs often between cancer cells, resulting in aneuploidy (polyploidy). Fusogenicity is the ability of cells to fuse the membranes and form binuclear cells (heterokaryon) or a giant nuclei, resulting from nuclear fusion (synkaryon)[10,28]. The fusogenicity is quantified by the % of fusion events observed in defined cell population.

Proliferation analysis. About 20–24 mono-spheroids or mixed spheroids were transferred into 2 mL microcentrifuge tubes (Eppendorf) after 1, 3 and 5 days of culture, dissociated with trypsin/EDTA (Corning, Life Sciences, USA), blocked with growth medium (DMEM plus 10% FBS), centrifuged, and resuspended in 100 µL phosphate-buffered saline for cell counting. The cell numbers, diameters and volumes were determined using a handheld automated cell counter (Scepter; Merck-Millipore, Billerica, MA, USA), using 40 µm and 60 µm cell filters for the sensor. The number of cells per spheroid in each tube was determined by dividing the total number of cells counted in each tube by the initial number of spheroids. For proliferation determination of the different cell types in coculture (U87dsRed, U373eGFP and BM-MSC), a parallel analysis was performed by flow cytometry with the same samples. As different cell types were distinguished by flow cytometry, it was also possible to analyse proportions of each cell type in co-culture and spheroids. The data were gathered from three independent experiments. The significance of differences between mono-culture and co-culture conditions was determined using ANOVA two-way and Student's t-tests, and $P < 0.05$ was considered as significant.

Determination of cell doubling time. Following the use of the automated cell counter (Scepter; Millipore), the doubling time of cell proliferation at each assayed time point was determined using Equation (1) (Roth V. 2006 Doubling Time Computing, Available from: http://www.doubling-time.com/compute.php):

$$\text{Doubling Time} = \text{Duration} \times \log(2)/\log(\text{Final Concentration}) - \log(\text{Initial Concentration}). \quad (1)$$

This equation was used for the calculation of the doubling time of each cell population.

Cell cycle and DNA content analyses. Bone-marrow MSC were pre-loaded with DiO and DiL, and were cultured in 2D co-cultures together with U87dsRed or U373eGFP cells, for 24 h or 72 h. The cells were then harvested, and washed with DMEM without serum, and 5×10^5 cells/mL were incubated with 5 µM Vibranty Dye Ruby (Life Technologies) for 15 min, according to the instructions of the supplier. Cell cycle analyses were performed with a flow cytometer (FACS Calibur; Becton and Dickinson, CA, USA) using 488 nm and 633/5 nm as excitation wavelength, and >670 nm as emission wavelength (linear scale). Fluorescence emission data of DiO or GFP (FL1,488 nm excitation, 533/30 nm emission band-pass filter) and fluorescence emission data of dsRed or DiL (FL2, FL1, 488 nm excitation, 585/40 emission band-pass filter) were used to determine the gates for the different cell populations. Three independent experiments were performed. The data were analysed using the FlowJo V10 software (FlowJo, LLC, OR, USA) to determine the fractions of cells in the sub-G0/G1, G0/G1, S and G2/M phases of the cell cycle.

Spheroid viability measurements (MTS assay). Cell viability within the spheroids was determined using the MTS assay. After 1, 3 and 5 days, for all control and treated spheroids grown in U-bottomed plates with 100 uL media/well, 20 µLMTS agent was added (Promega, Fitchburg, WI, USA). The spheroids were incubated at 37 °C for 3 h, and their absorbance was measured at 490/630 nm using a microplate reader (Genios; Tecan, Bradenton, FL, USA). The measurements were performed in triplicate and repeated in three independent experiments.

Flow cytometry analysis of 2D coculture and mesenchymal-specific markers. Different types of mixed spheroids (U87dsRed/BM-MSC, U373eGFP/BM-MSC) were cultured for 1, 3 and 5 days. They were then dissociated, and single-cell suspensions were subjected to flow cytometry analysis (FACS Calibur; BD Biosciences, NJ, USA). Forward and side light scatter signals were used to detect the size of each cell population in the co-cultures. GBM cells and MSC were discriminated based on the GFP (FL1-H) or dsRed (FL2-H) fluorescence signals, following compensation for eliminating non-specific signals.

Experiments for quantification of MSC-specific markers, CD29, CD90 and CD105, were performed according to Pillat *et al.*[21] MSC were pre-loaded with DiO and then seeded in monocultures or 2D co-cultures together with U87dsRed cells for 72 h. Cells were dissociated from the flasks using trypsin and FBS. Single cells were fixed for at least 20 min in 4% para-formaldehyde, washed with PBS 1% FBS, and incubated with antibodies anti-CD90 APC (5 µL:100 µL; BDPharmingen; cat 559862; FL4) and anti-CD29 PE-Cy^{TM}5 (20 µL:100 µL; BD Pharmingen; cat 559882; FL3) or anti-CD105 APC (5 µL:100 µL; BD Pharmingen; cat 562408; FL4) for 30 min at room temperature. Cells were washed with PBS and, then analysed in a flow cytometer. A minimum of 10,000 events was acquired per sample, and the data were displayed at logarithmic scales and analysed with the FlowJo V10 software.

DsRed positive cell selection. MSC were pre-loaded with DiO, and were seeded in monocultures or 2D co-cultures together with U87-dsRed cells for 8 days, with the medium change every 2 days. Control monoculture of U87dsRed and BM-MSC were set as well. On the 6th day, the 3rdmedia change was performed with the media supplemented with geneticin (G418) at 2 mg/ml to select for U87dsRed cells only as only those cells contain the Neo resistance cassette in their genome. On the 8th day the surviving cells out of U87dsRed monoculture and U87/BM-MSC coculture were collected and fixed with 4% paraformaldehyde for flow cytometry analysis (no BM-MSCs grown in monoculture survived the gentamicin treatment). Fixed cells were immunostained for CD29, CD90 and CD105 mesenchymal markers and analysed by flow cytometry.

Three-dimensional invasion assay. The 3D invasion assay was performed as described previously[65]. Briefly, the spheroids were covered with 5 mg/mL Matrigel (BD Bioscience) into 96-well U-bottomed plates. After a 45-min incubation at 37 °C and under 5% CO_2, the embedded spheroids were covered with DMEM with 10% FBS (control spheroids) and 100 nM DBK or R715 were added (treated spheroids). The initial distance of invasion (T0) was measured following an overnight incubation, and then on each successive day, for a total of 7 days. The distance was measured from the edge of the spheroid by using the NIS elements software 2.3 v (Nikon Instruments, Melville, NY, USA) and normalized to the size of the spheroid.

Three-dimensional migration assay. The migration assay was performed as described previously[11]. Briefly, the spheroids were transferred to 24-well plates (TPP, Trasadingen, Switzerland) and covered with 5 mg/mL Matrigel (BD Bioscience, USA). After a 45-min incubation at 37 °C under 5% CO_2, the embedded spheroids were covered with DMEM with 10% FBS (control spheroids) or 100 nM DBK or R715 were added (treated spheroids). Cell migration was determined by evaluating the distance between the cells and the edge of the spheroid over 3 successive days. Images were analysed with the NIS elements software 2.3 v (Nikon Instruments, Melville, NY, USA). Migration distances were normalized to the spheroid diameter.

Fusion, vesicle transfer and entosis analysis. Bone-marrow MSC were pre-stained for 30 min at 5 µM DiO or DiL (final concentrations; Thermo Fisher, MA, USA) at 37 °C under 5% CO_2 in a humidified incubator. They were then washed twice with 1 mL phosphate-buffered saline and set-up for a 2D co-cultures with

U87-dsRed or U373-GFP cells in 6-well plates, for 24 h and 72 h, as control cells and those treated with 100 nM R715 (antagonist). AT-MSC-GFP were used directly in co-cultures with U87dsRed cells under control and treatment conditions for 72 h. After these incubations, the cells were dissociated with 1 mL 0.25% trypsin/EGTA (Gibco-Thermofisher), blocked, and resuspended in phosphate-buffered saline for flow cytometry analysis (FACS Calibur; BD Biosciences, USA). Ten thousand events were acquired per sample, and the data were displayed on logarithmic scales. Forward and side light scatter signals were used to exclude dead cells and debris. DiO/GFP- and DsRed/DiL-positive cells were determined as the percentages of cells stained/with positive expression using the FL1-H and FL2-H channels, out of the total cells in each co-culture sample (U87dsRed/MSC-DiO, U373eGFP/MSC-DiL). Mono-culture control cells were used to determine the signal background and to set the gate boundaries. The data were analysed using the FlowJo V10 software (FlowJo, LLC, OR, USA).

Hyperploids cell populations were analysed and quantified using Vybrant Dye Cycle with the FL-4 (640 nm excitation, 675 nm emission, 25 nm band pass filter;675/25 nm). The diploid (2n) and <4n (diploid continuous = tetraploid, polyploid, aneuploid cells) populations were calculated based on (*A*) area × width (*W*). These parameters (*A vs. W*) were primarily set to discriminate single cells passing through the flow cell from cells that might not have spatial separation when passing through the flow cell of the cytometry; i.e. doublets (aggregated cells). Doublets will give an increased width measurement (26% increase for every doubling of volume of a cell, based on a spherical arithmetic model). Diploid cells result in increased area fluorescence signals without any increase in width fluorescence signals.

Cell treatment. The agonist Des-Arg^9-bradykinin (DBK) and the antagonist AcLys[D beta Nal^7, Ile^8] desArg^9-bradykinin(R-715) (both from Tocris, Fisher Scientific, Pittsburg, PA, USA) were added to the growth medium or matrigel of the 3D spheroids at final concentrations of 1 to 1000 nM. The spheroids were incubated with these for 24 h up to 168 h (7 days).

Viability MTT assay in BR1 activity testing. The effects of the B1R DBK agonist and R715 antagonist on the survival of GBM cells (U87dsRed, U373eGFP) and MSC in 2D monolayer cultures were determined using MTT (Sigma-Aldrich, St. Louis, MI, USA). The experiments were performed in 96-well plates (TPP; 8×10^3 cells/well). Control and treated cells were incubated with MTT at a final concentration of 1 mg/mL for 3 h. Then the cells were centrifuged, the medium was removed, and 50 µL isopropanol was added, with agitation for 1 min. The optical density of each sample was measured at 570/630 nm using a spectrophotometer microplate reader (Genios; Tecan). Three independent experiments were performed, with six replicate wells per condition. The data are given as percentages of viable treated cells, relative to untreated control cells.

Kinin-B1 receptor gene expression by real-time qPCR. Total RNA was isolated from three biological replicates of 2D monolayer mono-cultured U87, U373, U87dsRed and U373eGFP GBM cells, as well as BM-MSC and AT-MSC, using the Trizol reagent, according to manufacturer instructions (Invitrogen, Paisley, UK). The mRNA integrity was confirmed (Agilent 2100 Bioanalyser; Agilent Technologies, Santa Clara, CA, USA). The cDNA was generated from 1.0 µg total RNA using the High-Capacity cDNA Reverse Transcription kits (Applied Biosystems, Hilden, Germany). The relative quantification of gene expression levels of B1R was carried out using real-time PCR (ABI 7900 HT Sequence Detection System; Applied Biosystems, ThermoFisher, Waltham, MA, USA). These real-time PCR reactions were performed using 1:10 dilutions of each cDNA (1 µg/well), added to TaqMan Universal PCR Master Mix and TaqMan Gene Expression Assays (all from Applied Biosystems): for B1R-Hs00664201_s1 *versus* the amplification of glyceraldehyde 3-phosphate dehydrogenase (Pre-Developed TaqMan Assay Reagent No. 4310884E) as internal control. Here, 1, 1:10, 1:100, 1:1000 and 1:10000 dilutions of the template sample were used for relative B1R mRNA quantity determination in the samples. The SDS v2.2 software was used (Applied Biosystems) to analyse the data obtained from the TaqMan Gene Expression Assays. Independent experiments were performed in duplicate and repeated three times. Statistical significance between different cell lines was determined by two-tailed Student's t-tests, and $P < 0.05$ was considered significant.

Calcium Imaging. U87 and U373 GBM cells and human MSCs were seeded into 4 wells µ-Slide chamber ™ Ibidi (Munich-Germany) for 72 h at a density of 16.8 cells/cm^2. For direct co-cultures, the mix of MSC and U87-MG cells (1:1 ratio) were seeded and cultured for 72 h. Prior to calcium imaging, the cells were washed with PBS and loaded with 5 mM of Fluo 4-AM for 30 min at 37 °C in serum-free medium containing 0.06% of the non ionic surfactant pluronic acid F-127 (Sigma Aldrich), as published previously[21]. Cells were rinsed with serum-free medium and equilibrate in the chamber for 15 min before calcium images were recorded with Nikon fluorescence imaging microscope (ECLIPSE-TiS) (Nikon, Melville, NY) equipped with a 14 bit high-resolution CCD camera CoolSNAP HQ2 (Photometrics, Tucson, AZ) and analyzed with NIS-Element software 2.3 v(Nikon). Fluorescence excitation was done with a xenon lamp at wavelength 488 nm and the light emission was collected at 520 nm using a bandpass filter at 515–530 nm. Time kinetics of free intracellular calcium ($[Ca^{2+}]i$) variations were constructed from over 300 images collected in 1-s intervals. The fluorescence intensities (F) were calibrated in a solution containing 5 mM ionophore (Fmax) and 10 mM EGTA (Fmin) to provide an estimation of the absolute change in the intracellular calcium fluorescence using the following equation $\Delta F/F_{min}$. The cells were stimulated by 100 nM des-Arg^9-bradykinin (DBK) or 100 nM R715 following of DBK.The presented traces are average variations over time of at least 20 single cells.

Determination of proteases gene expression by real-time qPCR. Total RNA was isolated from 2D monolayer mono-cultured U87 cells and mixed co-cultures (U87/BM-MSC, U87/AT-MSC) using the TRIzol reagent (Life Technologies). Following DNase I treatment, 1 µg RNA was reverse transcribed into cDNA using SuperScript II Reverse Transcriptase (Life Technologies). Quantitative SYBR Green real-time PCR was performed (StepOnePlus; Life Technologies). Each 25 µL SYBR Green reaction consisted of 25 ng cDNA, 12.5 µL 2 × SYBR

Gene			Primers: forward (F)/reverse (R)
Access number	Species	Name	
NM_004995.3	*Homo sapiens*	Matrix metallopeptidase 14 (MMP14)	F: 5′GCTCTCTTCTGGATGCCCAA3′ R: 5′ GTACTCGCTATCCACTGCCC 3′
NM_001908.4	*Homo sapiens*	Cathepsin B (CTSB)	F: 5′TGCAATGTCACAACCTCTCTGA3′ R: 5′ TAGGAGGCAATCTGCAAACCA3′
NM_001257973.1	*Homo sapiens*	Cathepsin L (CTSL), transcript variant 5	F: 5′CAAGTGGAAGGCTGCAATGG3′ R: 5′ AGTCCAGGCCTCCATTATCCT3′
NM_001198868.1	*Homo sapiens*	Calpain 1 (CAPN1)	F: 5′ CCATAGACATCTCCAGCGTTCT3′ R: 5′CACGTTGTTCCACTCTGAGGA 3′
NM_001748.4	*Homo sapiens*	Calpain 2	F: 5′ CTCAACCAGGACTACGAGGC3′ R: 5′ TGATAAACTGGGGGTCAGCG 3′
NM_001005377.2	*Homo sapiens*	Plasminogen activator, urokinase receptor	F: 5′ACTCACGGACCGAAAAACCA3′ R: 5′TCCAGGTCTGGGTGGTTACA3′
GAPDH	*Homo sapiens*	Glyceraldehyde 3-phosphate dehydrogenase	F: 5′CCTCCCGCTTCGCTCTCT3′ R: 5′GCTGGCGACGCAAAAGA3′

Table 1. Primer sequences of the cDNAs coding for the proteases receptors and proteases-related enzymes used for the real-time PCR.

Green Universal PCR Master Mix (Life Technologies), and 200 nM respective forward and reverse primers. Unless otherwise stated, the primer sequences (Table 1) were designed using Primer-BLAST designer (https://www.ncbi.nlm.nih.gov/tools/primer-blast/). Real-time PCR was performed using the temperature protocol of 50 °C for 2 min, 95 °C for 10 min, followed by 40 cycles of 95 °C for 15 s and 60 °C for 1 min. The data were analysed following a dissociation curve protocol for evaluation of the specificity of the amplicon produced in each reaction. A distinct peak indicated that a single DNA sequence was amplified during the PCR. Standard curves were determined for each primer set and cDNA sample, to determine the efficiency of the reaction. Independent experiments were performed in triplicates for each gene analysed, and repeated three times. Glyceraldehyde-3-phosphate dehydrogenase gene expression levels were used as the endogenous control for relative quantification of gene expression levels (Table 1).

Live cell photomicrography. Images of live cells in the monolayers and as spheroids under control conditions and after addition of the agonist or antagonist (100 nM) were recorded after 24, 48, 72, 96 and 168 h using an inverted microscope (Nikon) coupled to a digital camera. The micrograph images were processed using the Software NIS-Elements 2.3 v software, for measuring the areas and cell distances, and for merging the fluorescent signals (GFP, dsRed, DiO, DiL). Five micrograph images were taken per experimental condition.

In time-lapse imaging, the cells were pre-loaded with respective dye, as described in fusion analysis. Cells were plated into 6 well and co-cultured for 48 h. All images of living cells were assisted by the Software NIS-Elements 2.3 v software, for automated focus and loop time was set at 7 min for 5 h.

Statistical analyses. Statistical comparisons between the different conditions were carried out using Student's t-tests, one-way analysis of variance (ANOVA), or two-way analysis of variance with Bonferroni *post-hoc* tests, using the GraphPad Prism 5.1 software (Graph-Pad Software, La Jolla, CA, USA). Unless otherwise stated, all of the data are expressed as means ± standard error of the mean (SEM), from at least three independent experiments. For flow cytometry, a minimum of 10000 events was analysed per cell sample. The criteria for statistical significance were set at $*P < 0.05$ and $**P < 0.001$.

Data availability statement. The data availability is in line with the Journal policy and Scientific Reports regulations and is available upon request.

References

1. Quail, D. F. & Joyce, J. A. The Microenvironmental Landscape of Brain Tumors. *Cancer Cell* **31**, 326–341 (2017).
2. Louis, D. N. *et al*. The2016 World Health Organization Classification of Tumors of the Central Nervous System: a summary. *Acta Neuropathol.* **131**, 803–820 (2016).
3. Schichor, C. *et al*. Mesenchymal stem cells and glioma cells form a structural as well as a functional syncytium *in vitro*. *Exp. Neurol.* **234**, 208–219 (2012).
4. Appaix, F. Brain mesenchymal stem cells: The other stem cells of the brain? *World J. Stem Cells* **6**, 134–147 (2014).
5. Behnan, J. *et al*. Recruited Brain Tumor-Derived Mesenchymal Stem Cells Contribute to Brain Tumor Progression. *Stem Cells* **2014**, 1110–1123 (2013).
6. Behnan, J. *et al*. Differential propagation of stroma and cancer stem cells dictates tumorigenesis and multipotency. *Oncogene* **36**, 570–584 (2017).
7. Baglio, S. R., Pegtel, D. M. & Baldini, N. Mesenchymal stem cell secreted vesicles provide novel opportunities in (stem) cell-free therapy. *Front. Physiol.* **3**, 359–372 (2012).
8. Alieva, M. *et al*. Glioblastoma therapy with cytotoxic mesenchymal stromal cells optimized by bioluminescence imaging of tumor and therapeutic cell response. *PLoS One* **7**, e35148 (2012).
9. Motaln, H. *et al*. Human mesenchymal stem cells exploit the immune response mediating chemokines to impact the phenotype of glioblastoma. *Cell Transplant.* **21**, 1529–1545 (2012).
10. Mercapide, J., Rappa, G. & Lorico, A. The intrinsic fusogenicity of glioma cells as a factor of transformation and progression in the tumor microenvironment. *Int. J. Cancer* **131**, 334–343 (2012).

11. Breznik, B., Motaln, H., Vittori, M., Rotter, A. & Lah, T. Mesenchymal stem cells differentially affect the invasion of distinct glioblastoma cell lines. *Oncotarget* **8**, 25482–25499 (2017).
12. Ulrich, H., do Nascimento, I. C., Bocsi, J. & Tárnok, A. Immunomodulation in Stem Cell Differentiation into Neurons and Brain Repair. *Stem Cell Rev. Reports* **11**, 474–486 (2015).
13. Trujillo, C. A. *et al*. Kinin-B2 receptor activity determines the differentiation fate of neural stem cells. *J. Biol. Chem.* **287**, 44046–44061 (2012).
14. Naaldijk, Y. M., Sack, U., Bittencourt, M. C. & Ulrich, H. Kinins and microglial responses in bipolar disorder: a neuroinflammation hypothesis. *Biol. Chem* **397**, 283–296 (2016).
15. Ishihara, K., Hayashi, I., Yamashina, S. & Majima, M. A potential role of bradykinin in angiogenesis and growth of S-180 mouse tumors. *Jpn. J. Pharmacol.* **87**, 318–326 (2001).
16. Marceau, F. & Regoli, D. Bradykinin receptor ligands: therapeutic perspectives. *Nat. Rev. Drug Discov.* **3**, 845–852 (2004).
17. da Costa, P. L. N., Sirois, P., Tannock, I. F. & Chammas, R. The role of kinin receptors in cancer and therapeutic opportunities. *Cancer Lett.* **345**, 27–38 (2014).
18. Ehrenfeld, P. *et al*. Activation of kinin B1 receptor increases the release of metalloproteases-2 and −9 from both estrogen-sensitive and -insensitive breast cancer cells. *Cancer Lett.* **301**, 106–118 (2011).
19. Lu, D. Y., Leung, Y. M., Huang, S. M. & Wong, K. L. Bradykinin-induced cell migration and COX-2 production mediated by the bradykinin B1 receptor in glioma cells. *J. Cell. Biochem.* **110**, 141–150 (2010).
20. Motaln, H. *et al*. Heterogeneous glioblastoma cell cross-talk promotes phenotype alterations and enhanced drug resistance. *Oncotarget*. https://doi.org/10.18632/oncotarget.570 (2015).
21. Pillat, M. M. *et al*. Glioblastoma-mesenchymal stem cell communication modulates expression patterns of kinin receptors: Possible involvement of bradykinin in information flow. *Cytom. Part A* **89**, 365–375 (2016).
22. Kashuba, E., Bailey, J., Allsup, D. & Cawkwell, L. The kinin–kallikrein system: physiological roles, pathophysiology and its relationship to cancer biomarkers. *Biomarkers* **18**, 279–296 (2013).
23. Whalley, E. T., Figueroa, C. D., Gera, L. & Bhoola, K. D. Discovery and therapeutic potential of kinin receptor antagonists. *Expert Opin. Drug Discov.* **1**, 1–20 (2012).
24. Kim, S. M. *et al*. *In vivo* near-infrared imaging for the tracking of systemically delivered mesenchymal stem cells: Tropism for brain tumors and biodistribution. *Int. J. Nanomedicine* **11**, 13–23 (2015).
25. Enriquez, V. A. *et al*. Tumorigenic hybrids between mesenchymal stem cells and gastric cancer cells enhanced cancer proliferation, migration and stemness. *RNA* **500**, 357–361 (2015).
26. Wang, R. *et al*. Spontaneous cancer-stromal cell fusion as a mechanism of prostate cancer androgen-independent progression. *PLoS One* **7**, e42653 (2012).
27. Del Fattore, A. *et al*. Differential effects of extracellular vesicles secreted by mesenchymal stem cells from different sources on glioblastoma cells. *Expert Opin. Biol. Ther.* **15**, 1–10 (2014).
28. Francesco, S., Aulicino, F., Theka, I. & Mesenchymal, M. P. C. stem cells generate distinct functional hybrids *in vitro* via cell fusion or entosis. *Sci. Rep.* **6**, 1–10 (2016).
29. Iwadate, Y. Epithelial-mesenchymal transition in glioblastoma progression. *Oncol. Lett.* **11**, 1615–1620 (2016).
30. Acquistapace, A. *et al*. Human Mesenchymal Stem Cells Reprogram Adult Cardiomyocytes Toward a Progenitor-Like State Through Partial Cell Fusion and Mitochondria Transfer. *Stem Cells* **29**, 812–824 (2011).
31. Stewart, J. M. *et al*. Bradykinin-related compounds as new drugs for cancer and inflammation. *Can J Physiol Pharmacol* **80**, 275–280 (2002).
32. Bougnaud, S. *et al*. Molecular crosstalk between tumour and brain parenchyma instructs histopathological features in glioblastoma. *Oncotarget* **7**, 31955–31971 (2016).
33. Verhaak, R. G. W. *et al*. Integrated Genomic Analysis Identifies Clinically Relevant Subtypes of Glioblastoma Characterized by Abnormalities in PDGFRA, IDH1, EGFR, and NF1. *Cancer Cell* **17**, 98–110 (2010).
34. Lin, N. *et al*. Prevalence and clinicopathologic characteristics of the molecular subtypes in malignant glioma: A multi-institutional analysis of 941 cases. *PLoS One* **9**, e94871 (2014).
35. Ricklefs, F. *et al*. Extracellular vesicles from high-grade glioma exchange diverse pro-oncogenic signals that maintain intratumoral heterogeneity. *Cancer Res.* **76**, 2876–2881 (2016).
36. Melzer, C., Yang, Y. & Hass, R. Interaction of MSC with tumor cells. *Cell Commun. Signal.* **14**, 20–35 (2016).
37. Noubissi, F. K. & Ogle, B. M. Cancer cell fusion: Mechanisms slowly unravel. *Int. J. Mol. Sci.* **17**, 1–10 (2016).
38. Bastida-Ruiz, D., Van Hoesen, K. & Cohen, M. The dark side of cell fusion. *Int. J. Mol. Sci.* **17**, 638–658 (2016).
39. Goldenberg, D. M. *et al*. Horizontal transmission and retention of malignancy, as well as functional human genes, after spontaneous fusion of human glioblastoma and hamster host cells *in vivo*. *Int. J. Cancer* **131**, 49–58 (2012).
40. Goldenberg, D. M., Rooney, R. J., Loo, M., Liu, D. & Chang, C. H. *In-vivo* fusion of human cancer and hamster stromal cells permanently transduces and transcribes human DNA. *PLoS One* **9**, e107927 (2014).
41. Yan, B., Wang, J. & Liu, L. Chemotherapy promotes tumour cell hybridization *in vivo*. *Tumor Biol.* **37**, 5025–5030 (2016).
42. Mohr, M., Zänker, K. S. & Dittmar, T. Cancer (stem) cell differentiation: An inherent or acquired property? *Med. Hypotheses* **85**, 1012–1018 (2015).
43. Pawelek, J. M. & Chakraborty, A. K. Explanation for Metastasis. *Gene Expr.* **8**, 377–386 (2008).
44. Pawelek, J. M. Fusion of bone marrow-derived cells with cancer cells: Metastasis as a secondary disease in cancer. *Chin. J. Cancer* **33**, 133–139 (2014).
45. Howcroft, T. K., Zhang, H. G., Dhodapkar, M. & Mohla, S. Vesicle transfer and cell fusion: Emerging concepts of cell-cell communication in the tumor microenvironment. *Cancer Biol. Ther.* **12**, 159–164 (2011).
46. De Toro, J., Herschlik, L., Waldner, C. & Mongini, C. Emerging roles of exosomes in normal and pathological conditions: new insights for diagnosis and therapeutic applications. *Front. Immunol.* **6**, 203–217 (2015).
47. Lamouille, S., Xu, J. & Derynck, R. Molecular mechanisms of epithelial-mesenchymal transition. *Natl. Rev. Mol. Cell Biol.* **15**, 178–196 (2014).
48. Rhee, K. J., Lee, J. I. & Eom, Y. W. Mesenchymal stem cell-mediated effects of tumor support or suppression. *Int. J. Mol. Sci.* **16**, 30015–30033 (2015).
49. Bryukhovetskiy, I. & Shevchenko, V. Molecular mechanisms of the effect of TGF-β1 on U87 human glioblastoma cells. *Oncol. Lett.* **12**, 1581–1590 (2016).
50. Overholtzer, M. *et al*. A Nonapoptotic Cell Death Process, Entosis, that Occurs by Cell-in-Cell Invasion. 966–979, https://doi.org/10.1016/j.cell.2007.10.040 (2007).
51. Bartosh, T. J., Ullah, M., Zeitouni, S., Beaver, J. & Prockop, D. J. Cancer cells enter dormancy after cannibalizing mesenchymal stem/stromal cells (MSCs). *Proc. Natl. Acad. Sci. USA* E6447–E6456, https://doi.org/10.1073/pnas.1612290113 (2016).
52. Akimoto, K. *et al*. Umbilical cord blood-derived mesenchymal stem cells inhibit, but adipose tissue-derived mesenchymal stem cells promote, glioblastoma multiforme proliferation. *Stem Cells Dev.* **22**, 1370–1386 (2013).
53. Svensson, A., Ramos-Moreno, T., Eberstål, S., Scheding, S. & Bengzon, J. Identification of two distinct mesenchymal stromal cell populations in human malignant glioma. *J. Neurooncol.* **131**, 245–254 (2017).
54. Vignais, M. L., Caicedo, A., Brondello, J. M. & Jorgensen, C. Cell connections by tunneling nanotubes: Effects of mitochondrial trafficking on target cell metabolism, homeostasis, and response to therapy. *Stem Cells Int.* **2017**, 14–19 (2017).

55. Dittmar, T. & Zänker, K. S. Tissue regeneration in the chronically inflamed tumor environment: Implications for cell fusion driven tumor progression and therapy resistant tumor hybrid cells. *Int. J. Mol. Sci.* **16**, 30362–30381 (2015).
56. Dittmar, T. & Rossbach, M. human pluripotent stem cells in regenerative and personalized medicine. *Curr Mol Med* **13**, 691–694 (2013).
57. Cavallo, F., De Giovanni, C., Nanni, P., Forni, G. & Lollini, P.-L. 2011: the immune hallmarks of cancer. *Cell* **60**, 319–326 (2011).
58. Singec, I. & Snyder, E. Y. Inflammation as a matchmaker: revisiting cell fusion. *Nat. Cell Biol.* **10**, 503–505 (2008).
59. Tidjane, N. *et al.* A primary role for kinin B1 receptor in inflammation, organ damage, and lethal thrombosis in a rat model of septic shock in diabetes. *Eur. J. Inflamm.* **13**, 40–52 (2015).
60. Mangani, D., Weller, M. & Roth, P. The network of immunosuppressive pathways in glioblastoma. *Biochem. Pharmacol.* **130**, 1–9 (2017).
61. Nicoletti, N. F. *et al.* Mechanisms involved in kinin-induced glioma cells proliferation: the role of ERK1/2 and PI3K/Akt pathways. *J. Neurooncol.* **120**, 235–244 (2014).
62. Seifert, S. & Sontheimer, H. Bradykinin enhances invasion of malignant glioma into the brain parenchyma by inducing cells to undergo amoeboid migration. *J. Physiol.* **592**, 5109–5127 (2014).
63. Wolf, K. & Friedl, P. Extracellular matrix determinants of proteolytic and non-proteolytic cell migration. *Trends Cell Biol.* **21**, 736–744 (2011).
64. Torsvik, A. *et al.* Spontaneous malignant transformation of human mesenchymal stem cells reflects cross-contamination: Putting the research field on track - Letter. *Cancer Res.* **70**, 6393–6396 (2010).
65. Vinci, M., Box, C. & Eccles, S. A. Three-dimensional (3D) tumor spheroid invasion assay. *J. Vis. Exp.* e52686, https://doi.org/10.3791/52686 (2015).

Acknowledgements

This study was financed by an ARRS grant (Project J1–02474; awarded to TTL) in Slovenia; National Counsel of Technological and Scientific Development (CNPq Linha 2 – Bolsa Pesquisador Visitante Especial, Edital No 61/2011 [Proc. No. 402468/2012-0]; São Paulo Research Foundation [FAPESP] Proc. No. 2012/50880-4, granted to H.U.)in Brazil. TTL was a Visiting Professor within the Science without Borders Programme of the CNPq. M.O. was the recipient of a CNPq Doctorate Fellowship in Brazil and of a sandwich Doctorate Fellowship for performing part of her PhD at the National Institute of Biology in Ljubljana, Slovenia, and was a PhD Fellow of the Jožef Stefan International Postgraduate School, Ljubljana, Slovenia. We acknowledge Dr. Christoph Berry for his valuable comments and English corrections. We acknowledge Sandi Ravbar for his valuable English correction.

Author Contributions

Conceived and designed the experiments: M.N.O., M.M.P., H.M., H.U., T.T.L. Performed the experiments: M.N.O., M.M.P., H.M. Analysed the data: M.N.O., M.M.P., H.M., H.U., T.T.L. Contributed reagents/materials/analysis tools: T.T.L., H.U.; Wrote the paper: M.N.O., M.M.P., H.M., H.U., T.T.L.

Additional Information

Supplementary information accompanies this paper at https://doi.org/10.1038/s41598-018-19359-1.

Competing Interests: The authors declare that they have no competing interests.

Publisher's note: Springer Nature remains neutral with regard to jurisdictional claims in published maps and institutional affiliations.

(Supplementary Information) Kinin-B1 Receptor Stimulation Promotes Invasion and is Involved in Cell-Cell Interaction of Co-Cultured Glioblastoma and Mesenchymal Stem Cells

Mona Oliveira, Helena Motaln, Micheli Pillat, Henning Ulrich, Tamara Lah

Reproduced from Scientific Reports. Accepted: December 21, 2017, published on January 18, 2018

Kinin-B1 Receptor Stimulation Promotes Invasion and is Involved in Cell-Cell Interaction of Co-Cultured Glioblastoma and Mesenchymal Stem Cells

Mona N. Oliveira[1,2,3],Micheli M. Pillat[1], Helena Motaln[2], Henning Ulrich[1,3]*and Tamara T. Lah[2,3,4]*

[1]Department of Biochemistry, Institute of Chemistry, University of São Paulo, Av. Prof. Lineus Prestes 748, São Paulo - SP, 05508-000, Brazil

[2]Department of Genetic Toxicology and Cancer Biology, National Institute of Biology, Večna pot 111, 1000 Ljubljana, Slovenia;

[3]Jožef Stefan International Postgraduate School, Jamova ulica 39, 1000 Ljubljana, Slovenia

[4]Department of Biochemistry, Faculty of Chemistry and Chemical Engineering, University of Ljubljana, Večna pot 113, 1000 Ljubljana, Slovenia

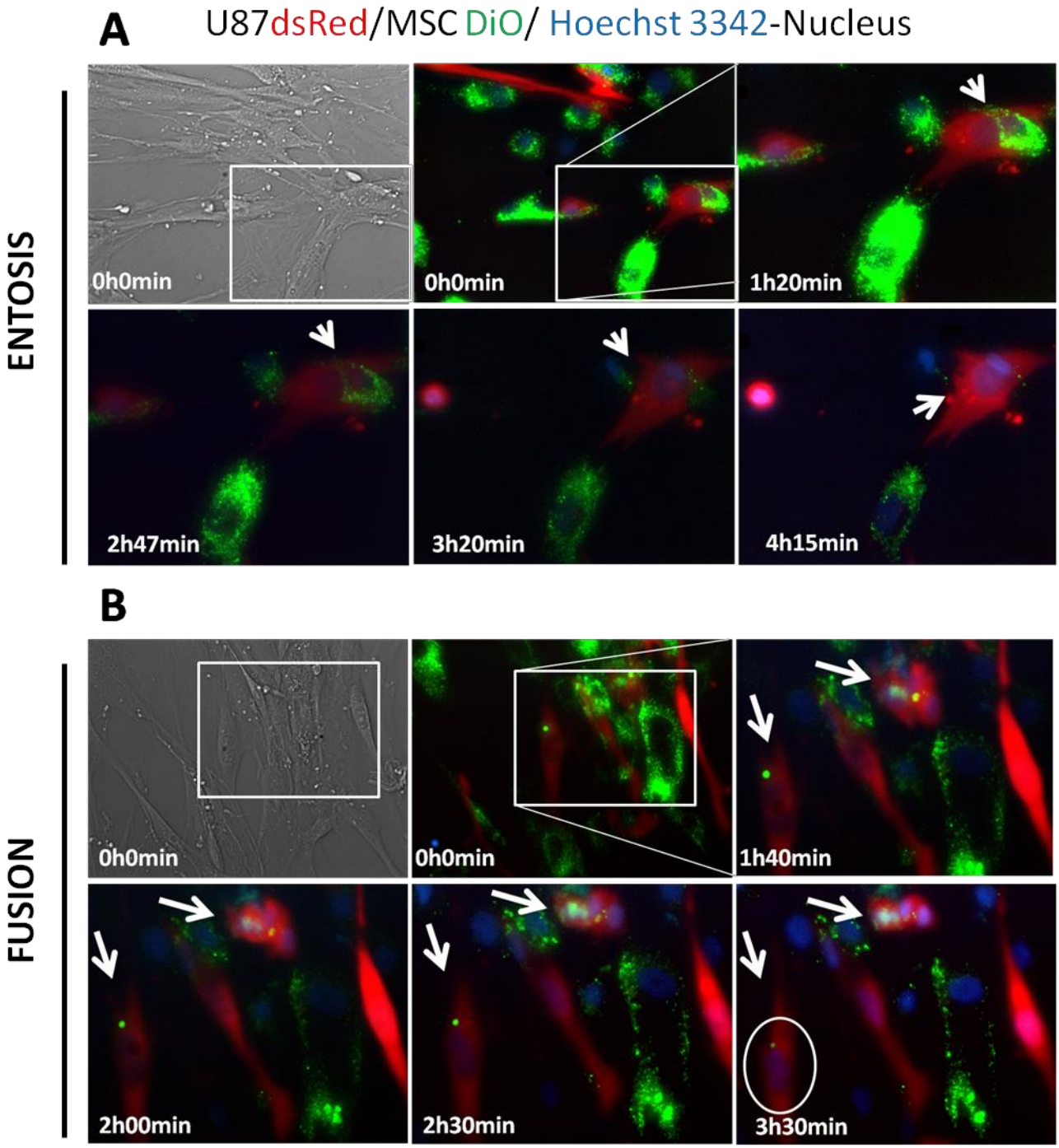

Supplementary Figure S1. Time lapse imaging of U87dsRed/BM-MSCDiO co-culture shows entosis, cell fusion and vesicle transfer after 48h. (A) Demonstration of the steps of process, similar to entosis of a BM-MSC DiO (green) and U87dsRed cells (red), following cells fusion event. (B)The time lapse demonstrate the steps of nuclear fusion. Fused cells progressively fuse the nuclei exhibiting a combined yellow staining marked by arrows. BM-MSC also secrete 6 large vesicle (in green) marked by a circle.

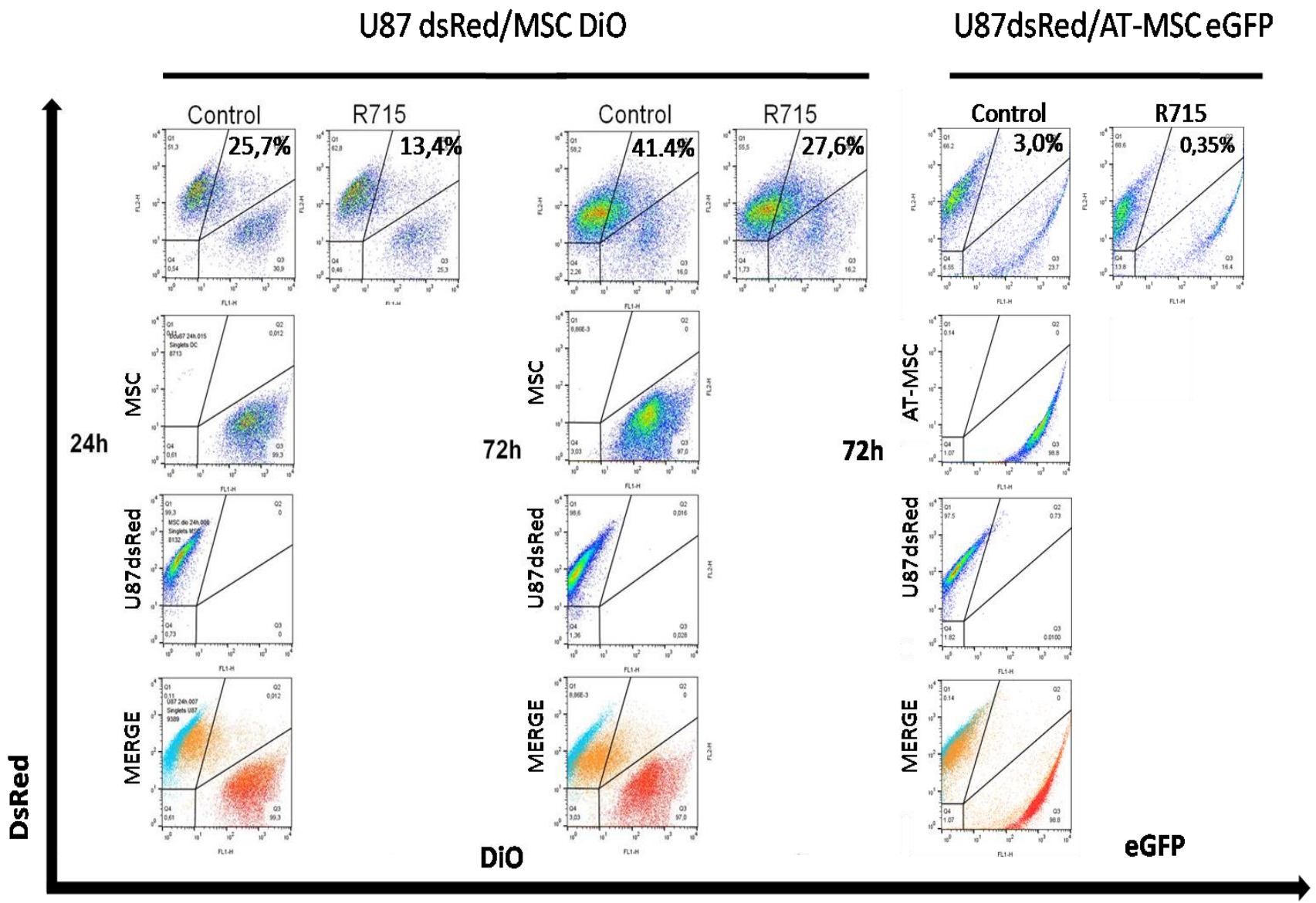

Supplementary Figure S2. Dot-plots of U87dsRed/BM-MSCDiO and U87dsRed/AT-MSCeGFP 9 co-culture shows cell fusion and vesicle transfer after 24h and 72h treatment with R715. Cell-cell interaction of U87 dsRed cell, BM-MSC DiO and AT-MSCeGFP were measured by flow cytometry. The representative dot-plots of control or treatment with R715 after 24h 12 and 72h are presented.

Chapter 4

Bradykinin Induces Epithelial-to-Mesenchymal Transition, Enhancing Invasion of Glioblastoma Cells in Co-Cultures with Mesenchymal Stem Cell

Mona N. Oliveira[1,2,3], Micheli Pillat[1], Tamara T. Lah[2,3] and Henning Ulrich[1]

[1] Department of Biochemistry, Institute of Chemistry, University of São Paulo, Av. Prof. Lineu Prestes 748, São Paulo - SP, 05508-000, Brazil
[2] Department of Genetic Toxicology and Cancer Biology, National Institute of Biology, Večna pot 111, 1000 Ljubljana, Slovenia;
[3] Jožef Stefan International Postgraduate School, Jamova 39, 1000 Ljubljana, Slovenia

Manuscript in preparation

Abstract

Glioblastoma (GBM) is the most common primary tumor of the central nervous system and is highly aggressive with a median survival of about 15 months. Pronounced tumor intra- tumor and inter- tumor heterogeneity, as well as cancer (stem) cells' plasticity create obstacles to efficient treatment of glioblastoma patients. Tumor progression involves interactions between cancer cells and exogenous components, including various types of stromal cells recruited to the tumor. Among these are mesenchymal stem cells that contribute to the tumor microenvironment. The mutual interactions among mesenchymal stem cells various subpopulations of cancer cells is still not sufficiently understood.

In this study we aimed to compare the effects of bone-marrow-derived mesenchymal stem cells (MSCs) on two glioblastoma U87 and U373 cells in direct co-cultures, modestly modeling heterogeneity of glioblastoma. The interactions among these cells was addressed in the in-vitro two-dimensional (monolayer) and three-dimensional (spheroid) co-cultures. The U87 cells expresses higher levels of bradykinin receptor1 (B1R) than U373 cells and their migration/invasion was greatly enhanced by the agonist bradykinin (BK), but blocked by B1R antagonist (R715) and B2R antagonist (HOE) alone and when co-cultured with MSCs. BK receptors' activation correlated with significantly higher U87/MSC cell-cell interactions (heterotypic fusion, vesicle transfer and enosis. i.e. "cell cannibalism". Furthermore, the kinins triggered invasion, F-actin expression as well as epithelial-to-mesenchymal transition genes' expression in U87 cells upon U87/MSC co-cultures. After treatment with both kinin receptors antagonists the invasion of U87 was significantly reduced. Altogether, these data support the on-going investigations of kinin receptors B2R and B1R as targets for adjuvant approach in glioblastoma therapy. Secondly, our results emphasize the need for further careful investigations of MSCs as potential candidates for cancer therapies, as they may adversely affect different cancer cell-subtypes, also depending on the levels of kinin/kinin receptors system.

Keywords: Bradykinin, Kinin Receptors, Epithelial-to-Mesenchymal Transition (EMT); Glioma, Mesenchymal Stem Cells.

4.1 Introduction

Glioblastoma (GBM) is characterized as most aggressive stage of glioma (WHO grade IV), mostly due to cooperative interactions among genetically distinct subclones, including the GBM stem cells, presenting barriers to effective therapy. Four genetically distinct subtypes: neural, proneural, classical and mesenchymal have been characterized (Verhaak et al. 2010), the latter being most invasive with the shortest survival rate of patients. Our previous work suggested that the standard GBM cells models used in vitro, comprising the U373/U251 and U87 cells, differ and that U373 is representing more mesenchymal, whereas U87 expresses more neuronal/proneural characteristics (Breznik et al. 2017). Motaln et al. (2015) reported that indirect interactions between these two heterogonous GBM cells resulted in enhanced drug resistance. The authors showed that their cross-talk altered the expression 264 genes in U87 cells that are associated with proliferation, inflammation, migration, and adhesion, and 221 genes in U373 cells that are associated with apoptosis, the cell cycle, cell differentiation and migration. Indirect and direct co-culturing of U87 and U373 cells showed mutually opposite effects on temozolomide resistance. Furthermore, Breznik et al (2017) first pointed on U87 and U373 cell-type-specific responses to bone-marrow derived mesenchymal stem cells (MSCs). In 2D and 3D direct co-cultures MSCs inhibited the invasion of U87 cells and enhanced the invasion of U373. MSC-enhanced invasion of U373 cells was assisted by overexpression of various invasion associated

proteases, such as cathepsin B, urokinase plasminogen activator (u-PA) and metalloproteases (MMP 2 and MMP 9).

These data suggest that tumor infiltrating cells, the so called "stromal cells", such as fibroblasts, macrophages, endothelial cells, pericytes and immune cells crucially change tumor microenvironment. (Quail and Joyce 2017; Zarkoob et al. 2013; Melzer et.al 2016). Among these, mesenchymal stem cells, also termed mesenchymal stromal cells, have special role as they can transdifferentiate into tumor-associated fibroblasts (TAF), pericytes, and possibly even to GBM stem cells (reviewed in Apaix et al. 2014). As glioma cells, as well as MSCs differentially express connexins, Schichor et al. (2012) speculated that they interact via gap-junctional coupling and found that besides this so-called functional syncytium formation cell fusion events, i.e. structural syncytium formation is enabled. On the other hand, MSCs play an important immunomodulatory role, producing and secreting a plethora of cytokines (Motaln et al, 2012; Motaln and Lah 2016; Behnan et al. 2013) and exchange these with cancer cells, either directly or via extracellular vesicles (EVs) (Baglio et al. 2012; Del Fattore et al. 2014). As MSCs have inherent tumor-trophic migratory properties, and have been indeed engineered to express anti-proliferative, pro-apoptotic, anti-angiogenic agents, they may serve as vehicles that specifically deliver and target different cancer types (Sasportas et al. 2009; Shah et al. 2012; Li et al. 2015).

Among the pro-inflammatory mediators, the kallikrein-kinin system plays a special role in tumor microenvironment. The endogenous kallikrein related proteolytic cascade, stating from plasma or tissue kininogens, results in the release of bioactive kinins (bradykinin and kallidin). Kinins are involved in many pathophysiological processes, such as regulation of blood pressure, renal and cardiac function acute and chronic inflammation Stewart et al. 2002) as well as cancer(Kashuba et al. 2013), including glioma (Uchida et al. 2002 ; Seifert et al. 2014). Kallikrein-kinin system activities are mediated by two cell membrane bradykinin receptors type 1 (B1R) and type 2 (B2R) receptor, which convey different pharmacological effects. The B2R is activated by bradykinin and kallidin, obtained by cleavage of low and high molecular weight kininogens, whereas B1R is activated by its metabolite, originating from the kinin cleavage of the Arg C-terminal by type I kinases (carboxy peptidases (Zhang et al. 2012)) that release des-Arg9-bradykinin and des-Arg10-kallidin (Maurer et al. 2011). In contrast to the B2R, which is expressed in a wide variety of cells and tissues, the B1R is poorly expressed under normal conditions, but can be induced in vivo and in vitro by endotoxins, cytokines and growth factors, indicating specific roles in pathological processes (Tidjane et al. 2015).

Pillat et al. (2014) have previously shown that both B1R and B2R are expressed in U87 cells and in MSCs and that in indirect and direct U87/MSC co-cultures, B1R gene and protein increased this being correlated with their enhanced invasiveness via induction of metalloproteases. Later, we demonstrated differential responses of U87 and U373 GBM cells to MSC in terms of cell proliferation, cell cycle and in heterotypic cell-cell interaction (Oliveira et al. 2018). B1R agonist des-Arg9-BK stimulated only U87/MSC, but not U373/MSC mixed spheroids and increased migration/invasion of U87 cells. We think that this is most likely due to significantly lower BR1 expression in U373 cells. Here we aimed to further investigate the role of bradykinin in two GBM cell models U87 (transfected with Red-ds) and U373 (transfected with eGFP) cells, that were co-cultured with bone marrow and adipose MSCs to determine the mechanisms of invasion and of previously suggested co-stimulation effects between B1R and B2R (Pillat et al. 2014). We proposed here that upon activation of BR signaling with kinin agonist and antagonists, these had an impact on cell invasion via an epithelial-to mesenchymal –like cell transition.

4.2 Results

Bradykinin receptor agonists and antagonists affect cell viability in glioblastoma cell and in their cultures with mesenchymal stem cells.

The effects of increasing doses of antagonists of B1R (R715) and B2R (HOE140) in the mono and co-culture conditions was measured at increasing (1nM, 3nM, 30nM and 100 nM) concentrations in the absence of fetal bovine serum (FBS) after 3 days cultures by the MTT assay (Figure 4.1.A). Glioblastoma cells were not significantly affected by HOE140, but the R715 significantly decreased the viability of do 50% in the dose dependent manner, whereas both antagonists decreased MSC viability down to 70-80%. In the co-cultures, the cytotoxic effects of antagonists were not significant both in 2D and 3D cultures (Figure 4.1.B), most likely due to due to lower exposure of bradykinin receptors on cell surfaces, or a possible induction of drug-resistance mechanisms such as gp180/MDR proteins activation upon co-cultures (Delphine et al. 2015). Interestingly, treatment of monocultures with agonist BK for 5 days significantly increased proliferation (Figure 4.2.B). However, in the co-cultures, there was no such proliferative effect observed by BK treatment, indicating more on the lack of receptors' availability to ligands' binding in the co-cultures (Figure 4.1.C,D), as also observed with antagonists binding (Figure 4.1.B).

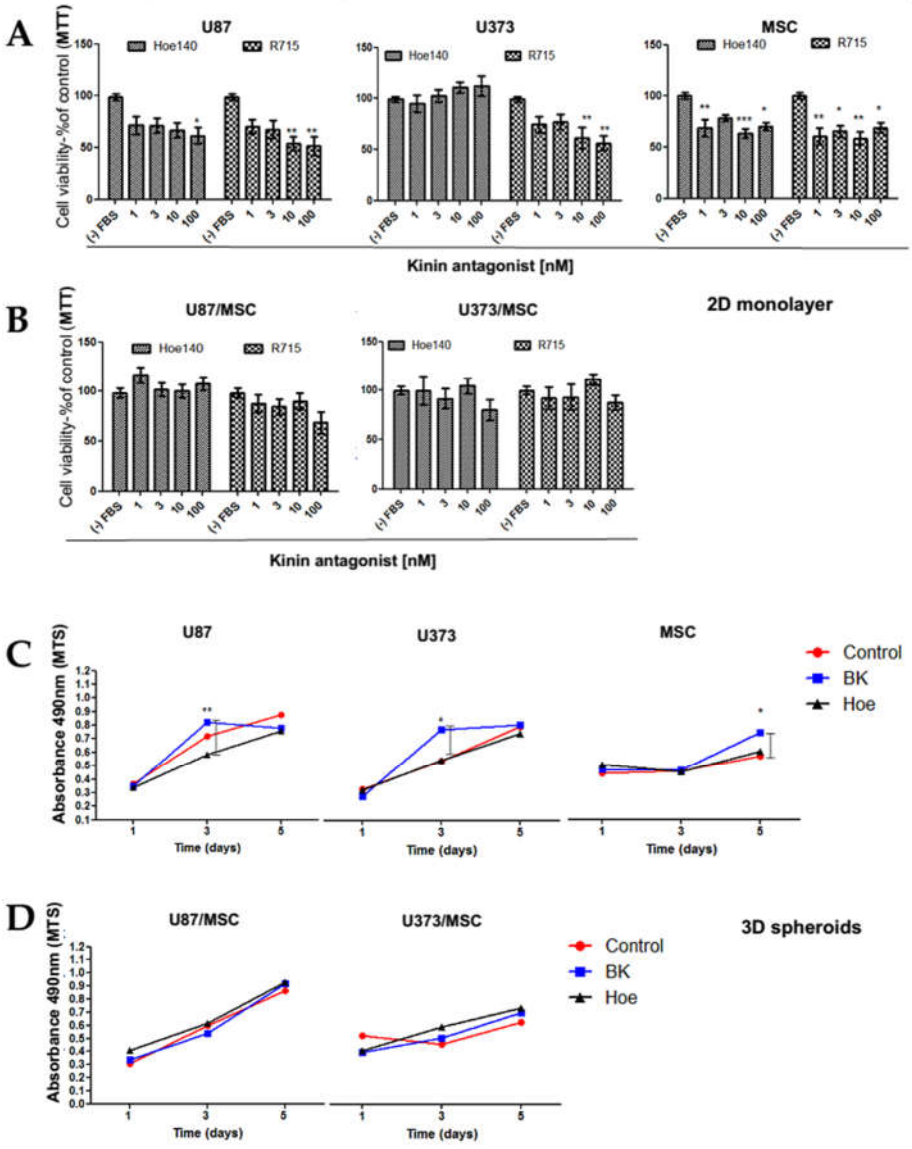

Figure 4.1: The effects of kinin receptors' antagonists and agonists on cell viability.
A) Cell viability in 2D cell cultures treated with kinin antagonist (HOE140 and R715) at 1 nM, 3 nM, 10 nM and 100nM for 72h of U87 and U373 and MSC monocultures in the absence of FBS, as determined by the MTT assay, as described in Methods.

B) Cell viability of U87/MSC and U373/MSC co-cultures, treated as above (A).
C) Cell viability of 3D spheroids after treatment with agonist (at 100 nM BK) and antagonist (HOE140 at 100 nM) for 1, 3 and 5 days of U87 and U373, and MSC monocultures, determined by the MTS assay, as described in Methods.
D) Cell viability of U87/MSC and U373/MSC co-cultures, as described under C). One-way analysis of variance was performed following Bonferroni's multiple comparison Test. P value*<0.05. Two-way analysis was performed following Bonferroni's multiple comparison Test. P# value <0, 05 and ### <0.0001 is representative of three independent experiments.

Activation of B1R and B2R receptors in glioblastoma cells and when co-cultured with mesenchymal stem cells.

We examined the intracellular calcium oscillations after bradykinin and antagonists HOE and R715 treatment under different experimental conditions (monocultures and co-cultures) of U373 and U87 cells, using calcium image, which shows cytosolic calcium concentration transients (Δ[Ca2+]i) after treatment with agonist bradykinin (100 nM) (Figure 4.2.A). Figure 4.2.B presented the wave of excitation in the monocultures of U87, U373 cells, which after 1 min returned to the desensitized state. However, it was only in the U87/MSC co-culture, where the formation of an excitatory plateau was observed, which was extended for over 2 min with amplitudes similar to that of the monoculture. To confirm the presence of co-stimulation of both receptors, as previously reported by Zhang et.al. (2018), a second experiment, using the antagonist to B1R and B2R was performed. The results showed strong evidence that there is a co-stimulatory effect of B2R and B1R, since BK is rapidly converted in DBK (Figure 4.2 C). The Δ[Ca2+]I of calcium observed in monoculture conditions is a typical B2R response. Furthermore, the Δ[Ca2+]I observed in the co-culture agrees with a response profile of type B1R co-stimulation and it is only reduced to that observed in U87 and MSC monoculture after R715-antagonist treatment.

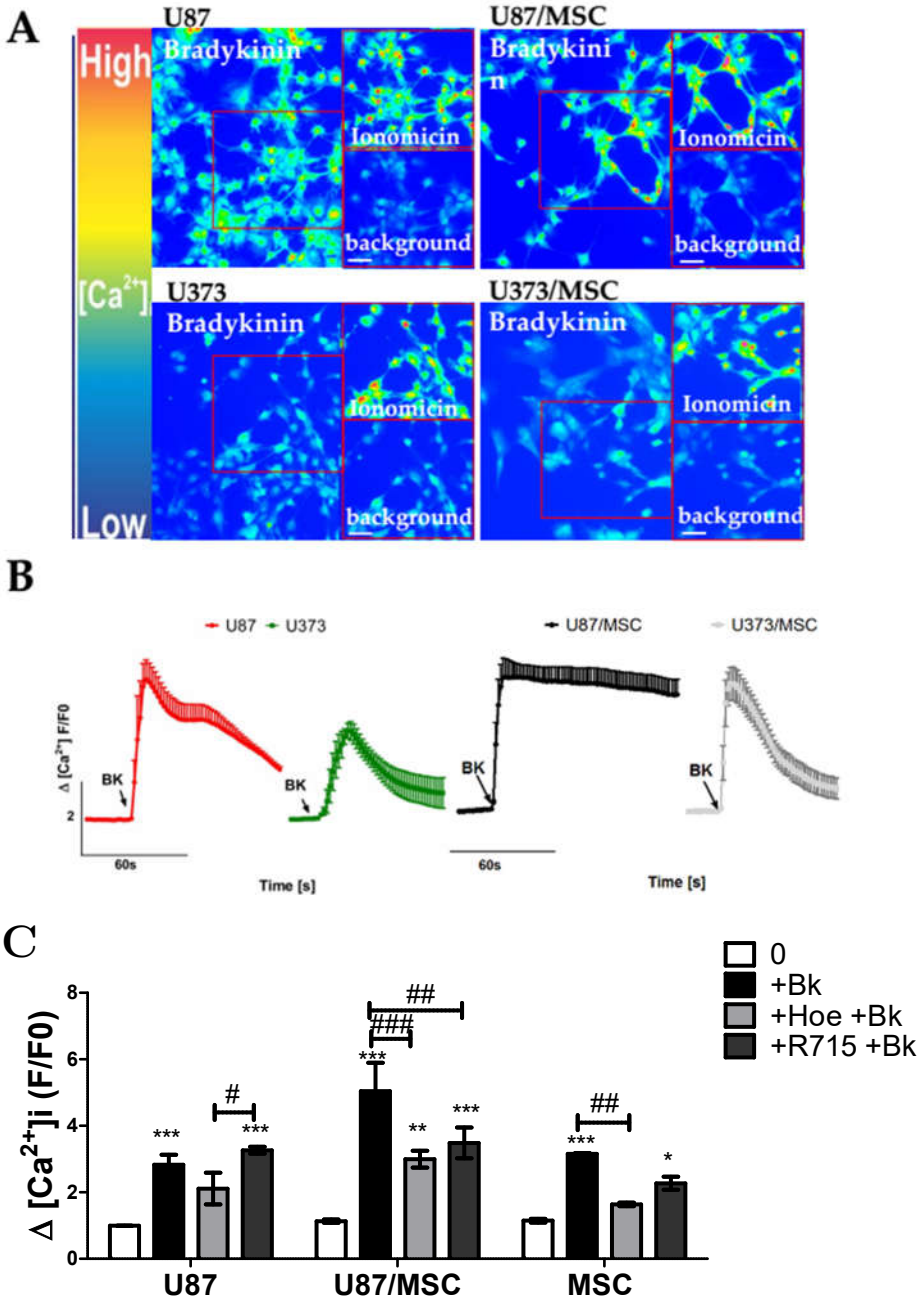

Figure 4.2: Activation of B1R and B2R after bradykinin treatment in U87/MSC co-culture.

A) The intracellular calcium flow vs time were monitored by calcium image in live cells after stimulation with bradykinin.

B) Calcium imaging wave plots of U87 cells (red line) and U373 cells (green line) in mono culture (right panel) and in U87/MSC and U373/MSC co-cultured cells (middle panel). Representative images of calcium intracellular detection after bradykinin.

C) Effect of B2R antagonist (HOE140 at 100nM) and B1R antagonist (R715 at 100nM) treatment on the calcium wave in U87 cell, U87/MSC cells and in MSCs. The intracellular calcium levels were monitoring by calcium image. One-way variance analysis was performed following Bonferroni's multiple comparison test. P value*<0.05. Two-way analysis was Performed Following Bonferroni's Multiple Comparison Test. # P value <0, 05 and ## <0.001 is representative three

independent experiments.

Mesenchymal stem cells trans-differentiation in co-cultures cancer-associated fibroblast formation.

As our previous data showed that U87 cell lines interacted with MSC to about ten times much greater extent than U373, thus we have further investigated U87/MSC co-cultures. We have also previously reported that U87 dsRed cells acquired mesenchymal phenotype when co-cultured with MSC, reflected in the increased expression of mesenchymal-specific membrane markers, adhesion protein CD29 and MSC markers CD90 and CD105 in co-cultures by flow cytometry that we interpreted either as U87 trans-differentiation or that the hybrid cell population that we have detected upon prolonged co-culture incubation induced the expressed of these markers. We used time-lapse microscopy of co-cultures compared to monocultures (Figure 4.3). Interestingly, co-cultures showed higher cell motility and interaction by formation of protrusion between U87 and MSC. The vesicles transfer between MSC cell and U87 was observed after 3-6h in both directions. Figure 4.3.B shows cell fusion event after 8h incubation between U87dsRed and MSCDiO-green-labeled cells, with nuclei visualized by Hoechst staining. Figure 4.3.C suggests cell cannibalism event, where a (green) MSC cell is internalized by the neighbor cell (U87). The nucleus of the host cell has been monitored to confirm the presence of the cannibalism. It is observed that the nucleus acquires a moon-like shape during cell internalization and is afterwards relocated, during vacuole formation, indicated by arrows (full lines: U87 host nucleus: dashed lines: MSC hosted cells) on Figure 4.3.C. Last, we analyzed the cell motility by monitoring cell angulations (directionality) by the local gradient variation of cell positioning during a specific timeframe as described in Methods, using the open source Fiji. 3.0 software. The histogram shows the amount of cells that change positions during the time in the co-culture conditions and co-culture after treatment with antagonist HOE140 and R715. When we treated these cells with antagonists HOE140 and R715 at (100nM final concentration) to inactivate both kinin receptors, there is clear a reduction of cell motility (Supplementary 5 video frame) and a reduction of the cell numbers that move to different angulations (Figure 4.3.D, left panel), indicating that these processes are mediated kinin receptors activities.

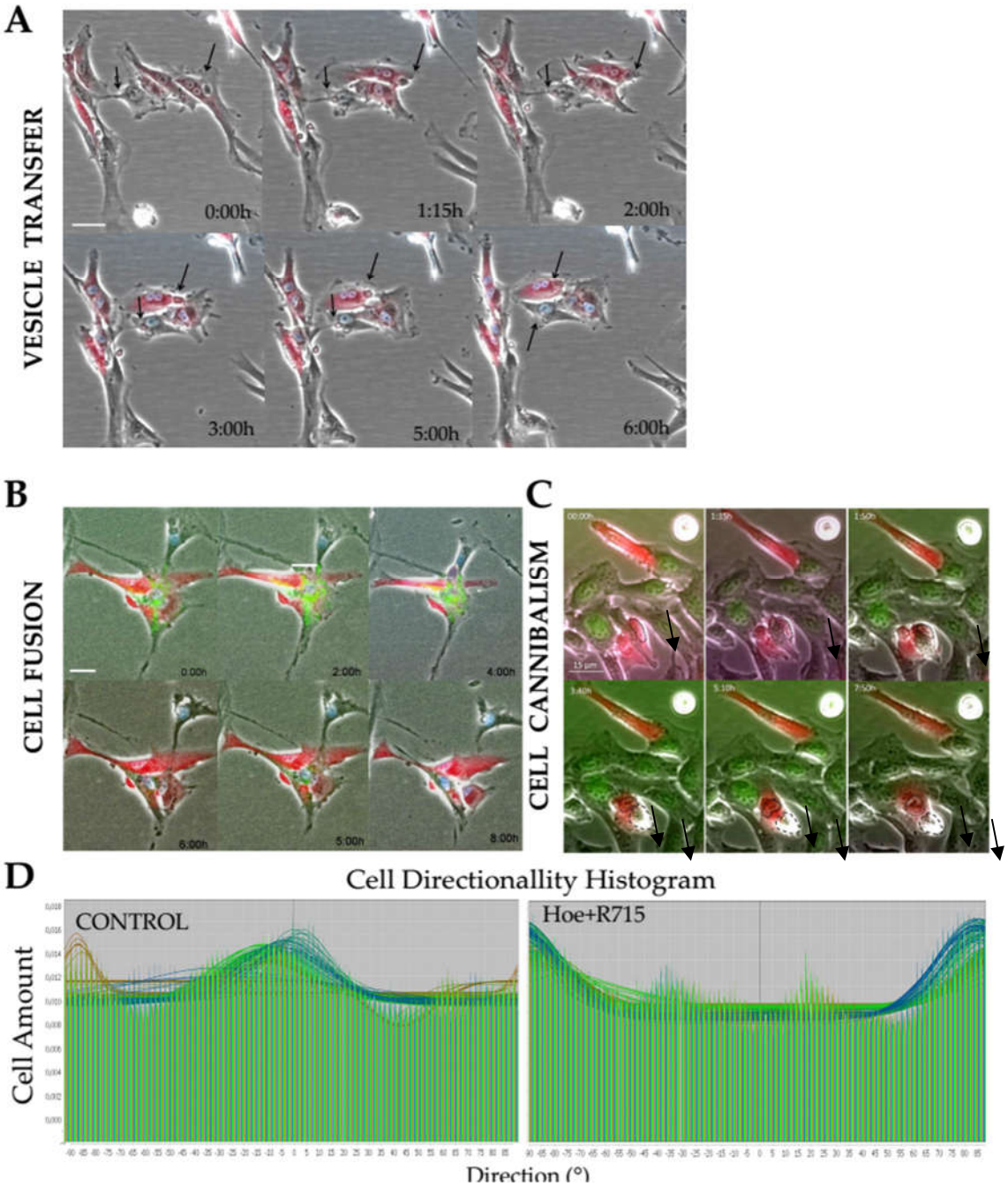

Figure 4.3: Cell-cell interactions and cell motility are reduced after –co-treatment with HOE140 and R715 of antagonists of U87/MSC cell co-cultures.

A) Time-lapse microscopy of U87dsRed cells and MSC (non-labelled, grey) were pre-cultured v for 3 days, (scale bar=25µm) for 8-6 hours observation. The arrows show ectosomes (vesicles) transfer between the cells.

B) Time-lapse microscopy of U87dsRed and MSC (stained DiO green) pre-cultured for 3 days, shows the cell fusion process (scale bar=25µm) within 1-6 hours.

C) Time-lapse of U87dsRed cells and MSCeGFP (nucleus) pre-cultured for 3 days, arrows shown the suggesting entosis, i.e. cell cannibalism processes (scale bar=15µm).

D) Directionality histogram of cell motility in the area was measured as described in Methods. Local gradient analysis was used to calculate the number of cells in a certain direction (angulations°). The points were monitored along the time scale,

and the plot presents the cells number in known angulations and the angulations variation along time.

Bradykinin activity affected F-actin expression and promoted the cell-cell interaction.

For further investigations of the cell-cell interaction fate and the relevance of kinins in this process, we evaluated the F-actin expression after co-culture and treatment with kinin receptor agonists and antagonists using immunocytochemistry and flow cytometry assay. Figure 4.4.A shows the higher induction of F-actin expression after co-culture for 3 days (see also supplementary data 6 ICC image). In U87 monoculture, where 27% of cells expressed F-actin, increasing by about 2-3-fold in U87/MSC co-cultures. Bradykinin treatment increased F actin expression in co-cultures by about 20%, being reduced after treatment with HOE140 and by more than 50% after treatment with both antagonists (HOE140 and R715) (Figure 4.4.B, C). This result demonstrates the relevance of co-stimulation between od both B1R and B2R for regulation of i F-actin expression. F-actin bundled is crucial for lamellipodia formation on the periphery of the cell, the most prominent cytoskeleton structure that drives cell locomotion (Johnson et al. 2015). These results show that bradykinin plays an important role in cell-cell interaction trough F-actin expression, which affects various processes, related to cell movements (Kozma et al. 1995).

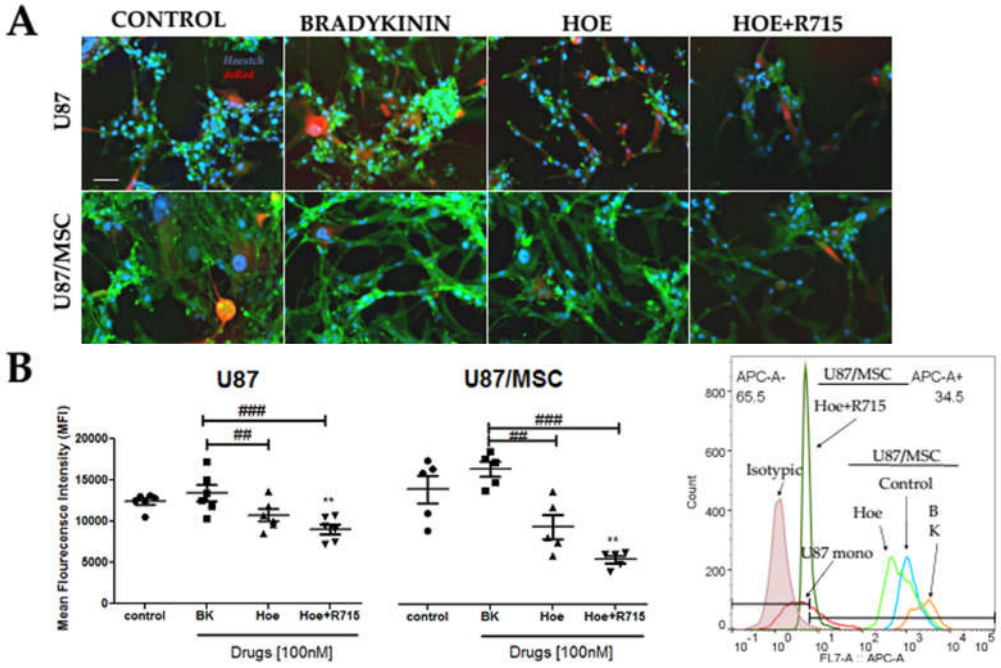

Figure 4.4: Bradykinin-mediated up-regulation of F-actin

A) Representative immunocytochemistry images of F-actin expression, labelled by antibodies and stained by Phalloidin Alexa Fluor 488) in U87 monoculture and U87/MSC co-culture and MSCs in the control and treatment condition, using BK=bradykinin,HOE140, and HOE140 R715) after 3 days in green and Ds RED, where nuclei are stained by Hoechst blue (scale bar= 100 µm).

B) Quantification of mean fluorescence intensity measured by Fuji software image analysis 3.0 of images generated from three experiment, (left panel) representative histogram of F-actin positive cells (phaloidin-647nm light emission), as determined by flow cytometry analysis of U87 cell and U87/MSC co-cultured cells after treatment with bradykinin (BK), HOE (HOE140) and HOE+R715.

Bradykinin induced the epithelial to-mesenchymal transition genes' expression and enhanced invasion in U87 cells and U87/MSC co-cultures.

Due to pronounced effects of kinin system on F-actin, we hypothesized that the BK would enhance invasion of U87 cells in monocultures and in co-cultures (U87/MSC) after treatment with BK. The glioblastoma U87 were grown in cells 3D spheres, covered with Matrigel and the area of cell invasion were measured over time. BK increased the invasive potential of U87 cells, and showed that the co-culture after 7 days was more invasive than the monoculture (Figure 4.5.B). The B2R inhibition by HOE140 reduced invasion by 40% compared by BK treatment (Fig. 5.B). To reveal the mechanism, underlying the enhanced F-actin induction, leading to enhanced invasion, we separated the U87 cells from co-cultures, using with the media supplemented with geneticin (G418) at 2 mg/ml to select for U87dsRed cells only as only those cells contain the Neo resistance cassette in their genome, but eliminate MSCs. On the 4th day the surviving cells out of U87dsRed monoculture and U87/BM-MSC co-culture were collected and mRNA was extracted. The genes related to EMT were determined by RT-PCR in U87 mono- and co-cultures, the latter selected and separated from MSC in co-cultures (Figure 4.5.C, left panel). To reveal if the BR1 and BR2 receptors activation was playing a role in EMT genes induction, we treated the U87 monocultures and co-cultures with bradykinin, HOE140 and R175 (Figure 4.5.C right panel). Taken together, these results show that bradykinin triggered the EMT genes' expression and invasion (Figure 4.5.B) under both culture conditions. The activation by bradykinin is inducing vimentin, CD44, Snail and TGFß in U87 cells alone (see first three bars) and even more in U87, separated from co-cultures (last three bars) all, being hindered by HOE140 alone and HOE140 and R175 treatment.

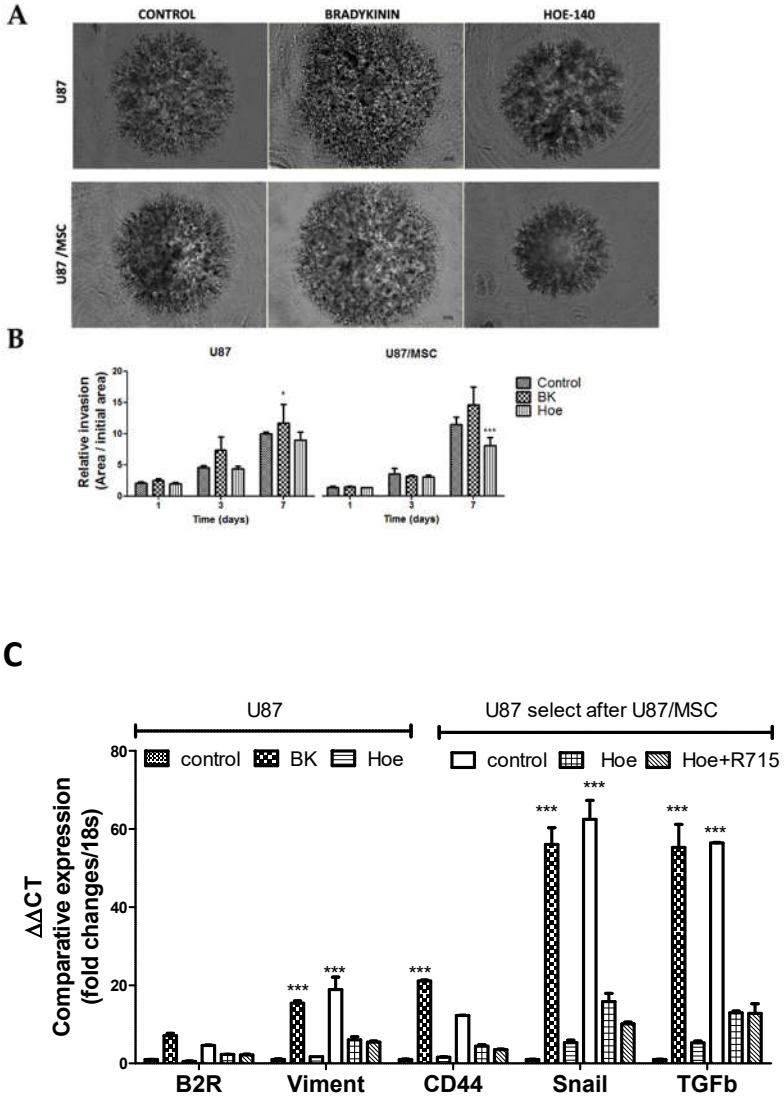

Figure 4.5: Bradykinin trigged invasion by upregulation of EMT-associated genes expression in U87 cell monoculture and co-cultures.

A) Spheroids were prepared either from U87dsRed, and U87/MSC co-cultures in 1: 1 ratio, embedded in Matrigel as described in Methods. Representative images of U87 and U87/MSC mixed spheroids were taken after 1, 2, and 3 days at 4x magnification. Initial invasion area and spheroid area were measured with the NIS-element v 2.13 software (Nikon Corporation Ltd.).

B) Invasion (%) was calculated according to the equation (X area initial area T0 / 100) tx = mean time of the day were collected measure, T0 = mean area of migration sphere day 0. One-way analysis of variance was performed following Bonferroni's multiple comparison test. P value*<0.05. Two-way analysis was performed following the Bonferroni's multiple comparison test. *** P value <0.0001 is representative of three independent experiments.

C) Total RNA was isolated from 2D monolayer mono-cultured U87 cells and from U87 cells isolated from mixed co-cultures after geneticin selection (U87/BM-MSC) with medium (control) or after treatment with bradykinin (BK), HOE140 and HOE140+R715 using the Trizol reagent. The relative quantification of gene expression levels of B2R, Vimentin, CD44, Snail, TGFβ and GADPH were carried out using real-time PCR, as described in Methods.

4.3 Discussion

Tumor microenvironment is becoming increasingly recognized to have substantial effects on tumor progression and thus new approaches, targeting the less resistant stromal cells are very attracting. Thus, interrupting the molecular crosstalk between glioma and brain parenchyma that is instructing histopathological features in GBM, may alter GBM cells response to its microenvironment (Bougnaud et al. 2016). We believe that targeting interactions between glioblastoma (GBM) cells and mesenchymal stem cells (MSCs) that have multiple effects on GBM progression is promising.

Here, we focused on their impact on GBM –MSC crosstalk and proved that this is tightly associated with kinin/kinin receptors. Their signaling is present in normal brain and related mostly to blood brain barrier homeostasis and angiogenesis (da Costa et al. 2012; Cote et al. 2014). Bradykinin kinin B2 receptors (B2R) expression in glioma tissues correlated with the stage of malignancy (Montana and Sontheimer, 2014), whereas B1R expression was induced in GBM by high levels of inflammatory cytokines, produced by tumor infiltrating immune cells and MSCs. We have previously confirmed that both B2R and B1R are highly expressed in GBM U87 cells, but not in GBM U373 cells, and both receptors were also constitutively expressed in MSCs (Pillat et al. 2012) However, upon direct or indirect co-culture the MSC expression levels of both receptors were down-regulated or not altered (Oliveira et al. 2018).

The activation of the kinin B1 and B2 receptors resulted in the proliferation of U87 and U373 cells in monocultures, but not in co-cultures (Figure 4.1). Our data on the effects of BR those by Lu et al (2010), demonstrating that upon the biding the ligands, DBK and BK, the B1R andB2R, respectively are increasing proliferation of GBM cell lines. Our results also demonstrate "co-stimulation" of the kinin-B1 and B2 receptors that is not due to their direct interactions, but rather by their signaling pathways crosslinking. Direct proof of the importance of communication between these two receptors was the reduction of invasion by the addition of two B2R and B1R selective antagonists, HOE140 and R175, respectively, although these have not totally block by the agonists. This may be due to the metabolic dynamics of bradykinin derivatives that may influence the communication between these two receptors (Barki-Harrington et al. 2003). Recently, various antagonists of both receptors have been used as promising tools for treating prostate cancer in clinical phase II (Whalley et al. 2012). However, the effects of kinins does depend on the type of cancer. It has been is observed, for example, that activation of the B1R suppresses growth of melanoma cells (Dillenburg-Pilla et al. 2013), while promoting the proliferation of estrogen-sensitive breast cancer cells (Molina et al. 2009).

Additionally, kinin receptors, when activated, influence chemotaxis and tumor invasion. Both receptors are coupled Gq protein receptors activating phospholipase C (PLC)-βyielding diacylglycerol (DAG) and inositol 1,4,5 triphosphate (IP3) and triggers Ca ions fluctuation. In U87/MSCs co-culture condition we observed a continuous release endoplasmic calcium ([Ca2+]i) release after stimulation with BK (Figure 4.2). Seifert et al (2014) reported that cytosolic calcium ([Ca2+] i) release directly stimulated glioma cell invasion, by inducing the formation of small bleb-like protrusions at their plasma membrane, resulting in contraction of the cytoskeleton, cytoplasmic flow and activation of Ca ions-dependent K+ and Cl− channels that stimulate an amoeboid phenotype of migration. The mechanism involves the ions fluctuations to reduce glioma cell to volume down to 33% of its original size, and remove free cytoplasmic water outside the cell via Cl− efflux (Thompson and Sontheimer 2016). On the other hand, the increased motility of glioma cells may also result from B1R downstream signaling via PI3K/ Akt pathways. affecting the transcription factors c-Jun/AP-1, known to affect cell invasion and migration.

Here we demonstrated that the BR1 signaling mechanisms is directly affecting the migration (Figure 4.3) by inducing the genes, associated with epithelial-to-mesenchymal transition (EMT). During this transition, the cells lose the epithelial morphology and gain

mesenchymal phenotype, such as spindle-like morphology and enhanced migratory capacity. EMT is triggered by major transcription factor TGF-β, and further by Snail1/2 and ZEB that regulated the expression of membrane protein CD44 and cytosolic vimentin, and actin proteins (Dezso et al. 2014; Kalluri and Weinberg 2009; Gu et al. 2016). A shift towards the mesenchymal subtype appears to be a common pattern in cancer progression by which cancer cells acquire a more aggressive phenotype (Iwadate 2016) Similar to Bryukhovetskiy and Shevchenko (2016), we found that TGF-β is triggered in U87 cells by kinin agonists, whereas the antagonists prevented the EMT (Figure 4.5) The BR1 activation of EMT was highly increased in U87 after being co-cultured with MSCs and separates for the EMT-associated gene analyses.. On the other hand, MSC co-culturing alone was sufficient to enhance the invasion of mesenchymal GBM-subtype U373 cells, that express very low levels of bradykinin receptors (Oliveira et al., 2018). but express TGF-β responsive genes (Breznik et al., 2016). Presumably, these were triggered by MSC secreted/ transduced factors to become more invasive. However, the induced invasiveness of U87 cells in mixed spheroids with MSC appeared to be delayed, up to between 4-7 days and this coincided with the appearance of heterotypic fusion events (see below). Taken together this data may suggest selective roles of bradykinin receptors in neural/proneural vs mesenchymal GBM subtype interactions with MSCs. In TH GBM microenvironment in vivo, inflammatory cytokines may enhance kinin production and thereby enhance neural/proneural GB invasion. By the same token, kinin receptors antagonists may be suggested as beneficial for a more individualized treatment of patients with this GBM subtypes.

EMT alone may not be sufficient to be involved in tumors invasion and metastasis, as suggested by Sheng et al. (2015), showing that within a predominantly epithelial metastatic tumor, only a small proportion of tumor cells did undergo EMT. Notably, lung metastases mainly consist of non-EMT tumor cells that maintain their epithelial phenotype. However, we have shown that upon B1R activation, along with invasion due to EMT transition, we observed changes in adherence (Oliveira et al. 2018) and cytoskeletal rearrangements, associated with highly upregulated levels of F-actin in U87 cell in the co-cultures, as it was completely inhibited only after the addition o its antagonist R175 to HOE140 (Figure 4.A). As GBM cell invasion is associated with cell extension of invadopodia/ lamellipoda, or microspikes (Hood and Cheresh, 2002); Maiuri et al. 2015). Our data are well in line with previous reports on bradykinin as an important mediator for microspike formation in 3T3 fibroblast (Kozma et al. 1995). We found much lower F-actin induction MSCs, as found by Kim et al. (2008). Cytosolic F-actin or microfilaments are able to undergo very fast polymerization and depolymerization dynamics. We observed that in most cells F-actin filaments formed larger networks that are essential for other cellular processes besides cell motility, such as cell division and cytokinesis, vesicle and organelle movement, cell signaling, and the establishment and maintenance of cell junctions and cell shape., the latter may also be the role of F-actin in U87/MSC co-cultures. Many of these processes are mediated by extensive and intimate interactions of actin with cellular membranes, where bradykinin receptors are localized.

In addition to invasion, we have previously reported on heterotypic cell fusion and the formation of U87/MSC cell hybrids appeared within 3 days (Oliveira et al. 2018), as has also been first reported by Mercapide et al. (2012). This process started with increased levels of adherence junctions, as described for U373/MSC by Schichor et al. (2012). Heterotypic cell fusion continued by U87 cells engulfing the MSC that increasingly invade upon co-cultures in various directions (Breznik et al. 2017), apparently also into the U87 cells, where they were presumably degraded by lysosomal enzymes. Recently, similar was demonstrated and termed entosis, or “cell cannibalism” of MSC by in 3D co-cultures of breast cancer cells (Bartosch et al. 2015). According to Bartosch et al. (2015) the MSC were mobilized from the bone marrow and migrated into the tumor environment. Furthermore, cell fusion of MSC by tumor cells would augment the liberation of pro-

inflammatory factors and by the same token a plethora of other cytokines would induce expression of B1R.

4.4 Conclusions

Taken together, in this study we have shown that in mono cultures bradykinin stimulated glioblastoma cells U87 and U373, but had lower effects on MSCs cell viability. The co-stimulation of kinin receptors B1R and B2R in U87 cells, but not U373 cells, in mono-cultures and in co-cultures with MSCs highly induced transient [Ca2+]i influx. Bradykinin treatment also increased the locomotion and invasion of U87 cells alone and in particular in the mixed co-cultures what was associated with higher expression of F-actin protein. These processes were impaired by the BR2 antagonist HOE140 and even more so after also BR1 antagonist R175 was added. We demonstrated that U87 cells, separated after bradykinin-treated co-cultures with MSCs, induced the epithelial-to-mesenchymal transition the associated genes what was prevented by kinin receptors antagonists. A fraction of glioblastoma U87 cells in the co-cultures fused with MSCs, forming hetero-hybrid cells. Accidental entosis events, i.e. cell cannibalism was observed, besides the extracellular vesicles transfer.

Altogether, our study supports the notion of an important role of kinin receptor agonists and antagonists in regulating glioblastoma microenvironment with respect to MSCs infiltration. This supports the on-going investigation of kinin antagonists as candidates in the development anti-invasive agents for adjuvant glioblastoma therapy. Possible clinical applications of our findings confirmed previously suggested B1R as biomarker for targeting, a theranostic for cancer therapy. In addition, the present study also has important information to be taken into accounts for potential MSC therapy designs, providing mechanisms of their interactions with tumor cells.

4.5 Materials and Methods

4.5.1 Cell Lines and Culture Maintenance

The U87 human GBM cell line was obtained from American Type Culture Collection (USA) and regularly authenticated, according to Torsvik et al. (2010). The dsRed-transfected U87 cells (U87dsRed) were established as described previously (Schichor et al. 2012). Cells were grown in complete growth medium consisting of Dulbecco's modified Eagle's medium (DMEM) and supplemented with 10% fetal bovine serum (FBS), non-essential amino acids, 4MmL-glutamine, 100 U/mL penicillin and 100 µg/mL streptomycin (Gibco). U87dsRed cells were routinely propagated in the medium with additional antibiotic 1mg/mL G-418 (Sigma-Aldrich). The cells were cultured at 37°C, in 5% CO2, and the medium was changed every 3 days. These cells were passaged after reaching 75% confluence and plated for culture maintenance at a density of 15000 cells/cm2.

Human bone-marrow MSCs, derived from a healthy volunteer (clone MSC-2) were purchased from Lonza Bioscience Walkersville (Walkersville, MD, USA). After resuscitation, the cells were plated and grown in the same medium as the GBM cells, however, without the addition of antibiotic G-418. MSCs were passaged after reaching 75% confluence at a density of 7000 cells/cm2. Bone marrow (BM)M-MSC of passages 8-12, and U87/U87dsRed GBM cells of passages 40-58 were used in culture medium containing 10% FBS. Adipose tissue derived MSCs (AT-MSCs) were isolated from healthy volunteers, as described by Kološa (PhD Thesis, 2016). Adipose tissue samples were collected from patients undergoing surgical removal of subcutaneous adipose tissue and the study was approved by the National Ethics Committee of the Republic of Slovenia (Doc. No.:

134/01/11). Isolation of AT-MSCs was performed according to the standard procedures (Mahmoudifar et al., 2010) with minor modifications.

4.5.2 Two-Dimensional and Three-Dimensional Cell Co-Cultures

For two-dimensional (2D) direct mixed cells co-cultures, GBM cells and MSCs: U87/MSC, U87dsRed/MSC, U373/ MSC, U373-GFP/MSC and U87dsRd/AT-MSC-GFP were plated into 6-well plates at 1:1 ratio and cultured for 1-7 days. For preparation of the three-dimensional (3D) spheroid cultures (mono-spheroids, mixed spheroids), the GBM cells and MSCs were mixed in 1:1 ratio and seeded into 96-well U-bottomed plates (2.5 ×103cells/well; Corning, Life Sciences, MA, USA) in 200 µL complete DMEM growth medium containing 4% methylcellulose. The cells were centrifuged for 90 min at 850×g and left in culture for 1 day at 37°C under 5% CO2, to form one spheroid in each well.

4.5.3 DsRed-Positive Cell Selection

MSC were pre-loaded with DiO, and were seeded in monocultures or 2D co-cultures together with U87-dsRed cells for 8 days, with the medium change every 2 days. Control monoculture of U87dsRed and BM-MSC were set in parallel. On the 3th day, the media were changed for the medium supplemented with geneticin (G418) at 2 mg/ml to select for U87dsRed cells, as only those cells contain the Neo resistance cassette in their genome. On the 8th day the surviving cells in U87dsRed monoculture and U87/BM-MSC co-culture were collected with trizol to perform the Real time analysis.

4.5.4 Cell Viability After Treatment With Agonists and Antagonists (MTT)

The agonist bradykinin (BK) and the antagonist AcLys[D beta Nal7, Ile8] desArg9-bradykinin(R-715) and HOE140 (both from Tocris, Fisher Scientific, Pittsburg, PA, USA) were added to the growth medium or matrigel of the 3D spheroids at final concentrations of 1 to 1000 nM. The spheroids were incubated with these for 24 h up to 168 h (7 days). The cells were incubated for 3 days in 96-well plates. The respective plate was removed from the incubator and the same added new medium with 20 l of MTT reagent to each well and incubated for 4h at 37 ° C. The formazan crystals were dissolved in isopropanol 100% and in 2 min maximum was made after the absorbance reading at 540nmusing a microplate reader (Genios; Tecan, Bradenton, FL). The measurements were performed in triplicate and repeated in three independent experiments.

4.5.5 Flow Cytometry Analysis of 2D Co-Culture Trans-Differentiation

Different types of mixed spheroids (U87-dsR/BM-MSC, U373-GFP/BM-MSC) were cultured for 3 after treatment with BK and HOE. They were then dissociated, and single-cell suspensions were subjected to flow cytometry analysis (FACS Calibur; BD Biosciences, NJ). Forward and side light scatter signals were used to detect the size of each cell population in the co-cultures. GBM cells and MSC were discriminated based on the GFP (FL1-H) or dsRed (FL2-H) fluorescence signals, following compensation for eliminating non-specific signals. Experiments for quantification of CD90 and F-actin expression were performed according to (Pillat et al. 2016). MSC were seeded in monocultures or 2D co-cultures together with U87-dsR cells for 72 h. Cells were dissociated from the flasks using

trypsin and FBS. Single cells were fixed for at least 20 min in 4% paraformaldehyde, washed with PBS 1% FBS, and incubated separated with primary antibodies conjugated with APC anti-CD90 and anti-phalloidin for 30 min at room temperature. Cells were washed with PBS and, then analyzed in a flow cytometer (MACSQuantAnalyser 10, Miltenyi Biotech, Germany). A minimum of 10,000 events was acquired per sample, and the data were displayed at logarithmic scales and analyzed with the FlowJo V10 software.

4.5.6 Spheroid 3D Analyses

4.5.6.1 Spheroid Viability Measurements (MTS Assay)

After the spheres prepared, we added 100ul of medium containing 2X concentration of the drugs tested, so that the final concentration was 100 nM in 200ul. Cell viability within the spheroids was determined using the MTS assay. After 1, 3 and 5 days, for all controls and treated spheroids grown in U-bottomed plates with 100uL media/well, 20 µLMTS agent was added (Promega, Fitchburg, WI, USA). The spheroids were incubated at 37°C for 3 h, and their absorbance was measured at 490/630 nm using a microplate reader (Genios; Tecan, Bradenton, FL, USA). The measurements were performed in triplicate and repeated in three independent experiments.

4.5.6.2 Three-Dimensional Invasion Assay

The 3D invasion assay was performed as described previously(Vinci, Box, and Eccles 2015). Briefly, the spheroids were covered with 5 mg/mL Matrigel (BD Bioscience). After a 45-min incubation at 37°C and under 5% CO2, the embedded spheroids were covered with DMEM with 10% FBS (control spheroids) and 100 nM BK or HOE-140were added (treated spheroids). The initial distance of invasion (T0) was measured following an overnight incubation, and then on each successive day, for a total of 7 days. The distance was measured from the edge of the spheroid by using the NIS elements software 2.3v (Nikon Instruments, Melville, NY, USA) and normalized to the size of the spheroid.

4.5.7 Calcium Imaging

Intracellular calcium transients were measured by fluorescence imaging of monoculture and co-culture cells using the calcium indicator dye fluo-4 AM as described by Pillat et al. (2016) elsewhere. Cells were loaded with 5 µM fluo-4 AM (Molecular Probes) in 0.5% DMSO and 0.1% of F-127 pluronic acid for 1 h at 37 °C. After three washes with culture medium, cells were placed in a warm chamber and fluorescence emissions were captured by a inverted microscope ECLIPSE-TiS (Nikon, Melville, NY) equipped with a 14 bit camera, high resolution, CCD CoolSnap HQ2 (Photometrics, Tucson, AZ, USA). Following pre-treatment with HOE140 and R715, the inhibitor was removed from the cell culture 2 min prior to calcium measurements by medium change performed twice. Fluo-4 AM was excited using the 488 nm line of argon ion laser, and the emitted light was detected at 515–530 nm using a band-pass filter. Time kinetics of free intracellular calcium ($[Ca2+]i$) variations were constructed from over 300 images collected in 1 second intervals. The fluorescence intensities (F) were calibrated in a solution containing 5 mM ionophore (Fmax) and 10 mM EGTA (Fmin) to provide an estimation of the absolute change in the intracellular calcium concentration using the following equation: $[Ca2+]i = Kd[(F - F\text{min})/(F\text{max} - F)]$; assuming a 450 nM Kd for fluo-4 AM. $[Ca2+]i$ levels of cell populations prior and following stimulation were calculated using the average value of

at least five fields of observation in independent experiments.

4.5.8 Determination of EMT Gene Expression by Real-Time qPCR

Total RNA was isolated from 2D monolayer mono-cultured U87 cells and mixed co-cultures (U87/BM-MSC, U87/AT-MSC) using the TRIzol reagent (Life Technologies). The mRNA integrity was confirmed (Agilent 2100 Bioanalyser; Agilent Technologies, Santa Clara, CA, USA). The cDNA was generated from 1.0 µg total RNA using the High-Capacity cDNA Reverse Transcription kits (Applied Biosystems, Hilden, Germany). The relative quantification of gene expression levels of B2R, Vimentin, CD44, Snail, TGFb and GADPH were carried out using real-time PCR (ABI 7900 HT Sequence Detection System; Applied Biosystems, ThermoFisher, Waltham, MA, USA). These reactions were performed using 1:10 dilutions of each cDNA (1 µg/well), added to TaqMan Universal PCR Master Mix and TaqMan Gene Expression Assays (all from Applied Biosystems): for B2R-Hs00176121_m1, Vimentin-Hs00185584_m1, CD44-Hs00174139_m1, Snail-Hs00195591_m1, Tgfb2-Hs00234244_m1 versus the amplification of glyceraldehyde 3-phosphate dehydrogenase (pre-Developed TaqMan Assay Reagent No. 4310884E) as internal control. Here, 1, 1:10, 1:100, 1:1,000 and 1:10,000 dilutions of the template sample were used for relative B1R mRNA quantity determination in the samples. The SDS v2.2 software was used (Applied Biosystems) to analyze the data obtained from the TaqMan Gene Expression Assays. Independent experiments were performed in duplicate and repeated three times. Statistical significance between different cell lines was determined by two-tailed Student's t-tests, and $P<0.05$ was considered significant.

4.5.9 Immunofluorescence Analyses

The mono-cultures of MSC and U87dsRed cells as well as co-cultures (1:1 ratio) were set up. Upon 72 h in co-cultures cells were fixed with 4% paraformaldehyde (PFA) in PBS for 15 min, washed three times and exposed for 30 min to a blocking solution containing 0.05% Triton-X 100 and 2% FBS. Cells were incubated for 30 min with Phalloidin-iFluor 488 Reagent | CytoPainter (ab176753) to marker F-actin filament (1:100, Abcam, UK). Samples were washed three times with PBS, followed by incubation for 15 min Hoechst 333482 counterstaining of cell nuclei. Following another washing step, slides were mounted with Vectashield (Vector Laboratories, Burlingame, CA USA) and analyzed on an NIKON epifluorescence microscope (Nikon, Japan), equipped with a Nikon camera and NIKON image analysis program. Alexa Fluor 488 and dsRed images were merged for detection of F-actin with cell nucleus detection in co-cultured U87-MG and MSC cells.

4.5.10 Live Cell Imaging

Images of live cells in the monolayers and as spheroids under control conditions and after addition of the agonist or antagonist (100nM) were recorded after 24h, 48h, 72h, 96h and 168h using an inverted microscope (Nikon) coupled to a digital camera. The micrograph images were processed using the Software NIS-Elements 2.3v software for measuring the areas and cell distances, and for merging the fluorescent signals (GFP, dsRed, DiO, DiL). Five micrograph images were taken per experimental condition. To time-lapse imaging, the cells were pre-loaded with the respective dye, as described in Oliveira et al. (2018). Cells were plated into 25 cm3 bottles and co-cultured for 48h. The bottles were filled up with medium supplemented with HEPES at 5mM and DAPI. All images of living cells were assisted by the Software NIS-Elements 2.3v software, for automated focus and loop time

was set at 7min for 12h.

4.5.11 Directionality Cell Analysis

The directionality Fiji plugin (open source Java image processing program ImageJ) was used to infer the preferred orientation of structures present in the input image. It computes a histogram indicating the amount of structures in a given direction. Images with completely isotropic content are expected to give a flat histogram, whereas images in which there is a preferred orientation are expected to give a histogram with a peak at that orientation. The method used was the local gradient orientation. The local gradient of the image was calculated using a 5x5 Sobel filter, which is used to derive the local gradient orientation. This orientation was then used to build the histogram, by putting the square of the gradient norm in the adequate bin. The plugin used a fit by a Gaussian to compute directionality parameters, where the Gaussian fit has the following Equation (4.1).

$$y = a + (b - a) * \exp\left(-\frac{(x - c)^2}{2d^2}\right) \tag{4.1}$$

Chapter 5

Conclusions

In this Thesis the diversity of microenvironment effects on tumor behavior in a model of glioblastoma (GBM) cells and mesenchymal stem cells (MSC) was explored with the emphasis on the role of kinin system. In three chapters we focused on understanding the relevance of kinin-mediated signaling and modulation of several processes, being altered upon interaction between two genetically different subtypes of GBM cells and a bone-marrow and adipose tissue derived MSC. GBM cell lines differ in their phenotype (Breznik et al. 2017) and also in the expression of kinin receptors, the U87 GBM cells, expressing 10 times more kinin receptor than the U373 GBM cell line. They also behave differently upon co-culturing with MSCs and the role of kinin- kininogen systems.

We observed that by co-culturing U87 and MSC cells, the expression of kinin receptors increased, either after direct or indirect cell contact, and even more so when pre-treated with their agonist, the bradykinin. B1R seems to be a more relevant mediator of kinin signaling. As cell-cell interaction increases in inflammatory conditions, we speculate that kinin / B1R system is a good candidate to trigger these events and indeed we found that B1R inhibition by its antagonist reduced cell-cell interactions. Furthermore, the epithelial-to-mesenchymal transition was triggered by bradykinin and U87/MSC interaction in co-cultures. Furthermore, antagonist treatment down regulated the expression of EMT genes as well as cell invasion by 40% compared to control conditions, whereas we found that the B1R also mediated migration and invasion in the U87 3D model.

However, we also observed co-stimulation of B2R in co-culture treatment with bradykinin. Cell-cell interactions prolonged intracellular calcium wave time prolongation, and in co-culture the B1R and B2R increased cell survival. Both kinin receptor antagonists (Hoe-140+R715) reduced cell-cell interactions. Our results strongly support the notion of high relevance of kinin receptors in tumor microenvironment as an important agent in modulating tumor cell (GBM cells) migration, invasion in possibly even more complex microenvironment than just in the presence of MSCs (Figure 5.1).

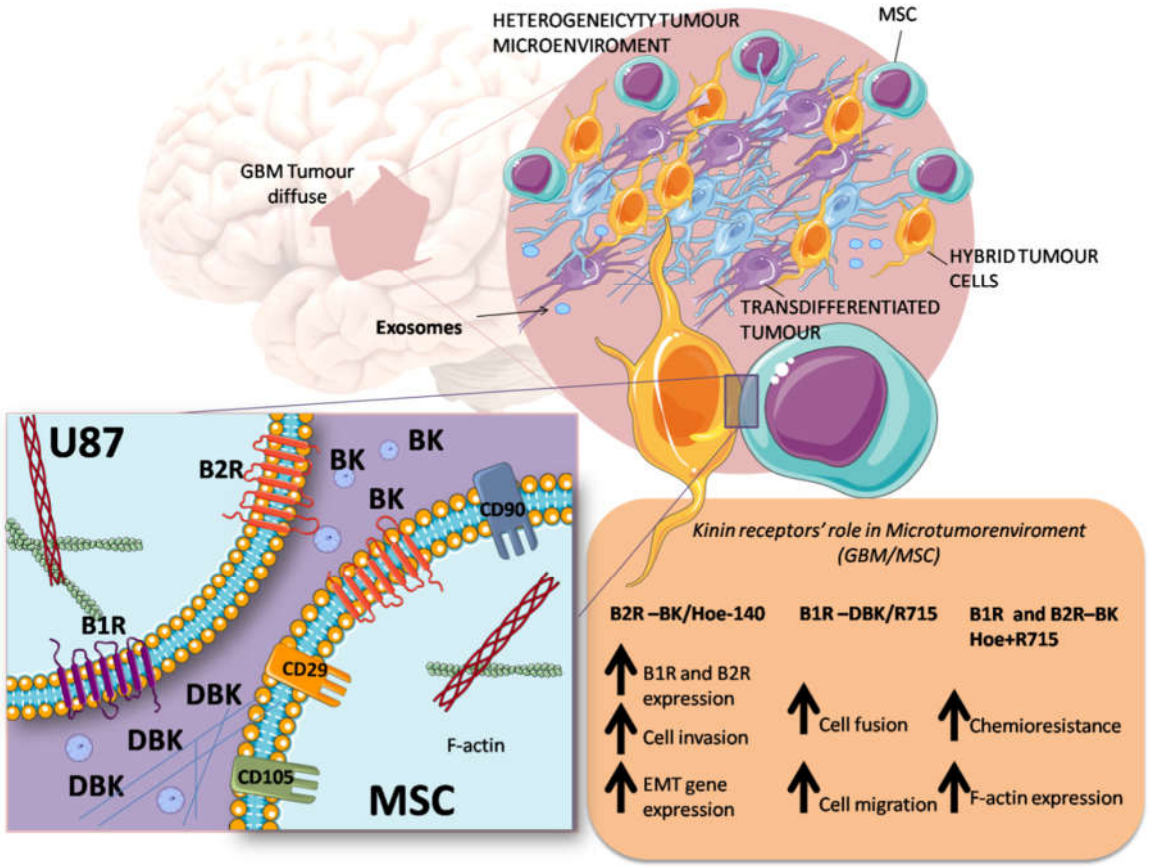

Figure 5.1: Schematic image of Kinin receptors' role of GBM-MSC interaction in the microtumor environment.

.

References

Appaix, F, Nissou, M-F., van der Sanden, B, Dreyfus, M., Berger, F., Issartel, J.-P., & Wion, D. (2014). Brain mesenchymal stem cells: The other stem cells of the brain? World Journal of Stem Cells, 6(2), 134–43. http://doi.org/10.4252/wjsc.v6.i2.134

Augello, A, Roberta T, Negrini S. M, Amateis A, Indiveri F, Cancedda R, and Pennesi G. (2005). "Bone Marrow Mesenchymal Progenitor Cells Inhibit Lymphocyte Proliferation by Activation of the Programmed Death 1 Pathway." Eur. J. Immunol. Journal 35:1482–90. https://doi.org/10.1002/eji.200425405.

Baglio, S. R, Pegtel D M, and Baldini N. (2012). "Mesenchymal Stem Cell Secreted Vesicles Provide Novel Opportunities in (Stem) Cell-Free Therapy." Frontiers in Physiology 3 (September):359–72. https://doi.org/10.3389/fphys.2012.00359.

Balyasnikova, I. V, Sherise D Ferguson, Sadhak Sengupta, Yu Han, and Maciej S Lesniak. (2010). "Mesenchymal Stem Cells Modified with a Single-Chain Antibody against EGFRvIII Successfully Inhibit the Growth of Human Xenograft Malignant Glioma." PloS One 5 (3):e9750. https://doi.org/10.1371/journal.pone.0009750.

Barki-Harrington, L, Angela L B, Gaofeng W, Lamb M E, Leeb-Lundberg L M F, and Yehia Daaka. (2003). "Requirement for Direct Cross-Talk between B1 and B2 Kinin Receptors for the Proliferation of Androgen-Insensitive Prostate Cancer PC3 Cells." The Biochemical Journal 371 (Pt 2):581–87. https://doi.org/10.1042/BJ20021708.

Bartosh, T. J., Ullah, M., Zeitouni, S., Beaver, J., & Prockop, D. J. (2016)." Cancer cells enter dormancy after cannibalizing mesenchymal stem/stromal cells (MSCs)". Proceedings of the National Academy of Sciences of the United States of America, 113(42), E6447–E6456. https://doi.org/10.1073/pnas.1612290113

Behnan, J, B Stangeland, S A M Hosainey, M Joel, T K Olsen, F Micci, J C Glover, P Isakson, and J E Brinchmann. (2017). "Differential Propagation of Stroma and Cancer Stem Cells Dictates Tumourigenesis and Multipotency." Oncogene 36 (4). Nature Publishing Group:570–84. https://doi.org/10.1038/onc.2016.230.

Behnan, J, Pauline I, Mrinal J, Corrado C, Langmoen Iver A, Vik-Mo E. O, and Wiaam Badn. (2013). "Recruited Brain Tumour-Derived Mesenchymal Stem Cells Contribute to Brain Tumour Progression." Stem Cells 2014 (32):1110–23. https://doi.org/http://dx.doi.org/ 10.1002/stem.1614.

Bougnaud, S, A. Golebiewska, A. Oudin, O. Keunen, P. N Harter, L. Mäder, F. Azuaje (2016). "Molecular Crosstalk between Tumour and Brain Parenchyma Instructs Histopathological Features in Glioblastoma." Oncotarget 7 (22):31955–71. https://doi.org/10.18632/oncotarget.7454.

Breznik, B, Motaln H, Vittori M, Rotter A, and Lah T. (2017). "Mesenchymal Stem Cells Differentially Affect the Invasion of Distinct Glioblastoma Cell Lines." Oncotarget 8 (15):25482–25499. https://doi.org/doi:10.18632/oncotarget.16041.

Bryukhovetskiy, I, and V. Shevchenko. (2016). "Molecular Mechanisms of the Effect of TGF-B1 on U87 Human Glioblastoma Cells." Oncology Letters 12 (2):1581–90. https://doi.org/10.3892/ol.2016.4756.

Cayla, C, VF Merino, and DA Cabrini. (2002). "Structure of the Mammalian Kinin

Receptor Gene Locus." International Immunopharmacology 2:1721–27. http://www.sciencedirect.com/science/article/pii/S1567576902001753.

Chamberlain, G, James F, Ashton B, and Jim Middleton. (2007). "Concise Review: Mesenchymal Stem Cells: Their Phenotype, Differentiation Capacity, Immunological Features, and Potential for Homing." Stem Cells 25 (11):2739–49. https://doi.org/10.1634/stemcells.2007-0197.

Cote J, Bovenzi V, Savard M, Dubuc C, Fortier A, Neugebauer W, Tremblay L, Mueller-Esterl W, Tsanaclis AM, Lepage M (2012). Induction of selective blood-tumor barrier permeability and macromolecular transport by a biostable kinin B1 receptor agonist in a glioma rat model. PLoS One ;2012 7:e37

da Costa, P.L.N, Sirois P, Tannock IF, Chammas R. (2014). The role of kinin receptors in cancer and therapeutic opportunities. Cancer Lett;345:27–38.

Delphine, A., Burckel, H. Josset, E., Noel, G. (2015). Three-Dimensional Cell Culture: A Breakthrough in Vivo. International Journal of Molecular Sciences. https://doi.org/10.3390/ijms16035517.

Dezso, Z, Oestreicher J, Weaver A, S. Santiago, S. Agoulnik, J. Chow, Y. Oda, and Y. Funahashi. (2014). "Gene Expression Profiling Reveals Epithelial Mesenchymal Transition (EMT) Genes Can Selectively Differentiate Eribulin Sensitive Breast Cancer Cells." PLoS ONE 9 (8). https://doi.org/10.1371/journal.pone.0106131.

Dillenburg-Pilla, P., Andrea G. M, Rosana I. R, Floriano E. M, Pereira C. D., Luiz De Lucca F., Ramos G. S., Pesquero J. B,. Jasiulionis M. G, and C. M. Costa-Neto. (2013). "Activation of the Kinin B1 Receptor Attenuates Melanoma Tumour Growth and Metastasis." PLoS ONE 8 (5):1–11. https://doi.org/10.1371/journal.pone.0064453.

Fattore, A. Del, Rosa L., R. Saracino, G. Battafarano, C. Rizzo, L. Pascucci, G. Alessandri (2014). "Differential Effects of Extracellular Vesicles Secreted by Mesenchymal Stem Cells from Different Sources on Glioblastoma Cells." Expert Opinion on Biological Therapy 15 (04):1–10. https://doi.org/10.1517/14712598.2015.997706.

Gu, S., Yanjing L, Bowen Z, Ke D, Tso P. Y, Fenfang C, Lixing Z,. (2016). "Loss of α-Tubulin Acetylation Is Associated with TGF-beta-Induced Epithelial-Mesenchymal Transition." Journal of Biological Chemistry 291 (10):5396–5405. https://doi.org/10.1074/jbc.M115.713123.

Hood, John D., and David A. Cheresh. (2002). "Role of Integrins in Cell Invasion and Migration." Nature Reviews Cancer 2 (2):91–100. https://doi.org/10.1038/nrc727.

Iwadate, Y. (2016). "Epithelial-Mesenchymal Transition in Glioblastoma Progression." Oncology Letters 11 (3):1615–20. https://doi.org/10.3892/ol.2016.4113.

Kalluri, R., and R. Weinberg. (2009). "Review Series The Basics of Epithelial-Mesenchymal Transition." Journal of Clinical Investigation 119 (6):1420–28. https://doi.org/10.1172/JCI39104.1420.

Kashuba, E, J. Bailey, D. Allsup, and L. Cawkwell. (2013). "The Kinin–kallikrein System: Physiological Roles, Pathophysiology and Its Relationship to Cancer Biomarkers." Biomarkers 18 (4):279–96. https://doi.org/10.3109/1354750X.2013.787544.

Kim, Y. Mi, E. S. Jeon, M. R. Kim, J. S. Lee, and J. H. Kim. (2008). "Bradykinin-Induced Expression of Alpha-Smooth Muscle Actin in Human Mesenchymal Stem Cells." Cellular Signalling 20 (10):1882–89. https://doi.org/10.1016/j.cellsig.2008.06.021.

Kološa K. (2016)."Optimization of human mesenchymal stem cells production and their mutual interactions with tumor cells: Doctoral Dissertation" http://www.digitalna-knjiznica.bf.uni-lj.si/biologija/dd_kolosa_katja.pdf.

Lah TT, Durán Alonso MB, Van Noorden CJ. (2006). "Antiprotease therapy in cancer: hot or not?" Expert Opin Biol Ther 6:257–279. https://doi.org/10.1517/14712598.6.3.257

Kozma, R, S Ahmed, A Best, and L Lim. (1995). "The Ras-Related Protein Cdc42Hs and

Bradykinin Promote Formation of Peripheral Actin Microspikes and Filopodia in Swiss 3T3 Fibroblasts." Molecular and Cellular Biology 15 (4):1942–52. https://doi.org/10.1128/MCB.15.4.1944.

Li, Z., Dongmei F., and D. Xiong. (2015). "Mesenchymal Stem Cells as Delivery Vectors for Anti-Tumour Therapy." Stem Cell Investigation 2 (6):1–5. https://doi.org/10.3978/j.issn.2306-9759.2015.03.01.

Lu, D. Y, Y. M. Leung, S. M. Huang, and K. L. Wong. (2010). "Bradykinin-Induced Cell Migration and COX-2 Production Mediated by the Bradykinin B1 Receptor in Glioma Cells." Journal of Cellular Biochemistry 110 (1):141–50. https://doi.org/10.1002/jcb.22520.

Mahmoudifar, N. and Doran, .P.M., (2010). Chondrogenic differentiation of human adipose-derived stem cells in polyglycolic acid mesh scaffolds under dynamic culture conditions. Biomaterials, 31, 14: 3858-3867

Maiuri, P., J. F. Rupprecht, S. Wieser, V. Ruprecht, O. Bénichou, N. Carpi, M. Coppey (2015). "Actin Flows Mediate a Universal Coupling between Cell Speed and Cell Persistence." Cell 161 (2):374–86. https://doi.org/10.1016/j.cell.2015.01.056.

Melzer, C., J. Von Der Ohe, and R. Hass. (2018). "Enhanced Metastatic Capacity of Breast Cancer Cells after Interaction and Hybrid Formation with Mesenchymal Stroma/Stem Cells (MSC)." Cell Communication and Signaling 16 (1). Cell Communication and Signaling:1–15. https://doi.org/10.1186/s12964-018-0215-4.

Melzer, C., Y. Yang, and R. Hass. (2016). "Interaction of MSC with Tumour Cells." Cell Communication and Signaling 14 (1). Cell Communication and Signaling:20–35. https://doi.org/10.1186/s12964-016-0143-0.

Mercapide, J., G. Rappa, and A. Lorico. (2012). "The Intrinsic Fusogenicity of Glioma Cells as a Factor of Transformation and Progression in the Tumour Microenvironment." International Journal of Cancer 131 (2):334–43. https://doi.org/10.1002/ijc.26361.

Molina, L, Carola E. M, A Astroza, F. Pavicic, E. Tapia, C. Toledo, J. A. Perez. (2009). "Stimulation of the Bradykinin B1 Receptor Induces the Proliferation of Estrogen-Sensitive Breast Cancer Cells and Activates the ERK1/2 Signaling Pathway." Breast Cancer Research and Treatment 118 (3):499–510. https://doi.org/10.1007/s10549-009-0314-4.

Montana, V., and H. Sontheimer. (2011). "Bradykinin Promotes the Chemotactic Invasion of Primary Brain Tumours." Journal of Neuroscience 31 (13):4858–67. https://doi.org/10.1523/JNEUROSCI.3825-10.2011.

Motaln, H., Gruden, K., Hren, M., Schichor, C., Primon, M., Rotter, A., & Lah, T. T. (2012). Human mesenchymal stem cells exploit the immune response mediating chemokines to impact the phenotype of glioblastoma. Cell Transplantation, 1–46.

Motaln, H., Koren, A., Gruden, K., Ramšak, Ž., Schichor, C., & Lah, T. T. (2015). Heterogeneous glioblastoma cell cross-talk promotes phenotype alterations and enhanced drug resistance. Oncotarget. http://doi.org/10.18632/oncotarget.5701

Motaln, H., & Turnsek, T. L. (2015). Cytokines play a key role in communication between mesenchymal stem cells and brain cancer cells. Protein and Peptide Letters, 22(4), 322–31.

Negraes, P. D., C. A. Trujillo, M. M. Pillat, Y. D. Teng, and H. Ulrich. 2015. "Roles of Kinins in the Nervous System." Cell Transplantation 24 (4):613–23. https://doi.org/10.3727/096368915X687778.

Obiezu, Christina V., and Eleftherios P. Diamandis. (2005). "Human Tissue Kallikrein Gene Family: Applications in Cancer." Cancer Letters 224 (1):1–22. https://doi.org/10.1016/j.canlet.2004.09.024.

Oliveira, M. N., M. M. Pillat, H. Motaln, H. Ulrich, and T. T. Lah. (2018). "Kinin-B1

Receptor Stimulation Promotes Invasion and Is Involved in Cell-Cell Interaction of Co-Cultured Glioblastoma and Mesenchymal Stem Cells." Scientific Reports 8 (1). Springer US:1299. https://doi.org/10.1038/s41598-018-19359-1.

Patel, Anoop P, I. Tirosh, J. J Trombetta, A. K Shalek, M Shawn, H. Wakimoto, D. P Cahill, et al. (2014). "Single-Cell RNA-Seq Highlights IntraTumoural Heterogeneity in Primary Glioblastoma Anoop." Science 344 (6190):1396–1401. https://doi.org/10.1126/science.1254257.Single-cell.

Patil, V, Jagriti Pal, and Kumaravel Somasundaram. (2015). "Elucidating the Cancer-Specific Genetic Alteration Spectrum of Glioblastoma Derived Cell Lines from Whole Exome and RNA Sequencing." Oncotarget 6 (41). https://doi.org/10.18632/oncotarget.6171.

Pesquero, J B, C J Lindsey, K Zeh, a C Paiva, D Ganten, and M Bader. (1994). "Molecular Structure and Expression of Rat Bradykinin B2 Receptor Gene. Evidence for Alternative Splicing." The Journal of Biological Chemistry 269 (43):26920–25. http://www.ncbi.nlm.nih.gov/pubmed/7929432.

Pillat, Micheli M., Mona N. Oliveira, Helena Motaln, Barbara Breznik, Talita Glaser, Tamara T. Lah, and Henning Ulrich. (2016). "Glioblastoma-Mesenchymal Stem Cell Communication Modulates Expression Patterns of Kinin Receptors: Possible Involvement of Bradykinin in Information Flow." Cytometry Part A 89 (4):365–75. https://doi.org/10.1002/cyto.a.22800.

Quail, Daniela F., and Johanna A. Joyce. (2017). "The Microenvironmental Landscape of Brain Tumours." Cancer Cell 31 (3). Elsevier Inc.:326–41. https://doi.org/10.1016/j.ccell.2017.02.009.

Sasportas, Laura S, Randa Kasmieh, Hiroaki Wakimoto, Shawn Hingtgen, Jeroen a J M Van De Water, Gayatry Mohapatra, Jose Luiz Figueiredo, Robert L Martuza, Ralph Weissleder, and Khalid Shah. (2009). "Assessment of Therapeutic Efficacy and Fate of Engineered Human Mesenchymal Stem Cells for Cancer Therapy." Proceedings of the National Academy of Sciences of the United States of America 106 (12). National Academy of Sciences:4822–27. http://www.pubmedcentral.nih.gov/articlerender.fcgi?artid=2660771&tool=pmcentrez&rendertype=abstract.

Schichor, C, Albrecht V, Korte B, Buchner A, Riesenberg R, Mysliwietz J, Paron I, et al. (2012). "Mesenchymal Stem Cells and Glioma Cells Form a Structural as Well as a Functional Syncytium in Vitro." Experimental Neurology 234 (1):208–19.

Seifert, S, and H Sontheimer. (2014). "Bradykinin Enhances Invasion of Malignant Glioma into the Brain Parenchyma by Inducing Cells to Undergo Amoeboid Migration." The Journal of Physiology 592 (Pt 22):5109–27. https://doi.org/10.1113/jphysiol.2014.274498.

Shah, Khalid. (2012). "Mesenchymal Stem Cells Engineered for Cancer Therapy." Adv Drug Deliv Rev 64 (8):739–48. https://doi.org/10.1016/j.addr.2011.06.010.Mesenchymal.

Sheng, J., Altorki, N. K., Schwabe, R. F., Li, F., Mittal, V., Lee, S., Gao, D. (2015). Epithelial-to-mesenchymal transition is not required for lung metastasis but contributes to chemoresistance. Nature, 527(7579), 472–476. https://doi.org/10.1038/nature157

Stewart, J M, L Gera, D C Chan, P A Bunn Jr., E J York, V Simkeviciene, and B Helfrich. (2002). "Bradykinin-Related Compounds as New Drugs for Cancer and Inflammation." Can J Physiol Pharmacol 80 (4):275–80. https://doi.org/10.1139/y02-030.

Thompson, Emily G., and Harald Sontheimer. (2016). "A Role for Ion Channels in Perivascular Glioma Invasion." European Biophysics Journal 45 (7):635–48.

https://doi.org/10.1007/s00249-016-1154-x.

Tidjane, N; Hachem, A; Zaid, Y.; Merhi, Y.; Gaboury, L.; Girolami, J .P.; Couture, R. (2015). “A Primary Role for Kinin B1 Receptor in Inflammation, Organ Damage, and Lethal Thrombosis in a Rat Model of Septic Shock in Diabetes.” European Journal of Inflammation 13 (1):40–52. https://doi.org/10.1177/1721727X15577736.A.

Torsvik, A, Gro V. Røsland, A Svendsen, A Molven, Immervoll H, McCormack E, Per Eystein Lønning, et al. (2010). “Spontaneous Malignant Transformation of Human Mesenchymal Stem Cells Reflects Cross-Contamination: Putting the Research Field on Track - Letter.” Cancer Research 70 (15):6393–96. https://doi.org/10.1158/0008-5472.CAN-10-1305.

Uchida, M, Zutang C, Yunhui L, and Keith L Black. (2002). “Overexpression of Bradykinin Type 2 Receptors on Glioma Cells Enhances Bradykinin-Mediated Blood – Brain Tumour Barrier Permeability Increase” 24:739–46.

Verhaak, R. G.W., Katherine A. H, Purdom E, Wang V, Yuan Qi, Matthew D. Wilkerson, C. Ryan Miller, et al. (2010). “Integrated Genomic Analysis Identifies Clinically Relevant Subtypes of Glioblastoma Characterized by Abnormalities in PDGFRA, IDH1, EGFR, and NF1.” Cancer Cell 17 (1). Elsevier Ltd:98–110. https://doi.org/10.1016/j.ccr.2009.12.020.

Vinci, Maria, Carol Box, and Suzanne A Eccles. (2015). “Three-Dimensional (3D) Tumour Spheroid Invasion Assay.” Journal of Visualized Experiments : JoVE, no. 99:e52686. https://doi.org/10.3791/52686.

Whalley, Eric T, Carlos D Figueroa, Lajos Gera, and Kanti D Bhoola. (2012). “Discovery and Therapeutic Potential of Kinin Receptor Antagonists.” Expert Opinion on Drug Discovery 1:1–20. https://doi.org/10.1517/17460441.2012.729038.

Yoon, Seon Jin, Jin Kyoung Shim, Jong Hee Chang, Ju Hyung Moon, Tae Hoon Roh, Kyoung Su Sung, Ji Hyun Lee, et al. (2016). “Tumour Mesenchymal Stem-Like Cell as a Prognostic Marker in Primary Glioblastoma.” Stem Cells International 2016. Hindawi Publishing Corporation. https://doi.org/10.1155/2016/6756983.

Zarkoob, H, Joseph H. T, Singh S. K, Sendurai A. Mani, and Mohammad Kohandel. (2013). “Investigating the Link between Molecular Subtypes of Glioblastoma, Epithelial-Mesenchymal Transition, and CD133 Cell Surface Protein.” PLoS ONE 8 (5). https://doi.org/10.1371/journal.pone.0064169.

Zhang, X, Fulong T, Yongkang Z, and Randal A. Skidgel. (2008). “Carboxypeptidase M and Kinin B1 Receptors Interact to Facilitate Efficient B1 Signaling from B2 Agonists.” Journal of Biological Chemistry 283 (12):7994–8004. https://doi.org/10.1074/jbc.M709837200.

Bibliography

Publications Related to the Thesis

Journal Articles

Pillat, M. M., Oliveira, M. N., Motaln, H., Breznik, B., Glaser, T., Lah, T. T., & Ulrich, H. (2016). Glioblastoma-mesenchymal stem cell communication modulates expression patterns of kinin receptors: Possible involvement of bradykinin in information flow. Cytometry Part A, 89(4), 365-375. *Micheli M. Pillat and Mona Oliveira share the first authorship.

Oliveira, M. N., Pillat, M. M., Motaln, H., Ulrich, H., & Lah, T. T. (2018). Kinin-B1 Receptor Stimulation Promotes Invasion and is Involved in Cell-Cell Interaction of Co-Cultured Glioblastoma and Mesenchymal Stem Cells. Scientific reports, 8(1), 1299. doi:10.1038/s41598-018-19359-1

Conference Paper

Oliveira, M.N, Breznik B, Pillat M. M, Lah T.T, and Ulrich H. (2014). Mesenchymal Stem Cells Enhance Invasion of Glioblastoma Cells via Kinin Receptor-mediated Activity. Fraunhofer Germany Symposium Leipzig, Leipzig, 2014.

Oliveira, M. N., Pillat, M. M., Motaln, H., Ulrich, H., & Lah, T. T. (2015). Kinin Receptor Expression and Activity in Co-cultured Mesenchymal Stem Cells and Glioblastoma Cells. In: FEBS+3 Molecules of life, 2015, Portorož. FEBS+3 Molecules of life, 2015.

Oliveira M.N. (2017). Kinin Receptors Activity Regulated Cell-Cell Interaction and Cell Fusion of Glioblastoma and Mesenchymal Stem Cell. In: Bilateral Cooperation SIKT and IQ, 2017, Leipzig. Leipzig University.

Oral Presentation Related with the Thesis

Oliveira, M. D. (2014). Mesenchymal Stem Cells Enhance Invasion of Glioblastoma Cells via Kinin Receptor-mediated Activity. Lecture presented at III Simposio Latino Americano de Neuroquimica e VI Simposio de Atualização de Farmacologia da UFBA in Health Sciences Institute of UFBA, Salvador da Bahia.

Other Publications

1. Oliveira, M. N., Pillat, M. M., Motaln, H., Ulrich, H., & Lah, T. T. (2018). Kinin-B1 Receptor Stimulation Promotes Invasion and is Involved in Cell-Cell Interaction of Co-Cultured Glioblastoma and Mesenchymal Stem Cells. Scientific reports, 8(1), 1299.

2. Cunha, S., Serafim, J. C., de Santana, L. L. B., Damasceno, F., Correia, J. T. M., Santos, A. O., ... & Costa, S. L. (2017). One-Step Synthesis of 3, 4-Diphenyl-2-pyrrolinones by Solvent-Free and Bi2O3-Catalyzed Approaches and Cytotoxicity Screening Against Glioma Cells. Journal of Heterocyclic Chemistry, 54(6), 3700-3710.

3. Coelho, P. L. C., Freitas, S. R. V. B. D., Pitanga, B. P. S., Silva, V. D. A. D., Oliveira, M. N., Grangeiro, M. S., ... & Nascimento, I. L. D. O. (2016). Flavonoids from the Brazilian plant Croton betulaster inhibit the growth of human glioblastoma cells and induce apoptosis. Revista Brasileira de Farmacognosia, 26(1), 34-43.

4. Coelho, P. L., Oliveira, M. N., da Silva, A. B., Pitanga, B. P., Silva, V. D., Faria, G. P., ... & Costa, S. L. (2016). The flavonoid apigenin from Croton betulaster Mull inhibits proliferation, induces differentiation and regulates the inflammatory profile of glioma cells. Anti-cancer drugs, 27(10), 960-969.

5. Pillat, M. M., Oliveira, M. N., Motaln, H., Breznik, B., Glaser, T., Lah, T. T., & Ulrich, H. (2016). Glioblastoma-mesenchymal stem cell communication modulates expression patterns of kinin receptors: Possible involvement of bradykinin in information flow. Cytometry Part A, 89(4), 365-375. *the authors share the first authorship.

6. Santos, B. L., Oliveira, M. N., Coelho, P. L., Pitanga, B. P., da Silva, A. B., Adelita, T., ... & Chneiweiss, H. (2015). Flavonoids suppress human glioblastoma cell growth by inhibiting cell metabolism, migration, and by regulating extracellular matrix proteins and metalloproteinases expression. Chemico-biological interactions, 242, 123-138. *the authors share the first authorship.

7. Santos, B. L., Silva, A. R., Pitanga, B. P. S., Sousa, C. S., Grangeiro, M. S., Fragomeni, B. O., ... & El-Bachá, R. D. S. (2011). Antiproliferative, proapoptotic and morphogenic effects of the flavonoid rutin on human glioblastoma cells. Food chemistry, 127(2), 404-411.

Biography

Mona Oliveira was born on the 12th of January 1986 in Salvador da Bahia, Brazil. In 2005, she enrolled in the study program Veterinary Medicine at Federal University of Bahia (UFBA). In parallel, in 2007-2011 she was Course Assistant for *Veterinary Biochemistry I* and *Veterinary Biochemistry II* at the same university. She held responsibility for Laboratory and Practical Classes. She completed her studies in 2010 and she is a Veterinary Doctor by profession. In 2010, she enrolled in the additional MSc program Biotechnology at State University of Feira de Santana (UEFS), which she completed in 2012.

Starting in November 2011, she became acting Assistant Professor (Portuguese: *Professor substituto*) at the Federal University of Bahia (UFBA) undergraduate degree programme in Animal Husbandry (Portuguese: *Zootecnia*). For 3 semesters, she held lectures in:

- General, Analytical and Organic Chemistry (Portuguese: *Química geral, analítica e orgânica*),
- Molecular Biology (Portuguese: *Biologia Molecular*),
- Animal Reproduction I (Portuguese: *Reprodução animal I*)
- Mathematics Applied to Animal Husbandry (Portuguese: *Matemática aplicada à Zootecnia*).

She also served as academic advisor to students for scientific experiments.

In 2013, she enrolled in the PhD Program in Biological Sciences (Biochemistry) at the Institute of Chemistry, University of São Paulo (USP). She was under the supervision of Prof. Dr. Alexander Henning Ulrich. In 2015, she continued her research at National Institute of Biology in Slovenia under the co-supervision of Prof. Dr. Tamara Lah Turnšek. In Slovenia, she also enrolled in the PhD program Nanosciences and Nanotechnologies at Jožef Stefan International Postgraduate School (IPS) in order to pursue the double PhD degree between USP and IPS.

She presented her work related to Mesenchymal Stem Cells at several international conferences and meetings, such as *III Latin American Symposium of Neurochemistry* and *VI Pharmacology Update Symposium* at UFBA (Brazil), *Fraunhofer Germany Symposium Leipzig* (Germany), FEBS3+ Meeting (Slovenia) and at a seminar at the *Saxon Incubator for Clinical Translation* (Germany).

In 2018, she founded the biotech startup Biolinker, where she acts as the Chief Science Officer. The purpose of the company is to develop technologies and services to express and purify recombinant protein in hours instead of weeks. Biolinker raised BRL 200.000 of equity-free capital from São Paulo Research Foundation (FAPESP). In October 2018, Biolinker was named one of the Top 500 startups at Hello Tomorrow Challenge - the world's biggest early-stage startup competition for science and deep technology startups. The company was chosen by a rigorous panel of industry experts, scientists and entrepreneurs who reviewed over 4.500 applications to select startups that have the most potential.